COMBINATORICS OF ARC DIAGRAMS, FERRERS FILLINGS, YOUNG TABLEAUX AND LATTICE PATHS

by

Jacob Post
B.Sc., Portland State University, 2001

A THESIS SUBMITTED IN PARTIAL FULFILLMENT
OF THE REQUIREMENTS FOR THE DEGREE OF
MASTER OF SCIENCE
in the School
of
Computing Science

© Jacob Post 2009
SIMON FRASER UNIVERSITY
Summer 2009

All rights reserved. However, in accordance with the *Copyright Act of Canada*, this work may be reproduced, without authorization, under the conditions for *Fair Dealing*. Therefore, limited reproduction of this work for the purpose of private study, research, criticism, review and news reporting is likely to be in accordance with the law, particularly if cited appropriately.

APPROVAL

Name:	Jacob Post
Degree:	Master of Science
Title of thesis:	Combinatorics of Arc Diagrams, Ferrers Fillings, Young Tableaux and Lattice Paths
Examining Committee:	Dr. Ramesh Krishnamurti, Professor of Computing Science Chair
	Dr. Pavol Hell, Professor of Computing Science Senior Supervisor
	Dr. Cedric Chauve, Professor of Mathematics Co-supervisor
	Dr. Marni Mishna, Professor of Mathematics Supervisor
	Dr. Gábor Tardos, Professor of Computing Science Supervisor
	Dr. Jonathan Jedwab, Professor of Mathematics External Examiner
Date Approved:	July 22, 2009

SFU SIMON FRASER UNIVERSITY
LIBRARY

Declaration of
Partial Copyright Licence

The author, whose copyright is declared on the title page of this work, has granted to Simon Fraser University the right to lend this thesis, project or extended essay to users of the Simon Fraser University Library, and to make partial or single copies only for such users or in response to a request from the library of any other university, or other educational institution, on its own behalf or for one of its users.

The author has further granted permission to Simon Fraser University to keep or make a digital copy for use in its circulating collection (currently available to the public at the "Institutional Repository" link of the SFU Library website <www.lib.sfu.ca> at: <http://ir.lib.sfu.ca/handle/1892/112>) and, without changing the content, to translate the thesis/project or extended essays, if technically possible, to any medium or format for the purpose of preservation of the digital work.

The author has further agreed that permission for multiple copying of this work for scholarly purposes may be granted by either the author or the Dean of Graduate Studies.

It is understood that copying or publication of this work for financial gain shall not be allowed without the author's written permission.

Permission for public performance, or limited permission for private scholarly use, of any multimedia materials forming part of this work, may have been granted by the author. This information may be found on the separately catalogued multimedia material and in the signed Partial Copyright Licence.

While licensing SFU to permit the above uses, the author retains copyright in the thesis, project or extended essays, including the right to change the work for subsequent purposes, including editing and publishing the work in whole or in part, and licensing other parties, as the author may desire.

The original Partial Copyright Licence attesting to these terms, and signed by this author, may be found in the original bound copy of this work, retained in the Simon Fraser University Archive.

Simon Fraser University Library
Burnaby, BC, Canada

Abstract

Several recent works have explored the deep structure between arc diagrams, their nestings and crossings, and several other combinatorial objects including permutations, graphs, lattice paths, and walks in the Cartesian plane.

This thesis inspects a range of related combinatorial objects that can be represented by arc diagrams, relationships between them, and their connection to nestings and crossings. We prove a direct connection between nestings in involutions and the shape of Young tableaux, clarify Knuth transformations in terms of Young tableaux, present a local transformation on arc diagrams of involutions that we term involutive transformations, and describe variants to the well-known RSK correspondence.

Keywords: Arc diagrams, Ferrers filling, Young tableaux, Lattice paths, Bijections, Nestings, Crossings, RSK, Knuth transformations

Acknowledgments

I would like to acknowledge the continuing support of my co-supervisor Cedric Chauve. Additionally, my senior supervisor Pavol Hell has been very flexible in allowing me to follow my own interests. The nestings and crossings study group has also been very inspirational.

Contents

List of Figures

List of Notations

Preface

Everything starts with the paper of Chen et al. [8]. It describes interesting properties of nestings and crossings and their statistics in a representation of matchings and set partitions in terms of arc diagrams. In particular it links these objects to vacillating tableaux, that can be described as paths in the Young lattice, and to the classical RSK construction, that relates Young tableaux and permutations. The paper of Chen was then greatly generalized by Krattenthaler [29] in terms of Ferrers fillings and their growth diagrams.

Since then, several other works have followed, exploring the deep structure between arc diagrams, their nestings and crossings, and several other combinatorial objects including permutations [10], graphs [12], lattice paths [26], walks in the Cartesian plane [37, 33], generating functions, and more.

From these works, arc diagrams appear to be a very general way to represent several families of combinatorial objects. In addition to the myriad of opportunities for new mathematical discoveries in this area, research is motivated by connections to RNA secondary structures and genome rearrangement scenarios. Two RNA secondary structures in particular are pseudoknots, which correspond to crossings, and helices, which correspond to nestings. There is, therefore, a strong connection between nestings and crossings and the analysis of RNA structures, which has been the subject of many recent works. See, for example, Jin et al. [24], Jin et al. [25], Huang et al. [23] and Chen et al. [9].

This thesis inspects a range of related combinatorial objects, relationships between them, and their connection to nestings and crossings. In the process, we clarify Knuth transformations in terms of Young tableaux, present involutive transformations, and extend one of the results in the Chen et al. paper.

Chapter 1

Introduction

In this chapter, we introduce a number of combinatorial objects which are used in the following chapters, and some fundamental relationships between them. Section 1.5 gives a summary of the objects and prior work in this research area, and an overview of the following chapters.

1.1 Integer Partitions, Ferrers Diagrams, and Young's Lattice

An integer partition can be represented by a *Ferrers diagram* consisting of cells in left-aligned rows of non-increasing length. We say that the *shape* of such a partition is $\lambda = \lambda_1, \lambda_2, \ldots$, where λ_i is the length of the ith row. (The empty partition is represented by $\emptyset = 0, 0, \ldots$)

The *conjugate* or *transposition* of λ, λ^T, is constructed by exchanging the rows and columns of λ. More formally, we can consider positions (r, c) in the diagram, with $(r, c) \in \lambda \iff 1 \leq c \leq \lambda_r$. Then, $(i, j) \in \lambda^T \iff (j, i) \in \lambda$. Figure 1.1 gives an example.

Figure 1.1: The Ferrers diagrams of an integer partition $\lambda = 5, 3, 2, 2$ and its conjugate $\lambda^T = 4, 4, 2, 1, 1$

Given two integer partitions λ and μ, we say that λ *contains* μ and write $\mu \preceq \lambda$ if, for all i, $\mu_i \leq \lambda_i$. Strict containment is analogously defined for $\prec$. This relation defines a poset over all integer partitions. The Hasse diagram on this poset is known as *Young's lattice*; see, for example, [45]. Here, we refer to the sublattice induced by the integer partitions contained in λ as Y_λ, and to the number of integer partitions thus contained as $|Y_\lambda|$. Figure 1.2 shows one such sublattice.

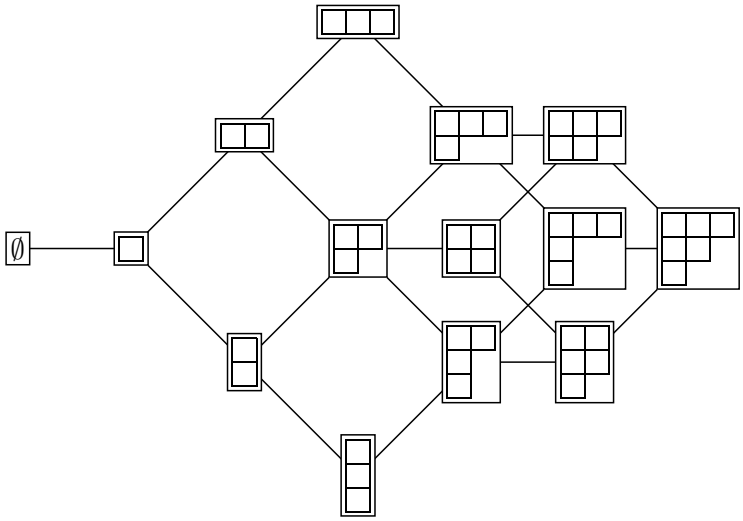

Figure 1.2: The lattice Y_λ for $\lambda = 3, 2, 1$. $|Y_\lambda| = 14$

Cells of a Ferrers diagram that can be removed to form a new Ferrers diagram are called corners, and positions where a cell can be added are called co-corners. Note that any removed corner becomes a co-corner, and any cell added at a co-corner becomes a corner. Examples are given in Figure 1.3.

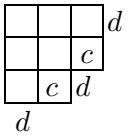

(a) A Ferrers diagram of $\lambda = 3, 3, 2$ with corners labeled c and co-corners labeled d.

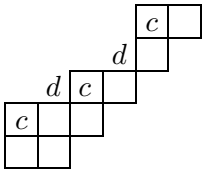

(b) A skew shape λ/μ with $\lambda = 6, 5, 4, 3, 2$ and $\mu = 4, 4, 2$. Inner corners are labeled with c and inner co-corners with d.

Figure 1.3: Examples of corners and co-corners

Finally, given $\mu \prec \lambda$, we define the skew shape λ/μ as $\{(r, c)|(r, c) \in \lambda \wedge (r, c) \notin \mu\}$. Corners of μ that are not corners of λ are called inner co-corners of λ/μ, and co-corners of μ that are not co-corners of λ are called inner corners of λ/μ, as shown in Figure 1.3.

1.2 Young Tableaux and the Robinson-Schensted-Knuth Correspondence

Filling each cell of a Ferrers diagram with numbers results in an object referred to as a *tableau* or *Ferrers filling*. The numbers are collectively called the *contents* of the tableau. Restricting the content leads to combinatorial objects with remarkable properties. In this thesis, we are primarily interested in two types of fillings, strict 0-1 Ferrers fillings (presented in Section 1.4) and Young tableaux (presented below).

1.2.1 Young Tableaux

A *tableau* P on shape $\mathrm{sh}(P) = \lambda$ and size $n = |\lambda|$ is defined as the Ferrers diagram of λ in which every cell is filled with a number. The numbers are collectively referred to as the contents of the tableau. If the numbers increase from left to right in each row, and increase downward in each column, it is defined as an *increasing Young tableau*. *Decreasing Young tableaux* and *skew Young tableaux* are analogously defined. If the numbers are $[n]$, we say that P is a *standard Young tableau* or *SYT*. Here, we usually work with increasing tableaux, and thus do not specify the direction of a Young tableau unless it is decreasing.

Note that the smallest number of a Young tableau must be located at the origin $(1, 1)$, and the largest number must be located at a corner. Inductively, the cells containing the

smallest k numbers form a sub-Young tableau, and those containing the largest $n-k$ numbers form a skew Young tableau. As a result, a Young tableau P with $\mathrm{sh}(P) = \lambda$ can also be defined as a monotonic walk in Y_λ from $\emptyset$ to λ. An example is given in Figure 1.4.

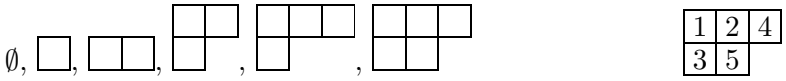

Figure 1.4: A monotonic walk in $Y_{3,2}$ from $\emptyset$ to $3,2$ and the corresponding SYT

Given a Young tableau P with contents $p_1 < p_2 < \ldots < p_n$, we define the *negation* of P, P^N, to be the decreasing Young tableau obtained by replacing p_i with p_{n-i+1}. We similarly define negation for decreasing Young tableaux, and note that $P^{NN} = P$. We define the *transposition* of a Young tableau P similarly to that of integer partitions, and write P^T. Note that $P^{TT} = P$ and $P^{NT} = P^{TN}$. If a value α is less than (resp. greater than) any value in the Young tableau, we write $\alpha < P$ (resp. $\alpha > P$). See Figure 1.5 for examples.

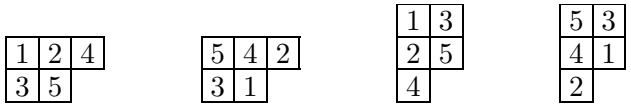

Figure 1.5: From left to right: A standard Young tableau P, P^N, P^T, and $P^{NT} = P^{TN}$

There are two well-known pairs of operations for adding or removing numbers from a Young tableau, namely *jeu de taquin* and *row insertion/deletion*. Jeu de taquin can also be used to define a transformation on Young tableaux called *evacuation*. Although the operations may seem unrelated on the surface, it has been shown that they in fact have deep connections to one another. The operations can also be used to show many correlations between standard Young tableaux, permutations, and other related structures.

We explore row insertion/deletion in the following section, as it is essential in showing a strong connection between permutations and Young tableaux via the Robinson-Schensted-Knuth correspondence. Jeu de taquin and evacuation are presented in Chapter 3, where they are used to generalize the Robinson-Schensted-Knuth correspondence and describe transformations of Young tableaux.

1.2.2 Robinson-Schensted-Knuth and Permutations

One pair of operations for adding and removing numbers from a Young tableau is *row insertion* and *row deletion*. Given a Young tableau P, we define the row insertion $\text{rins}(P, \alpha)$ as Algorithm 1.1.

Algorithm 1.1 $\text{rins}(P, \alpha)$: Row insertion of α into Young tableau P

Let $r \leftarrow 1$
while α is not larger than all values in row r **do**
  Let β be the smallest number in row r such that $\beta > \alpha$
  Let c be the column where β is located
  Replace β in (r, c) with α, then let $\alpha \leftarrow \beta$ and $r \leftarrow r + 1$
end while
Create a new cell at the end of row r and set the value to α

The operation is referred to as row insertion as a number is inserted into the first row, potentially "bumping" another number into the second row; the algorithm then continues recursively, bumping numbers from their original row to the row below. Figure 1.6 shows an example of a row insertion.

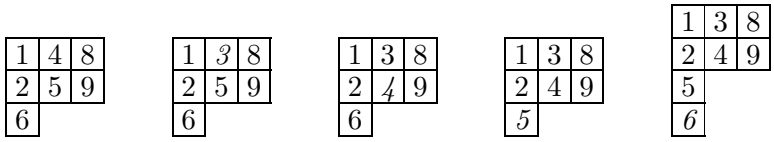

Figure 1.6: A row insertion of 3 into a Young tableau. Row deleting the new corner (containing 6) would reverse the process

It can be shown that this algorithm results in a new Young tableau. Moreover, the algorithm is reversible; $\text{rdel}(P, r, c)$ is defined as Algorithm 1.2.

Algorithm 1.2 rdel(P, r, c): Row deletion of corner (r, c) from Young tableau P

Require: (r, c) is a corner in P
  Let α be the contents of (r, c)
  Remove corner (r, c) from P
  while $r > 1$ **do**
    Let $r \leftarrow r - 1$
    Let β be the largest number in row r such that $\beta < \alpha$
    Let c be the column where β is located
    Place α into cell (r, c), then let $\alpha \leftarrow \beta$
  end while
  {The algorithm terminates and α is removed from P}

Although it is conventional to use the row-based operations defined above, column-based variants cins(P, α) and cdel(P, r, c) can also be defined.

$$\text{cins}(P, \alpha) = \text{rins}(P^T, \alpha)^T \tag{1.1}$$

$$\text{cdel}(P, r, c) = \text{rdel}(P^T, c, r)^T \tag{1.2}$$

It is also possible to prove (Schensted [38]) that column-base insertion and row-based insertion are remarkably independent; namely,

$$\text{rins}(\text{cins}(P, x), y) = \text{cins}(\text{rins}(P, y), x) \tag{1.3}$$

This property can in turn be used to prove some of the connections between Young tableaux and permutations explored in Chapter 3.3.

Row insertion can be used to prove a bijection between two-line arrays of a certain form with pairs of Young tableaux of the same shape. The bijection was first discovered for permutations by Robinson [11], and then independently rediscovered by Schensted [38]. Knuth later [27] generalized the Robinson-Schensted algorithm using two-line arrays. We do not use Knuth's generalization in this thesis, but still refer to the construction as the *RSK algorithm* due to the use of two-line arrays.

Theorem 1.1 (Robinson[11], Schensted[38], Knuth[27])**.** *Two-line arrays of the form*

$$A = \begin{pmatrix} q_1 & q_2 & \dots & q_n \\ p_1 & p_2 & \dots & p_n \end{pmatrix} \quad p_i \text{ distinct and } q_i < q_{i+1},\ 1 \le i < n$$

are in bijection with pairs of Young tableaux P with contents $p_1, \ldots, p_n$ and Q with contents $q_1, \ldots, q_n$ such that $\mathrm{sh}(Q) = \mathrm{sh}(P)$.

Proof. The proof is constructive. Algorithm 1.3 gives the process for constructing the two tableaux from the two-line array.

Algorithm 1.3 RSK construction of tableaux from a two-line array

Require: p_i distinct and $q_i < q_{i+1},\ 1 \leq i < n$

Let $P_0 \leftarrow \emptyset$ and $Q_0 \leftarrow \emptyset$

for $i = 1$ to n **do**

Let $P_i \leftarrow \mathrm{rins}(P_{i-1}, p_i)$ and let (r_i, c_i) be the resulting new corner

Let Q_i be the same as Q_{i-1}, and then place q_i into a new cell at position (r_i, c_i)

{Note that $\mathrm{sh}(Q_i) = \mathrm{sh}(P_i)$}

end for

Conventionally, $P = P_n$ is called the *insertion tableau* of A, and $Q = Q_n$ is called the *recording tableau*. If A corresponds to P and Q, we write $A \sim (P, Q)$, and let $\mathrm{sh}(A) = \mathrm{sh}(P) = \mathrm{sh}(Q)$. Figure 1.7 gives an example of the algorithm.

$$\begin{pmatrix} 1 & 3 & 5 & 7 & 9 \\ 4 & 8 & 2 & 0 & 6 \end{pmatrix}$$

(a) A two-line array A

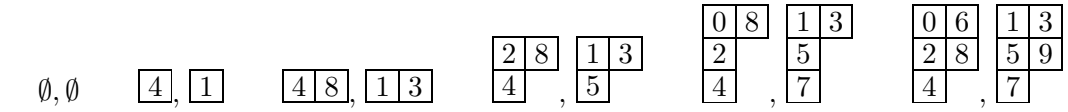

(b) P_0, Q_0 (c) P_1, Q_1 (d) P_2, Q_2 (e) P_3, Q_3 (f) P_4, Q_4 (g) P_5, Q_5

Figure 1.7: An example of Algorithm 1.3

Because the content of (r_i, c_i) in Q is q_i, it is simple to reverse the construction of Algorithm 1.3, yielding Algorithm 1.4.

Algorithm 1.4 RSK construction of a two-line array from tableaux

Require: $\mathrm{sh}(Q) = \mathrm{sh}(P)$

Let $P_n \leftarrow P$ and $Q_n \leftarrow Q$

for $i = n$ down to 1 **do**

Let q_i be the largest number in Q_i and let (r_i, c_i) be its location

Let Q_{i-1} be the same as Q_i, and then remove the corner at position (r_i, c_i)

Let $P_{i-1} \leftarrow \mathrm{rdel}(P_i, r_i, c_i)$ and let p_i be the number removed from P_i

end for

Let the two-line array be $\begin{pmatrix} q_1 & q_2 & \cdots & q_n \\ p_1 & p_2 & \cdots & p_n \end{pmatrix}$

This completes the bijection. □

Corollary 1.1.1. *Permutations of $[n]$ are in bijection with pairs of SYTs of size n and identical shape.*

1.3 Arc Diagrams, Nesting, and Crossing

In this section, we present arc diagrams, and show how they can represent a number of combinatorial objects, such as permutations, set partitions, and matchings. We also introduce natural statistics on arc diagrams, namely nestings and crossings. In the following chapter, bijections involving these objects are explored. Figure 1.14 gives a table of notations and a hierarchy for these classes.

1.3.1 Arc Diagrams

An *arc diagram* is a multigraph with labeled vertices in which the vertices are placed on the x axis in increasing order, and edges are drawn as arcs between the vertices.

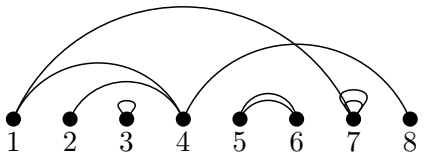

Figure 1.8: An example of an arc diagram

There are deep connections between general Ferrers fillings and general arc diagrams, as explored by de Mier [12].

Various classes of arc diagrams can represent many combinatorial objects. For example, a permutation σ can be represented by an arc diagram with bicoloured arcs; one colour for edge $(i, \sigma(i))$ when $\sigma(i) \geq i$, and another for edge $(\sigma(i), i)$ when $\sigma(i) < i$. (Every vertex will have degree 2 and there are no multi-edges; a vertex attached only to a loop is considered to have degree 2.) Conventionally, arcs of the first colour are drawn above the x axis and arcs of the second colour are drawn below, as shown in Figure 1.9.

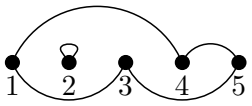

Figure 1.9: The arc diagram of the permutation 42153

This thesis is primarily concerned with the arc diagrams of set partitions, and subsets of set partitions. Set partitions can be represented by an arc diagram wherein elements in the same part are connected by a sequence of arcs, from the smallest element to the largest. Additionally, parts of size one can be represented by a vertex with a loop. Set partitions themselves can be considered a subset of permutations. For example, each part of a set partition can be reinterpreted as a cycle, as demonstrated in Figure 1.10.

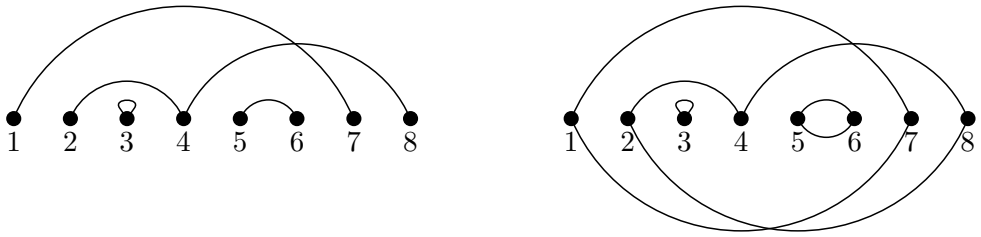

Figure 1.10: The set partition $\{1, 7\}\{2, 4, 8\}\{3\}\{5, 6\}$ and the permutation with cycles $[1, 7][2, 4, 8][3][5, 6]$

Restricting each part in a set partition to size 1 or 2 results in an involution, i.e. a permutation that is its own inverse. As can be seen in Figure 1.11, the arc diagram consists of vertices with loops (and no other arcs), and pairs of vertices with degree 1 connected by an arc. Involutions are also known as partial matchings.

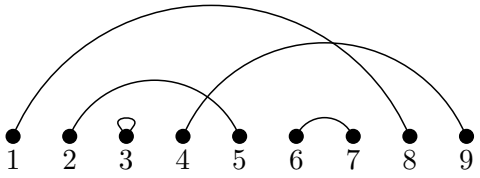

Figure 1.11: The arc diagram of an involution

Forbidding loops in a permutation results in a derangement, forbidding loops in a set partition results in a singleton-free set partition, and forbidding loops in an involution results in a (perfect) matching. Examples are given in Figure 1.12.

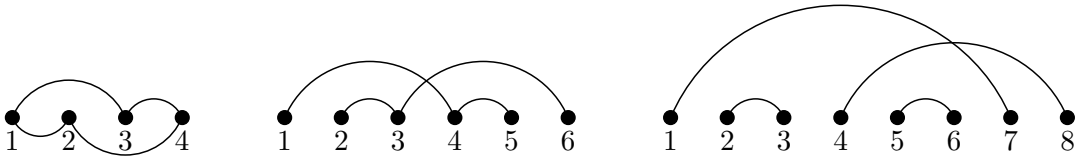

Figure 1.12: The arc diagrams of a derangement, a singleton-free set partition, and a matching

A *balanced matching* with $2n$ vertices is a matching which consists of arcs (i, j) such that $i \leq n$ and $j > n$. In other words, all arcs start on the left half of the diagram and end on the right half, as shown in Figure 1.13.

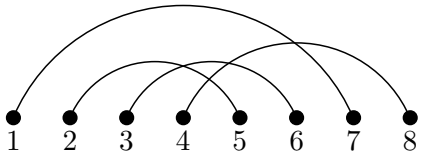

Figure 1.13: The arc diagram of a balanced matching

Together, these objects form a hierarchy; each one can be considered to be a subset of permutations, as illustrated in Figure 1.14. However, as we will demonstrate in Section 1.4, permutations of size k are in bijection with balanced matchings of size $2k$. Therefore, permutations can also be seen as a special case of matchings.

S_n	Permutations on $[n]$
D_n	Derangements on $[n]$
P_n	Set partitions of $[n]$
FP_n	Singleton-free set partitions of $[n]$
I_n	Involutions (self-inverse permutations) on $[n]$
M_n	Matchings on $[n]$ (n must be even)
BM_n	Balanced matchings on $[n]$ (n must be even)

$$\begin{array}{ccccccccc} S_n & \supset & P_n & \supset & I_n & & & & \\ \cup & & \cup & & \cup & & & & \\ D_n & \supset & FP_n & \supset & M_n = M_{2k} & \supset & BM_{2k} & \leftrightarrow & P_k \end{array}$$

Figure 1.14: Notations and a hierarchy for families of combinatorial objects that can be represented as arc diagrams

Most of this thesis concerns arc diagrams of one colour, in particular, set partitions and their subsets, such as matchings. These arc diagrams have four types of vertices, as illustrated in Figure 1.15. Namely, the four types are *left endpoints*, *right endpoints*, *transitory vertices*, and *singletons*.

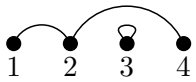

Figure 1.15: A left endpoint (1), transitory vertex (2), singleton (3), and right endpoint (4)

1.3.2 Nestings and Crossings

Following Chen et al. [8], we are primarily interested in the relationship between arcs in the diagram. In terms of a permutation σ, *nesting* can be defined as i and j such that $i < j < \sigma(j) < \sigma(i)$. In an arc diagram, nesting has the intuitive meaning of one arc being completely underneath another. Examples can be seen in Figure 1.16.

When considering singletons, there are at least two popular interpretations that have been considered. Under the *strong nesting* interpretation, singletons cannot be part of a nesting. Under the *weak nesting* interpretation, however, they may. In this case, the requirement can be stated as $i < j \leq \sigma(j) < \sigma(i)$. (In Chapter 4, we introduce a third interpretation.)

The concept of nesting can be generalized. A k-nesting is a set of k pairwise nesting arcs. In terms of the permutation, we have $i_1 < i_2 < \ldots < i_k < \sigma(i_k) < \ldots < \sigma(i_2) < \sigma(i_1)$ for strong k-nestings, and similar for weak k-nestings. When unqualified, the term nesting refers to 2-nestings.

Note that, in terms of a permutation, a k-nesting involving v vertices is a decreasing subsequence of length v.

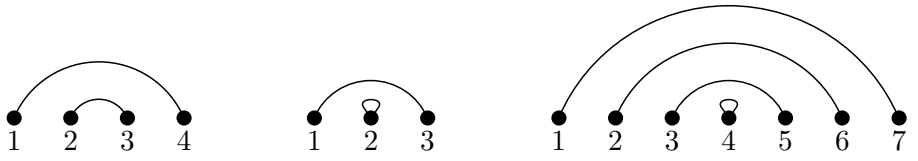

(a) A nesting (b) A weak nesting that is not a strong nesting (c) A weak 4-nesting that is a strong 3-nesting

Figure 1.16: Examples of nestings and k-nestings

Crossings and k-crossings can be similarly defined. In terms of a permutation, a strong k-crossing consists of k indices such that $i_1 < i_2 < \ldots < i_k < \sigma(i_1) < \sigma(i_2) < \ldots < \sigma(i_k)$. Within the arc diagram, crossings again have the intuitive meaning of two arcs that overlap (cross). There are also weak and strong interpretations for crossings; the *weak crossing* interpretation considers a transitory vertex to be a crossing, while the *strong crossing* interpretation does not. Examples are given in Figure 1.17.

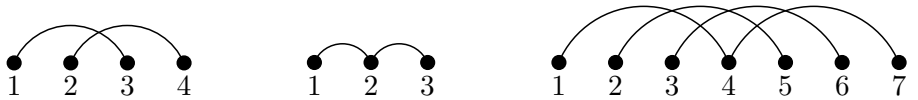

(a) A crossing (b) A weak crossing that is not a strong crossing (c) A weak 4-crossing that is a strong 3-crossing

Figure 1.17: Examples of crossings and k-crossings

In this thesis, we define an *alignment* to be two arcs that neither nest nor cross. (There is no standard interpretation of this term in the literature; for example, in [10] nestings are considered to be alignments, while in [26] they are not.) Figure 1.18 gives examples.

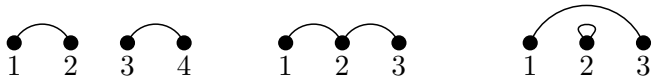

(a) An alignment (b) One type of strong alignment (c) Another type of strong alignment

Figure 1.18: Examples of alignments

1.4 Strict 0-1 Ferrers Filling and Permutation Matrices

In this section, we present another type of Ferrers filling. Krattenthaler [29] explores both general and restricted Ferrers fillings in depth. In particular he devotes a section to presenting evidence that Ferrers fillings are but a part of a much larger theory, encompassing such shapes as stack polyominoes and moon polyominoes.

A *strict 0-1 Ferrers filling* is a Ferrers diagram in which each cell contains either a 0 or a 1, and moreover, every column and every row contains exactly one 1. For ease of legibility, the diagrams for these objects are presented with 'X' replacing 1 and the 0s omitted, as demonstrated in Figure 1.19.

For the rest of this thesis, the term *Ferrers filling* will refer to a strict 0-1 Ferrers filling, unless explicitly noted otherwise.

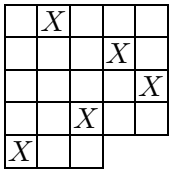

Figure 1.19: A strict 0-1 Ferrers filling

Given a permutation $\sigma \in S_n$, the *permutation matrix* of σ is a square $n \times n$ grid such that if $\sigma(i) = j$, then there is a mark in row i (counting from the left), column j (counting from the bottom). Clearly, a permutation matrix is a special case of a Ferrers filling. An example is given in Figure 1.20.

$$\begin{pmatrix} 1 & 2 & 3 & 4 & 5 \\ 1 & 5 & 2 & 4 & 3 \end{pmatrix}$$

(a) A permutation $\sigma = 15243$

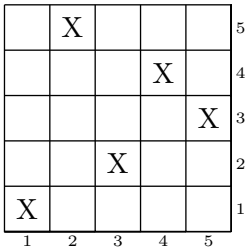

(b) The corresponding permutation matrix

Figure 1.20: An example of a permutation matrix, a special case of a strict 0-1 Ferrers filling

A matching is a permutation consisting solely of cycles of length two; such permutations must necessarily have an even number of elements. There is also a bijection between Ferrers fillings with n 1s, and matchings on $[2n]$, as implied by Krattenthaler [29] (theorem 1) and clarified by de Mier [12]. We supply our own proof here to emphasize the connection between the Ferrers filling and the permutation matrix of matchings.

Theorem 1.2. *Strict 0-1 Ferrers fillings with n 1s are in bijection with matchings on* $[2n]$.

Proof. A property of any matching μ is that if $\mu(i) = j$, then $\mu(j) = i$ and $i \neq j$. This means that the permutation matrix must be symmetric around the main diagonal, with no marks on the diagonal itself. Therefore, a matching can be represented by a triangular matrix with n marks, as shown in Figure 1.21b.

Removing the columns and rows which do not contain marks leaves a Ferrers filling. The mapping can be reversed by following the border from the lower-left corner to the upper-right corner as numbered in Figure 1.21c, inserting a blank row below each horizontal step, and a blank column to the right of every vertical step. □

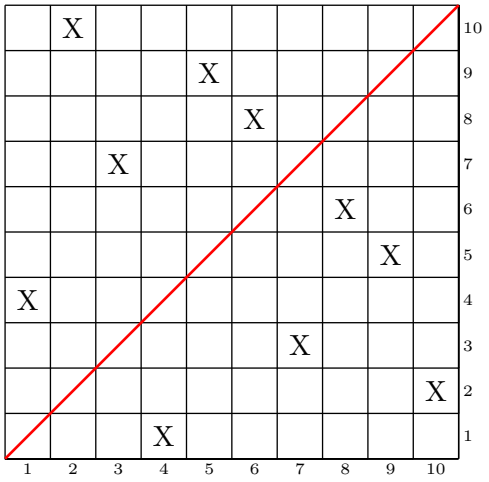

(a) The permutation matrix of a matching $\mu \in M_{10}$. The matrix is symmetric around the main diagonal, with no marks on the main diagonal

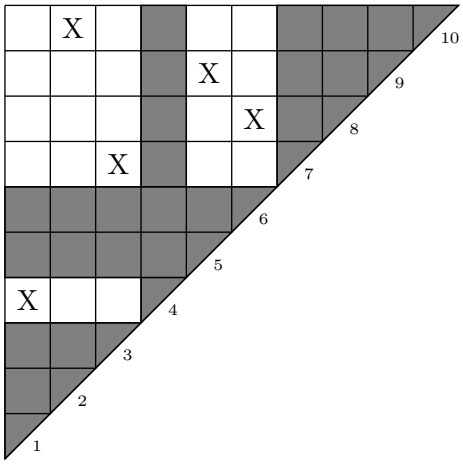

(b) The top half of the permutation matrix, with blank rows and columns highlighted. Every labeled diagonal step has a mark in the adjacent column or row, but not both

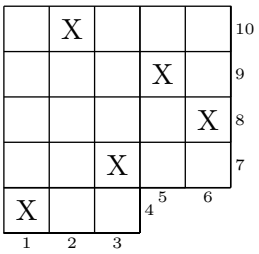

(c) The strict 0-1 Ferrers filling that remains after removing blank rows and columns

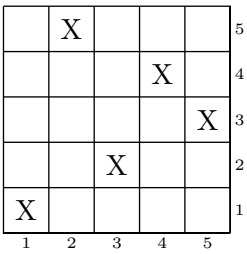

(d) The permutation matrix of $f(\mu) \in S_5$ (See comments following Theorem 1.3)

Figure 1.21: An example of the bijection between matchings on $[2n]$ and strict 0-1 Ferrers fillings with n marks

For any permutation σ, if $\sigma(i) > i$, i is referred to as an excedance. A matching $\mu \in M_{2n}$ must have exactly n excedances, corresponding to the smaller value in each of the n cycles of length 2. A matching β is a balanced matching if and only if it begins with n excedances ($\beta(i) > i$ for $1 \leq i \leq n$). This leads to a simple proof of the following well-known result.

Theorem 1.3. *BM_{2n} is in bijection with S_n.*

Proof. Note that if $\mu(i) > i$ in the bijection of Theorem 1.2, then the ith step along the border is horizontal, and otherwise it is vertical. Therefore the Ferrers filling of a balanced

matching $\beta \in BM_{2n}$ is a permutation matrix of some permutation $\sigma \in S_n$, and vice-versa.

The bijection between $\sigma \in S_n$ and $\beta \in BM_{2n}$ can also be described numerically:

$$\sigma(i) = j \iff \beta(i) = n + j \wedge \beta(n + j) = i \tag{1.4}$$

□

If $\sigma \in S_n$ is in bijection with $\beta \in BM_{2n}$, we use the following notations.

$$g(\sigma) = \beta$$
$$g^{-1}(\beta) = \sigma$$

Later, it will be useful to have an extension of this bijection to a surjection from M_{2n} to S_n. The Ferrers filling of a matching in M_{2n} has n marks, and thus necessarily has n rows and n columns. Thus, the Ferrers filling is contained within an $n \times n$ square, even if it is not a square.

Given a matching $\mu \in M_{2n}$, define $f(\mu)$ as follows. First form the corresponding Ferrers filling, and then extend the Ferrers filling to be an $n \times n$ square by adding blank cells. Let $\sigma \in S_n$ be the permutation corresponding to the resulting permutation matrix, and define $f(\mu) = \sigma$. Note that for $\beta \in BM_{2n}$, $f(\beta) = g^{-1}(\beta)$. Figure 1.21d gives an example.

There are actually deep connections between the arc diagram of a matching and its Ferrers filling, as illustrated in Figure 1.22.

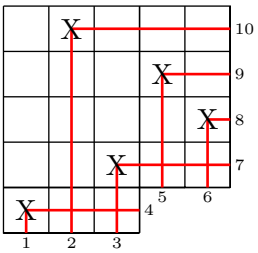

(a) Ferrers filling of $\mu \in M_{10}$, with arcs

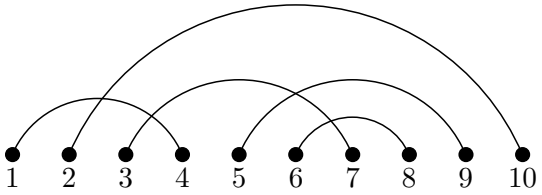

(b) The arc diagram of μ

Figure 1.22: The connection between Ferrers fillings and arc diagrams

When reading the border of the Ferrers filling from the lower left corner to the upper right corner as numbered, horizontal edges correspond to left endpoints in the arc diagram,

and vertical edges correspond to right endpoints. By connecting lines between the border and the marks, the arc diagram can be seen within the Ferrers filling.

1.5 Object Summary and Overview

1.5.1 Object Summary

Figure 1.23 summarizes some of the many objects and families of objects which are related to the study of arc diagrams, nestings, and crossings.

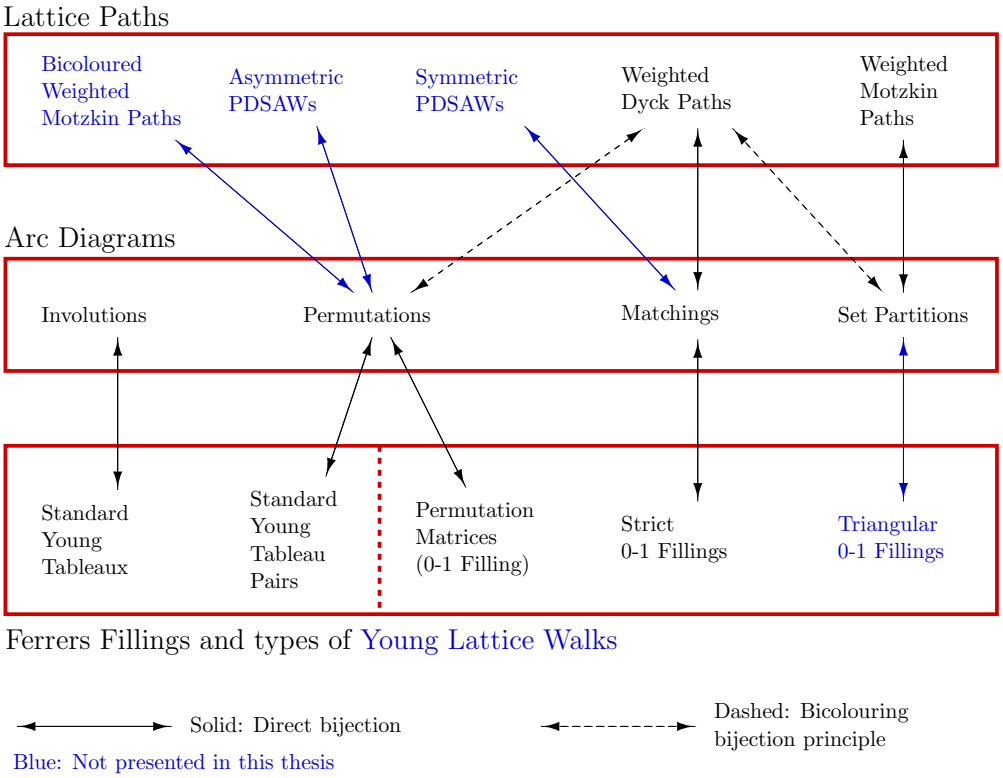

Figure 1.23: Some objects and their relationships

Many classical results involving Young tableaux revolve around the bijection between permutations (typically in their sequential form) and pairs of standard Young tableaux. This includes the work of Robinson [11], Schensted [38], Schützenberger [39], Knuth [27], Greene [22], and Reifegerste [35].

Chen et al. [8] use triangular 0-1 matrices to represent set partitions, and use an RSK-like algorithm to produce walks in Young's lattice which they term vacillating tableaux. They then use these objects to show the equidistribution of maximal nesting and maximal crossing for set partitions, among other results. Their main results were greatly generalized in terms of Ferrers fillings by Krattenthaler [29], whose work was further explored in terms of arc diagrams by de Mier [12].

Kasraoui and Zeng [26] use weighted Motzkin paths and weighted Dyck paths to show the equidistribution of (the total number of) nestings and crossings in set partitions and matchings. Corteel [10] then extended this work to permutations, and also showed connections to patterns in the sequential form of permutations.

Rubey [37] and Poznanović [33] also show connections between the nestings of matching and permutations and another type of lattice walk, partially-directed self-avoiding walks (PDSAWs).

The main result of this thesis involves the bijection between involutions and standard Young tableaux. Specifically, in Chapter 5 we show a direct correlation between nestings in the arc diagram of an involution and the shape of the associated tableau (Theorem 5.2). The result mirrors that of Greene [22], who showed the same connection between decreasing subsequences of a permutation and the shape of the associated tableaux.

In Section 2.4, we also find identities between statistics of families of objects that are in bijection, provided the bijection meets certain requirements. We term the requirements of the bijection and the resulting identities the bicolouring bijection principle, presented as Theorem 2.9. Concrete examples of such bijections are also presented, including bijections between a type of weighted Dyck path and derangements (singleton-free permutations), and also between a (different) type of weighted Dyck path and singleton-free set partitions (Sections 2.4.4 and 2.4.2 respectively).

1.5.2 Overview

The main goals of Section 2.1 are to set the stage for Sections 2.2–2.4, and to supply some tools for use later in the thesis. We present weighted Dyck paths and weighted Motzkin paths, as well as two bicolouring bijections between the two. We also present some surjections related to the bijections which are later used to prove some of the results in Chapter 5.

The bijections of Section 2.1 are part of a larger bicolouring bijection principle, which

gives identities between statistics of families of objects. The families of objects in the bicolouring bijection principle can be represented by sets of structures. Section 2.2 introduces sets of structures and shows their close connection to semilabeled structured trees, extending the results of Diaconis and Holmes [14], and of Erdös and Székely [15]. The cases for unlabeled and fully-labeled structured trees, also called enriched trees, have been studied by Labelle [31] and Bergeron et al. [3] in the context of combinatorial species. Series-reduced semilabeled plane trees and semilabeled unordered trees are also considered in [17], where they are called hierarchies.

Section 2.3 explores a system of statistics that applies to sets of structures. In Section 2.4 we develop the bicolouring bijection principle (Theorem 2.9) in terms of sets of structures and identities in terms of the statistics explored in Section 2.3. Concrete examples of bijections under the principle are also presented, which involve such well-known sequences as the Stirling numbers of the first and second kind, the second-order Eulerian numbers, and the Narayana numbers. Section 2.3 and Equation 2.30 include statistics of set partitions by the number of arcs in their arc diagram, which may be useful in the study of nestings and crossings. The other results of Sections 2.2–2.4 are not used outside of Chapter 2.

Chapter 3 examines the connection between the natural global transformations on permutations and global transformations on pairs of standard Young tableaux. The chapter is mainly a presentation of prior results by Robinson, Schensted, Schützenberger, and Knuth. However, four new variations of RSK (in addition to the four variations of Knuth) are also presented (Algorithm 3.4 and Theorem 3.3). The main result used in the following chapters is the classical result showing that involutions are in bijection with standard Young tableaux (Corollary 3.3.2).

In contrast, Chapter 4 examines local transformations of objects which preserve the shape of the corresponding tableaux. In particular, Knuth's classical result of Knuth transformations is explored. Knuth transformations relate local relationships and transformations in permutations to the global RSK correspondence. The results of Reifegerste [35] in describing these relationships in terms of Young tableaux are clarified (Theorem 4.2), and used to present involutive transformations in Section 4.2. Involutive transformations are local relationships and transformations in arc diagrams, analogous to Knuth transformations in permutations. Involutive transformations provide the main tool for proving the results of Chapter 5, and are also used in parts of Chapter 6. Figure 4.11 provides an exhaustive enumeration of involutive transformations in terms of arc diagrams.

Chapter 5 presents our main result, a Greene-like correspondence for the arc diagrams of involutions. In particular, Theorem 5.2 shows that the nestings of an involution correspond to the shape of its Young tableau under RSK. The result is important in that it shows a direct connection between the nestings of an object and the RSK shape of the same object, for involutions. The result is then extended to set partitions for both the weak and strong nesting interpretations (Corollary 5.5.2), giving an extension of one of the results of Chen et al. [8].

Chapter 6 examines graphs on all Young tableaux of the same shape implied by the results of Chapter 4. The results of Reifegerste [35] indicate that these graphs are in fact lattices. Some properties of these graphs for specific shapes are explored in Section 6.3.

Finally, Chapter 7 notes topics touched upon in this thesis that could be fruitful areas for further research.

Chapter 2

Bijections and Surjections

In this chapter, we present a number of bijections and surjections on set partitions, matchings, permutations, and related objects.

Section 2.1 introduces weighted Dyck paths and weighted Motzkin paths, and uses them to define bijections and surjections which will be useful in Chapter 5. In particular, two surjections are defined from set partitions to involutions which preserve all nestings. This will allow us to extend results on involutions in Chapter 5 to set partitions. Two surjections from set partitions to matchings are also defined: one which preserves strong nestings and crossings, and one which preserves weak nestings and crossings. These surjections will allow us to state the results of Chapter 5 in terms of either strong nestings or strong crossings, as is conventional.

The bijections are defined between weighted Dyck paths with bicoloured peaks or valleys and weighted Motzkin paths. They are part of a larger picture of bijections related to sets of structures. Section 2.2 sets the stage by presenting new bijections between sets of structures and semilabeled trees and forests. The contents of this section are related to the study of combinatorial species and enriched trees, as presented by Labelle [31] and Bergeron et al. [3]. Section 2.3 explores the statistics of these families of objects.

Finally, Section 2.4 presents a general bicolouring bijection principle (Theorem 2.9) which gives identities between the statistics of families of objects, such as matchings and singleton-free set partitions. The bicolouring bijection principle encompasses the bijections of Section 2.1. Examples of bijections encompassed by the principle are also presented, including some new combinatorial interpretations of known identities (Equations 2.31 and 2.35). The identities include such well-known sequences as the Stirling numbers of the first and second

kind, the second-order Eulerian numbers, and the Narayana numbers.

Section 2.3 and Equation 2.30 include statistics of set partitions by the number of arcs in their arc diagram, which may be useful in the study of nestings and crossings. The other results of Sections 2.2–2.4 are not used outside of this chapter.

2.1 Weighted Dyck and Motzkin Paths

2.1.1 Weighted Dyck Paths

As noted in Section 1.4, when reading the border of a Ferrers filling from the bottom left corner to the top right corner, horizontal edges correspond to left endpoints in the arc diagram and vertical edges correspond to right endpoints. Every right endpoint is connected by an arc to a preceding left endpoint. Therefore, the number of vertical edges seen during the reading never exceeds the number of horizontal edges seen.

This shows that the shape of a Ferrers filling with n marks describes a *Dyck path* of semilength n. A Dyck path of semilength n is a walk from $(0, 0)$ to $(2n, 0)$ using only up steps $(1, 1)$ and down steps (1,-1), and never going below the x-axis. A step with its lowest point at (x, y) has *height* y. There are necessarily n up steps and n down steps. Figure 2.1 gives an example.

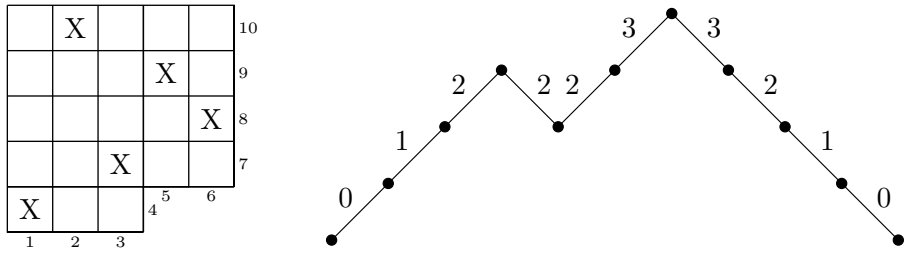

Figure 2.1: A Ferrers filling and the Dyck path that the border of the Ferrers filling describes. The Dyck path has steps (from left to right) up, up, up, down, up, up, down, down, down, down. The steps are labeled with their heights

A *weighted Dyck path* is a Dyck path in which each down step with height h has been given a weight w such that $0 \leq w \leq h$. Figure 2.2 gives an example.

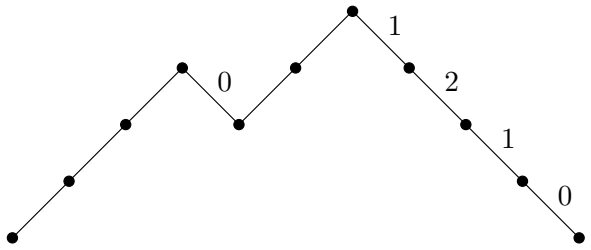

Figure 2.2: A weighted Dyck path

It is well-known that weighted Dyck paths correspond to matchings; see, for example, [16]. Figure 2.3 demonstrates the bijection. Kasraoui and Zeng [26] explore the bijection in more detail.

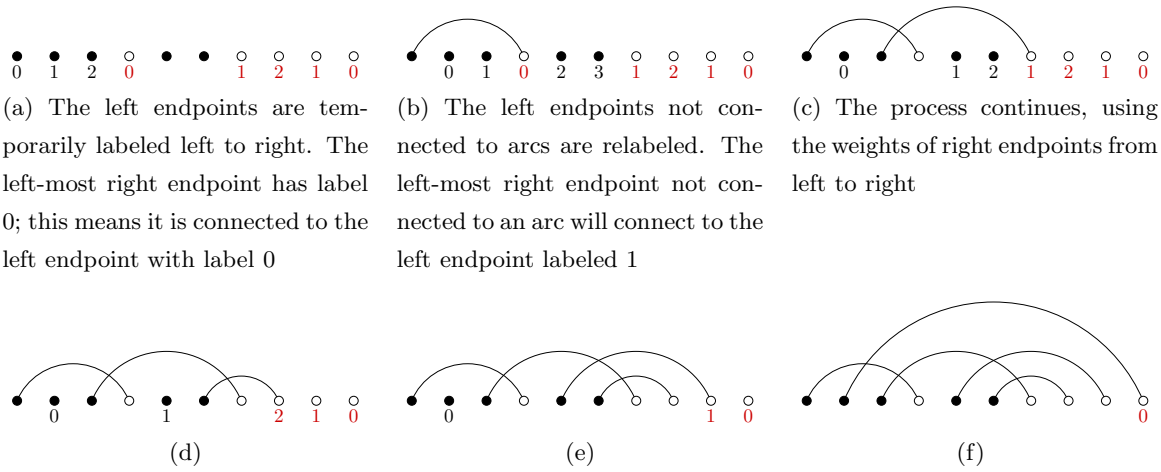

(a) The left endpoints are temporarily labeled left to right. The left-most right endpoint has label 0; this means it is connected to the left endpoint with label 0

(b) The left endpoints not connected to arcs are relabeled. The left-most right endpoint not connected to an arc will connect to the left endpoint labeled 1

(c) The process continues, using the weights of right endpoints from left to right

Figure 2.3: Construction of a matching from the weighted Dyck path in Figure 2.2. The up and down steps of the Dyck path indicate which vertices are left endpoints (black) and right endpoints (white). The right endpoints are labeled with their weights

Note that up steps in the weighted Dyck path correspond to left endpoints in the arc diagram, and down steps to right endpoints.

The weighted Dyck path of a matching can easily be recovered from the Ferrers filling, as demonstrated in Figure 2.4.

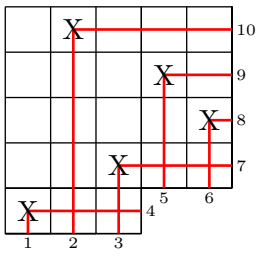

(a) The Ferrers filling in bijection with the matching of Figure 2.3f

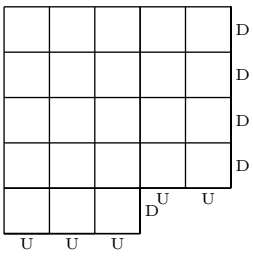

(b) The shape describes a Dyck path

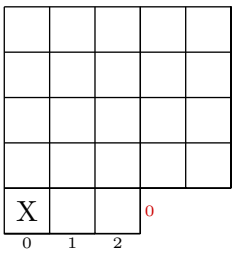

(c) There are three columns in the bottom row. The mark goes in column 0

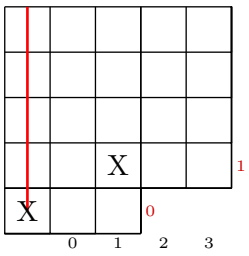

(d) In the next row, there are four unfilled columns. The mark goes in column 1

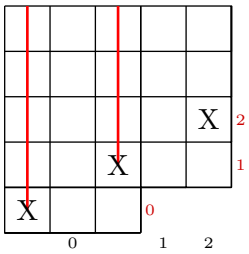

(e) There are three unfilled columns, and the mark goes in column 2

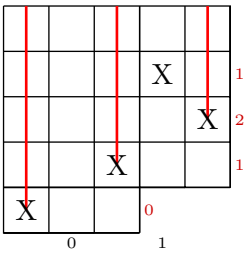

(f) There are two unfilled columns, and the mark goes in column 1

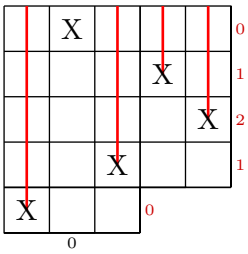

(g) There is only one unfilled column for the last mark, column 0

Figure 2.4: Construction of a weighted Dyck path from a Ferrers filling by filling rows from bottom to top, weighting the down steps. The result (Figure 2.4g) is the weighted Dyck path of Figure 2.2

For each weight w on a down step at height h, define the *complementary weight* to be $h - w$. Kasraoui and Zeng [26] proved that the sum of the weights in a weighted Dyck path equals the number of nestings in the corresponding arc diagram, and that the sum of the complementary weights is the number of crossings. It immediately follows that for every matching with n nestings and c crossings, there is a matching with c nestings and n crossings, as demonstrated in Figure 2.5.

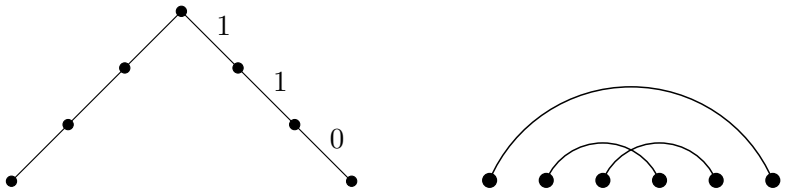

(a) A weighted Dyck path and the corresponding matching, with 2 nestings and 1 crossing

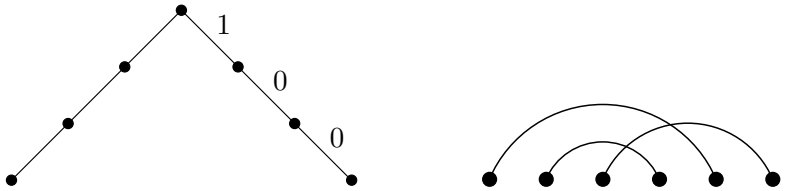

(b) The weighted Dyck path with complemented weights, having 1 nesting and 2 crossings

Figure 2.5: Exchanging the number of nestings and crossings in a matching

2.1.2 Weighted Motzkin Paths

A *Motzkin path* is a generalization of a Dyck path. A Motzkin path of length n is a walk from $(0, 0)$ to $(n, 0)$ with up steps $(1, 1)$, down steps $(1, -1)$ and horizontal steps $(1, 0)$. Like a Dyck path, a Motzkin path cannot go below the x-axis.

A *weighted Motzkin path* is a Motzkin path in which each down or horizontal step with height h has been given a weight w such that $0 \leq w \leq h$. As weighted Dyck paths are in bijection with matchings, weighted Motzkin paths are in bijection with set partitions. The bijection is very similar to that between weighted Dyck paths and matchings, illustrated in Figure 2.3 above. A horizontal step with maximum weight corresponds to a singleton, and a horizontal step with non-maximal weight corresponds to a transitory vertex. In terms of the construction, horizontal steps with non-maximal weight behave both like down steps (with the weight determining which arc connects to the left of the vertex), and like up steps (with another arc connected to the right of the vertex). Figure 2.6 gives an example.

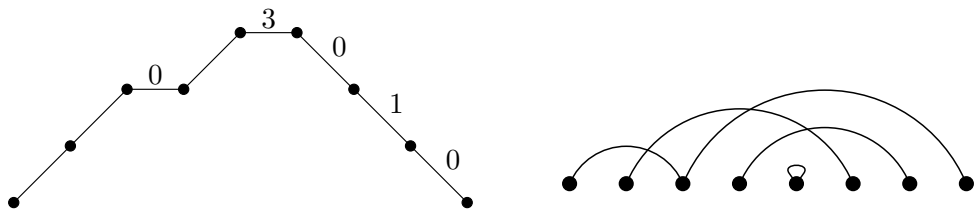

Figure 2.6: A weighted Motzkin path and the corresponding set partition

Note: An alternative representation that appears in the literature is to have two colours of horizontal steps, one colour for singletons (which are unweighted) and another for transitory vertices (which can never have maximal weight). The results for nestings and crossings that apply to matchings also apply to set partitions, for both weak nestings and crossings, and strong nestings and crossings. Details can be found in Kasraoui and Zeng's paper [26] and in Corteel's paper [10] regarding permutations.

2.1.3 Bijections

In this section, we present two simple bijections between weighted Dyck paths with bi-coloured points and weighted Motzkin paths. First, some terminology related to Dyck paths is required. A Dyck path with semilength n has n up steps, n down steps, and $2n-1$ places strictly between the steps. The places between steps are categorized as *peaks*, *valleys*, *strong rises*, or *strong falls* as demonstrated in Figure 2.7. Two up steps correspond to a strong rise, two down steps to a strong fall, an up step followed by a down step is a peak, and a down step followed by an up step is a valley. For matchings, we apply the same labels to places inbetween the vertices based on the corresponding weighted Dyck path. (Recall that left endpoints correspond to up steps, and right endpoints to down steps.)

Figure 2.7: Objects with labeled strong rises (r), peaks (p), valleys (v), and strong falls (f). For clarity, left endpoints in the arc diagram are coloured black, and right endpoints, white

If a Dyck path has semilength n and p peaks, then it also has $p-1$ valleys, $n-p$ strong rises, and $n-p$ strong falls. Deutsch [13] provides a deeper study of these statistics.

We are now ready for the bijections. (While we are unaware of any specific citation for these bijections, those familiar with weighted Dyck paths and weighted Motzkin paths will find them intuitive. The approach of these bijections in terms of arc diagrams is the same that de Mier [12] (Lemma 3.4) uses for a more general family of arc diagrams.)

Proposition 2.1. *There is a bijection between weighted Dyck paths with bicoloured peaks and weighted Motzkin paths, such that if a Dyck path has semilength n and has k coloured peaks, the corresponding Motzkin path has length $2n-k$ and exactly k horizontal steps.*

Proof. The bijection simply replaces the up step and down step of a peak at height h with a horizontal step at height h, preserving the weight of the down step. Figure 2.8 gives an example. The reverse mapping is trivial. The horizontal step has the same height as the original down step, and thus the same range of weights is possible for both steps. □

In terms of arc diagrams, Proposition 2.1 induces a bijection between matchings with bicoloured peaks and set partitions. Note that the number of arcs is preserved, as illustrated in Figure 2.8. Additionally, weak crossings and weak nestings are preserved. The exact transformation in terms of arc diagrams is explored more deeply in the following section.

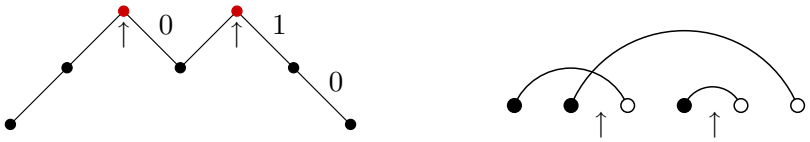

(a) A weighted Dyck path with two coloured peaks, and the corresponding matching

(b) The weighted Motzkin path after applying the bijection of Proposition 2.1, and the corresponding set partition

Figure 2.8: An illustration of Proposition 2.1

Proposition 2.2. *There is a bijection between weighted Dyck paths with bicoloured valleys and weighted Motzkin paths where all horizontal steps have non-maximal weight, such that*

if a Dyck path has semilength n and has k coloured valleys, the corresponding Motzkin path has length $2n-k$ and exactly k horizontal steps.

Proof. The bijection simply replaces the down step and up step of a valley at height h with a horizontal step at height $h+1$, preserving the weight of the down step. Figure 2.9 gives an example. The reverse mapping is trivial. As the height of the horizontal step is one higher than that of the original down step, the horizontal step never has maximal weight. This also forbids horizontal steps at height 0. □

In terms of arc diagrams, Proposition 2.2 is a bijection between matchings with bi-coloured valleys and singleton-free set partitions. Note that the number of arcs is preserved, as illustrated in Figure 2.9. Additionally, strong crossings and nestings are preserved.

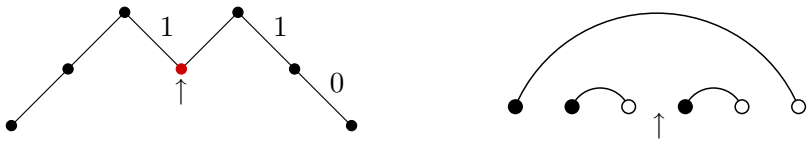

(a) A weighted Dyck path with a coloured valley, and the corresponding matching

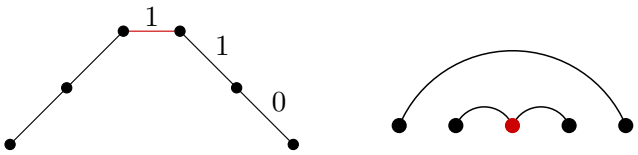

(b) The weighted Motzkin path after applying the bijection of Proposition 2.2, and the corresponding singleton-free set partition

Figure 2.9: An illustration of Proposition 2.2

2.1.4 Surjections

The bijections of Propositions 2.1 and 2.2 have useful properties when translated into the arc diagrams of matchings and set partitions. In particular, Proposition 2.1 preserves weak crossings and nestings, Proposition 2.2 preserves strong crossings and nestings, and both preserve the number of arcs, as will be illustrated below. The surjections are used in Chapter 5 to extend results on involutions to set partitions, for both the weak and strong interpretations.

We define two surjections from set partitions with k transitory vertices to involutions,

$\check{\eta} : P_{n+k} \to I_{n+2k}$ and $\hat{\eta} : P_{n+k} \to I_{n+2k}$. Let $\check{\eta}$ be defined by "breaking apart" transitory vertices into a right endpoint followed by a left endpoint, and let $\hat{\eta}$ be defined by instead breaking apart transitory vertices into a left endpoint followed by a right endpoint. Figure 2.10 gives examples.

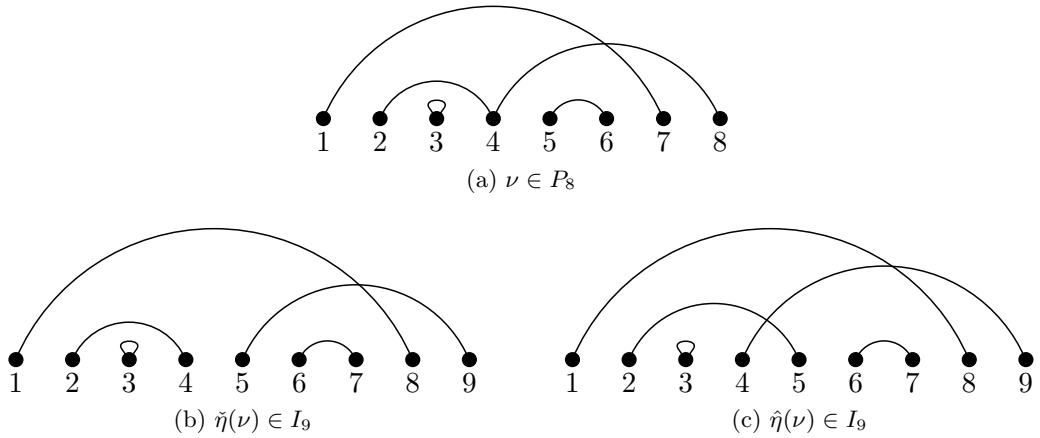

(a) $\nu \in P_8$

(b) $\check{\eta}(\nu) \in I_9$

(c) $\hat{\eta}(\nu) \in I_9$

Figure 2.10: Examples of the surjections from set partitions to involutions

In terms of the corresponding weighted Motzkin paths, $\check{\eta}$ turns horizontal steps with non-maximal weight into a valleys (analogous to Proposition 2.2), and $\hat{\eta}$ turns them into peaks (analogous to Proposition 2.1). Additionally, $\check{\eta}$ preserves strong crossings (as the arcs attached to transitory vertices become unambiguously non-crossing), and $\hat{\eta}$ preserves weak crossings (as the arcs attached to transitory vertices become unambiguously crossing). As the only changes are at transitory vertices, both surjections also preserve all nestings (weak and strong). The number of arcs is also preserved.

We also define two surjections from involutions with k singletons to matchings, $\check{h} : I_{n+s} \to M_n$ and $\hat{h} : I_{n+s} \to M_{n+2s}$. Let $\check{h}$ be defined by removing singletons, and let $\hat{h}$ be defined by turning singletons into a left endpoint and right endpoint connected by an arc.

In terms of the corresponding weighted Motzkin paths, $\check{h}$ removes horizontal steps with maximal weight, while $\hat{h}$ turns them into peaks (analogous to Proposition 2.1). Note that $\check{h}$ preserves strong nestings (as singletons are removed), while $\hat{h}$ preserves weak nestings (by making singletons into arcs between two vertices). Additionally, and both preserve all crossings. The number of arcs is also preserved by $\hat{h}$.

These surjections are extended to set partitions by letting $\check{h}(\nu) = \check{h}(\check{\eta}(\nu))$ and $\hat{h}(\nu) =$

$\hat{h}(\hat{\eta}(\nu))$ for any set partition ν. Figure 2.11 gives examples.

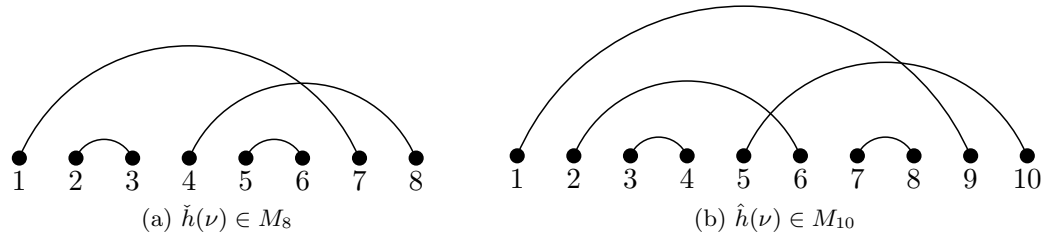

(a) $\check{h}(\nu) \in M_8$ (b) $\hat{h}(\nu) \in M_{10}$

Figure 2.11: Examples of the surjections to matchings. (ν is shown in Figure 2.10)

Note that $\hat{h}(\nu)$ corresponds to the bijection of Proposition 2.1. The bijection of Proposition 2.2 is between matchings and singleton-free set partitions; if ν is a singleton-free set partition, then $\check{h}(\nu) = \check{\eta}(\nu)$ corresponds to the bijection of Proposition 2.2.

The usefulness of these surjections stems from their property of preserving weak or strong nestings and crossings. Given a set partition ν, $\hat{h}(\nu)$ gives a matching with the same weak k-nestings and k-crossings. Similarly, $\check{h}(\nu)$ gives a matching with the same strong k-nestings and k-crossings. Therefore proofs regarding nestings and crossings of matchings can often be automatically extended to set partitions. This is the same approach as de Mier [12] (Lemma 3.4) uses for strict nesting and crossing in the more general context of general Ferrers fillings and singleton-free arc diagrams.

Finally, we follow Chen et al.'s lead and define surjections from set partitions to permutations. Recall the surjection $f : M_{2n} \to S_n$ from Section 1.4, wherein the Ferrers filling of a matching is extended to be a permutation matrix. We define two surjections $\check{f} : P_{n+j+k} \to S_{(n+2j)/2}$ and $\hat{f} : P_{n+j+k} \to S_{(n+2j+2k)/2}$ by letting $\check{f}(\nu) = f(\check{h}(\nu))$ and $\hat{f}(\nu) = f(\hat{h}(\nu))$ for any set partition ν having j transitory vertices and k singletons. Note that for $\mu \in M_{2n}$, $\check{f}(\mu) = \hat{f}(\mu) = f(\mu)$.

Chen et al. [8] (Proposition 8) define a similar surjection from set partitions to matchings, $\alpha(\nu)$. Our definition of $\check{f}$ is such that $\check{f}(\nu) = \alpha(\nu)^{-1}$. $\check{f}$ and $\hat{f}$ will be used in Chapter 5 to give an alternate proof of the results of Chen et al. [8] (Proposition 8 and Corollary 9), which involve the strong nesting interpretation, as well as the analogous result for the weak nesting interpretation (Corollary 5.5.2).

2.2 Structured Trees and Forests

In [15], Erdös and Székely present a bijection between unordered trees with labeled leaves and set partitions. Diaconis and Holmes later [14] gave a similar bijection between matchings and binary unordered trees with labeled leaves. In this chapter, we show how these bijections can be extended to combinatorial objects other than unordered trees and set partitions.

The particular families of objects we consider in this section are semilabeled structured forests, semilabeled structured trees, and sets of structures. The related families of unlabeled and fully-labeled structured trees, also called enriched trees or R-enriched trees, have been studied by Labelle [31] and Bergeron et al. [3] in the context of combinatorial species. Series-reduced semilabeled plane trees and series-reduced semilabeled unordered trees are also considered by Flajolet and Sedgewick in [17], where they are called hierarchies. Series-reduced semilabeled unordered trees are also known as phylogenetic trees. Taking sets of structures (cycles, sequences, ...) is a common theme in combinatorics, as also seen in [3, 17].

2.2.1 Notations and Terminology

A set partition can be viewed as a set of parts; each part is itself a set. A permutation can similarly be seen as a set of cycles. In this section, a *structure* is any arrangement of labeled objects, such as a set or cycle. The internals of the structure will not matter for the bijections presented; we need only be concerned with how many distinct structures there are for a given size. Let $\phi(k)$ be the number of structures given an underlying set of size k. For sets, $\phi(k) = 1$; for cycles, $\phi(k) = (k-1)!$. Structures of size 1 are referred to as *singletons*, and structures of size greater than 1 are called *non-singleton structures* or *NSS*s.

The bijections will involve sets of structures and *semilabeled structured trees* (and forests). A semilabeled tree is a rooted tree with labeled leaves (but unlabeled internal nodes). A structured tree is a rooted tree wherein a structure is imposed on all siblings except the root. For example, a tree structured by sets is an unordered tree (as the order of siblings is irrelevant), while a tree structured by sequences is a plane (ordered) tree (as the order of siblings is completely relevant). Sometimes the trees will be restricted to *series-reduced* trees, meaning that there are no internal nodes with only one child. A forest is considered to be a *set* of trees, regardless of the structure imposed on the trees. Figure 2.12 gives examples.

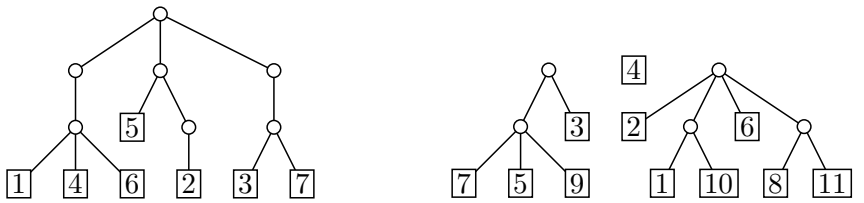

(a) A semilabeled tree (b) A semilabeled series-reduced forest

Figure 2.12: Examples of semilabeled objects

2.2.2 The Bijections

Here, we present two similar bijections which are both extensions of mappings given by Diaconis and Holmes [14]. The first bijection is an alternative to that of Erdös and Székely [15], and transports the same statistics. The second bijection is a variant of the first, using series-reduced forests in place of trees; as it is more constrained ($\phi(1)$ must be 1), we state the theorem separately. It is also interesting to note that in general, the bijections do not preserve the number of labels.

Theorem 2.1. *For any structure, there is a bijection between semilabeled structured trees and sets of structures such that for all $k > 0$, the number of internal nodes with k children in the tree is the same as the number of structures of size k in the corresponding set of structures.*

Theorem 2.1 clearly implies that the number of internal nodes in a tree is the same as the number of structures in the corresponding set of structures. Because every node in the tree except the root has one parent, Theorem 2.1 also implies that the number of nodes in the tree is one greater than the number of elements in the corresponding set of structures.

Theorem 2.2. *For any structure with $\phi(1) = 1$, there is a bijection between semilabeled series-reduced structured forests and sets of structures such that for all $k > 1$, the number of internal nodes with k children in the forest is the same as the number of structures of size k in the corresponding set of structures. Additionally, the number of trees in the forest is one greater than the number of singleton structures in the corresponding set of structures.*

Theorem 2.2 clearly implies that the number of internal nodes in a tree is the same as the number of NSSs in the corresponding set of structures. Because every node in the forest

except the roots have one parent, and because the number of singletons is one less than the number of roots (trees), Theorem 2.2 also implies that the number of nodes in the forest is one greater than the number of elements in the corresponding set of structures.

Note that the theorems are identical when considering only singleton-free sets of structures.

The two theorems can be combined to give the following corollary.

Corollary 2.2.1. *For any structure with $\phi(1) = 1$, there is a bijection between semilabeled series-reduced structured forests and semilabeled structured trees such that for all $k > 1$, the number of internal nodes with k children in the forest is the same as the number of internal nodes with k children in the corresponding tree. Additionally, the number of trees in the forest is one greater than the number of internal nodes with 1 child in the corresponding tree.*

The corollary implies that the forest and the tree have the same number of nodes, but not necessarily the same number of leaves (or internal nodes).

Proof. The proofs are constructive. For both bijections, the labeling is first extended to the entire forest (tree) by the following algorithm.

Algorithm 2.1 Extending the labeling of a semilabeled forest

Let F_v and F_l be the number of nodes and leaves in the forest, respectively
Let $k \leftarrow F_l + 1$
while $k \leq F_v$ **do**
  Let u be the node which
  1. is unlabeled,
  2. has no unlabeled children,
  3. has the child with the leastmost value out of all nodes satisfying the previous two requirements

  Label u with k
  Let $k \leftarrow k + 1$
end while

The result of the algorithm is a fully-labeled decreasing forest with certain properties enforced by the method of labeling, as shown in Figure 2.13.

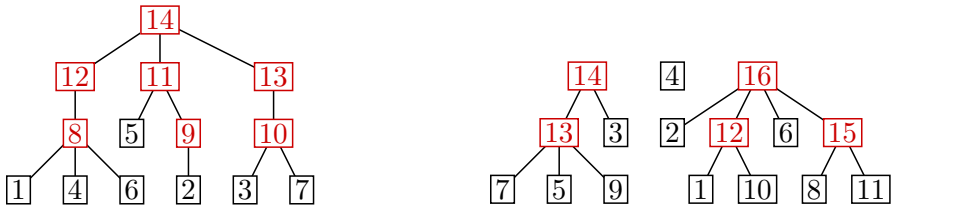

(a) A tree with extended labeling (b) A series-reduced forest with extended labeling

Figure 2.13: Extended labeling of the objects from Figure 2.12

For the bijection of Theorem 2.1, the structures of the tree, now fully-labeled, become the set of structures. The root is omitted.

For the bijection of Theorem 2.2, the structures of the forest, now fully-labeled, become the NSSs in the set of structures. Each root *except* for the one with the highest value become singletons in the set of structures. (The correspondence between roots (which are not structured) and singletons is the reason why $\phi(1)$ must be 1 for this bijection.)

Figure 2.14 gives examples, using sets as the structures.

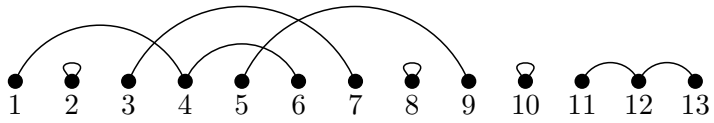

(a) The set partition corresponding to Figure 2.13a

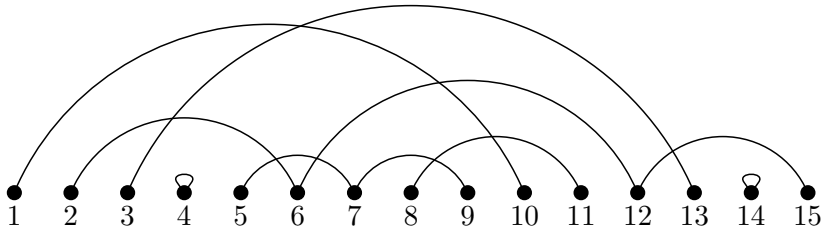

(b) The set partition corresponding to Figure 2.13b

Figure 2.14: Set partitions corresponding to Figure 2.13

Recovering the forest (or tree) from the set of structures is accomplished by constructing the decreasing forest from the set of structures. The constructions are similar for both bijections.

Algorithm 2.2 Recovering the decreasing tree of Algorithm 2.1

Let G_v and G_b be the number of elements and structures in the set of structures, respectively

Let $k \leftarrow G_v - G_b + 2$

$\{k-1$ is the number of leaves in the tree$\}$

while $k \leq G_v + 1$ **do**

Let s be the structure that

1. has not yet been chosen,
2. consists of elements strictly less than k,
3. has the element with the leastmost value out of all structures satisfying the previous two requirements

Give s the parent k in the tree

Let $k \leftarrow k + 1$

end while

We need to show that we can always find an appropriate structure s in Algorithm 2.2. Namely, there must be at least c structures with largest element $\leq G_v - G_b + c$ for $1 \leq c \leq G_b$. When $c = G_b$, there are trivially G_b structures with largest element $\leq G_v$. Next consider $c = G_b - i$. There are exactly i vertices greater than $G_v - i$, so there are at most i structures with an element greater than $G_v - i$. This implies that there are at least $G_b - i = c$ structures with an element less than or equal to $G_v - i$, and the condition is still satisfied.

In Algorithm 2.2, the method of choosing parents mirrors the method of labeling in Algorithm 2.1; the labels of the internal nodes are determined completely by the labels of the leaves. Discarding the labels of internal nodes results in a semilabeled structured tree.

Figure 2.15 gives an example of Algorithm 2.2, using sets as the structure.

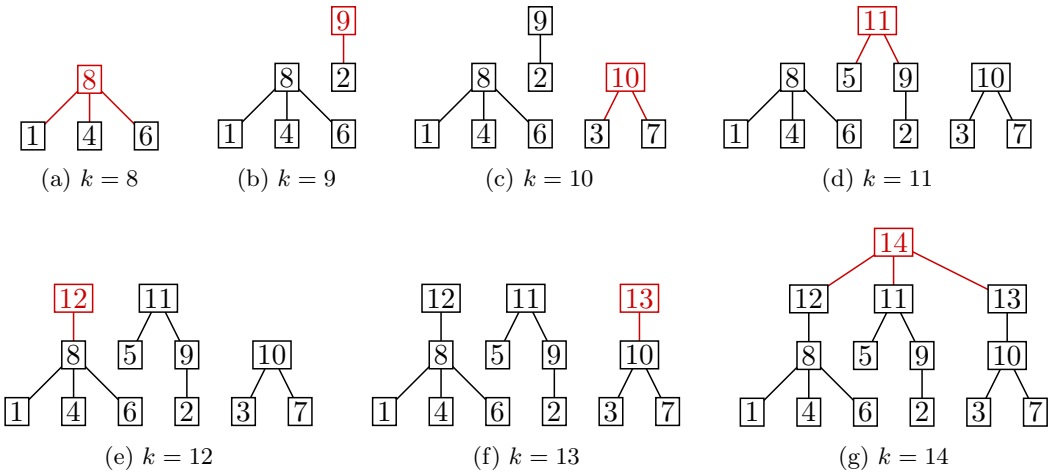

Figure 2.15: Recreating the tree from the set partition of Figure 2.14a

---

Algorithm 2.3 Recovering the decreasing series-reduced forest of Algorithm 2.1

Let G_v and G_h be the number of elements and NSSs in the set of structures, respectively

Let $k \leftarrow G_v - G_h + 2$

$\{k - 1$ is the number of leaves in the forest$\}$

Add all singletons with value $< k$ as trees of size 1 in the forest

while $k \leq G_v + 1$ **do**

Let s be the NSS that

1. has not yet been chosen,
2. consists of elements strictly less than k,
3. Has the element with the leastmost value out of all NSSs satisfying the previous two requirements

Give s the parent k in the forest

Let $k \leftarrow k + 1$

end while

We need to show that we can always find an appropriate NSS s in Algorithm 2.3. Namely, there must be at least c NSSs with largest element $\leq G_v - G_h + c$ for $1 \leq c \leq G_h$. When $c = G_h$, there are trivially G_h NSSs with largest element $\leq G_v$. Next consider $c = G_h - i$.

There are exactly i vertices greater than $G_v - i$, so there are at most i NSSs with an element greater than $G_v - i$. This implies that there are at least $G_h - i = c$ NSSs with an element less than or equal to $G_v - i$, and the condition is still satisfied.

In Algorithm 2.3, the method of choosing parents mirrors the method of labeling in Algorithm 2.1; the labels of the internal nodes are determined completely by the labels of the leaves. Discarding the labels of internal nodes results in a semilabeled series-reduced structured forest.

Figure 2.16 gives an example of Algorithm 2.3, using sets as the structure.

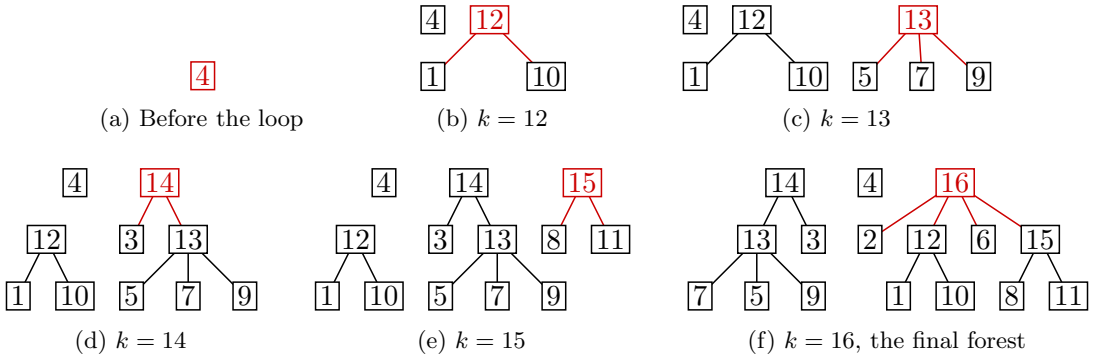

Figure 2.16: Recreating the forest from the set partition of Figure 2.14b

Note that at no point do the constructions rely on the internals of the structures. Structures are merely preserved on both sides of each bijection. □

The results presented in this section, namely bijections between semilabeled structured trees and structured arc diagrams, can be related to the Lagrange formal power series inversion formula (see [31] for example). This formula is one of the main tools to enumerate tree-like structures where all nodes are labeled (fully-labeled trees). The main combinatorial proofs rely on bijections between fully-labeled structured trees and structured sequential structures (endofunctions or words) [31, 34]. These bijections are very similar, both in principle and in their properties, to the bijections we described here. It would then be interesting to investigate the use of our bijections in the inversion of formal power series and in the extraction of the coefficients of the generating functions of semilabeled structured trees.

2.3 Statistics

In this section, we describe two methods of enumerating statistics on sets of structures, both in terms of the number of elements in the set of structures, and in terms of the number of labeled leaves in the corresponding semilabeled structured trees and series-reduced forests.

2.3.1 Statistics on Sets of Structures

We are mainly interested in the number of sets of k structures over n total elements, which we denote as $V_b(n,k)$. Another important statistic is the number of singleton-free sets of k structures over n total elements. We define this statistic as $V_b^0(n,k)$.

Other statistics include the number of of sets of structures on n elements with k singletons ($V_s(n,k)$), those with k NSSs ($V_h(n,k)$), and those with k NSSs and l singletons ($V(n,k,l)$).

The following theorem gives recursive identities for these statistics, using the classical approach of counting the ways to add a new structure to an existing set of structures.

Theorem 2.3.

$$V_b(n,k) = \sum_i \phi(i)\binom{n-1}{i-i}V_b(n-i,k-1) \tag{2.1}$$

$$V_b^0(n,k) = \sum_{i>1} \phi(i)\binom{n-1}{i-i}V_b^0(n-i,k-1) \tag{2.2}$$

$$V_s(n,k) = \phi(1)V_s(n-1,k-1)+\sum_{i>1} \phi(i)\binom{n-1}{i-1}V_s(n-i,k) \tag{2.3}$$

$$V_h(n,k) = \phi(1)V_h(n-1,k)+\sum_{i>1} \phi(i)\binom{n-1}{i-1}V_h(n-i,k-1) \tag{2.4}$$

$$V(n,k,l) = \phi(1)V(n-1,k,l-1)+\sum_{i>1} \phi(i)\binom{n-1}{i-1}V(n-i,k-1,l) \tag{2.5}$$

Proof. These statistics can be generated recursively by counting the number of sets of structures in which the largest element is in a structure of size i. To illustrate for $V_b(n,k)$, we first choose $i-1$ of the smaller $n-1$ elements to be part of the structure. Next, there are $\phi(i)$ structures involving the chosen i elements. Finally, there are $V_b(n-i,k-1)$ ways to arrange the remaining $k-1$ structures amongst the remaining $n-i$ elements.

For the first summation, i may take any non-zero value. However, the summand is 0 when $i<0$, so we can leave the index unrestricted. For the second equation, i must be larger than 1, as singletons are forbidden.

The other statistics follow similarly. For example, the term $\phi(1)V_s(n-1,k-1)$ in the recursion for $V_s(n,k)$ covers the case when the largest element is a singleton, and the remaining summation covers all other sizes. □

With the additional observation that there are only $\phi(1)$ ways to create a single set of structures from a single element, Theorem 2.3 implies that all of the statistics discussed can be calculated from ϕ alone.

We also define the statistics in terms of $V_b^0(n,k)$, as there are some situations where the recursive approach cannot be applied. Similar to the preceding theorem, this is a classical combinatorial technique.

Theorem 2.4.

$$V(n,k,l) = \phi(1)^l \binom{n}{l} V_b^0(n-l,k) \tag{2.6}$$

$$V_b(n,k) = \sum_i \phi(1)^i \binom{n}{i} V_b^0(n-i,k-i) \tag{2.7}$$

$$V_h(n,k) = \sum_i \phi(1)^i \binom{n}{i} V_b^0(n-i,k) \tag{2.8}$$

$$V_s(n,k) = \phi(1)^k \binom{n}{k} \sum_i V_b^0(n-k,i) \tag{2.9}$$

Proof. Equation 2.6 comes from choosing l of the n elements to be singletons, and then arranging the remaining $n-l$ elements into k NSSs. Equation 2.7 builds on Equation 2.6 by holding the total number of structures constant and sums over varying numbers of singletons. Equation 2.8 similarly holds the number of NSSs constant and sums over the number of singletons, and Equation 2.9 holds the number of singletons constant and sums over the number of NSSs.

The derivation of all four equations can be seen as adding singletons to a singleton-free set of structures. □

2.3.2 Statistics on Semilabeled Structured Trees

It is natural to enumerate labeled objects by the number of labels. In the case of semilabeled trees (and forests), this is the number of leaves. In this section, we consider the statistics of semilabeled series-reduced structured trees with n leaves and k internal nodes ($E_p^0(n,k)$), semilabeled structured trees with n leaves and k internal nodes ($E_p(n,k)$), those with n

leaves and k internal nodes with one child ($E_s(n,k)$), and those with n leaves and k internal nodes, l of which have one child ($E(n,k,l)$).

The bijection of Theorem 2.1 allows us to translate the classical results of the previous section to semilabeled structured trees.

Theorem 2.5.

$$E_p^0(n,k) = V_b^0(n+k-1,k) \tag{2.10}$$

$$E_p(n,k) = V_b(n+k-1,k) \tag{2.11}$$

$$E(n,k,l) = V(n+k-1,k-l,l) \tag{2.12}$$

Proof. In all three cases, the number of leaves (n) and the number of internal nodes (k) is known, and by the bijection of Theorem 2.1 these objects correspond to sets of structures with $n+k-1$ elements and k structures. □

Note that in the case of $E_s(n,k)$, the total number of internal nodes (and thus the number of nodes) is not known. However, we can also describe statistics in terms of $E_p^0(n,k)$.

Theorem 2.6.

$$E_p(n,k) = \sum_i \phi(1)^i \binom{n+k-1}{i} E_p^0(n,k-i) \tag{2.13}$$

$$E_s(n,k) = \phi(1)^k \sum_i \binom{n+i-1}{k} E_p^0(n,i-k) \tag{2.14}$$

$$E(n,k,l) = \phi(1)^l \binom{n+k-1}{l} E_p^0(n,k-l) \tag{2.15}$$

Proof. For $E(n,k,l)$, the equation can be derived from $V(n,k,l)$ in terms of sets of structures. Analogously to the proof of Theorem 2.4, the other statistics follow by holding the number of internal nodes or the number of internal nodes with one child constant. □

2.3.3 Statistics on Semilabeled Series-Reduced Structured Forests

The statistics for this section are similar to the last section. The statistics for semilabeled series-reduced trees with n leaves and k internal nodes are $L_p^0(n,k) = E_p^0(n,k)$. The statistics for semilabeled series-reduced forests with n leaves and k internal nodes are $L_p(n,k)$, those with n leaves and k trees are $L_t(n,k)$, and those with n leaves, k internal nodes, and l trees are $L(n,k,l)$.

It is also of note that when the structure is a set (and thus the set of structures is a set partition), there is a direct relationship between the number of leaves in the semilabeled series-reduced structured forest and the number of arcs in the arc diagram of the corresponding set partition. A singleton has one arc, and a NSS of size m has $m-1$ arcs. Therefore, the arc diagram of a set partition G with G_v vertices and G_h NSSs has $G_v - G_h$ arcs. If G corresponds to the forest F, then by as implied by Theorem 2.2, the number of leaves in the forest F is $G_v + 1 - G_h$. (The forest has one more node than the set partition has elements, and the number of NSSs is the same as the number of internal nodes.) In other words, F has one more leaf than G has arcs. Note that as the structure is a set, the forest is a set of phylogenetic trees.

As the number of arcs determines the number of possible nestings and crossings, we are also interested in the statistics of semilabeled series-reduced structured forests with n leaves corresponding to sets of structures with k structures, $L_b(n,k)$. (We will also revisit this statistic in Equation 2.30 below.)

The bijection of Theorem 2.2 allows us to translate the classical results of the previous section to semilabeled structured trees. Recalling that $\phi(1) = 1$ for this case, the following equations hold.

Theorem 2.7.

$$L_p^0(n,k) = E_p^0(n,k) = V_b^0(n+k-1,k) \tag{2.16}$$

$$L_p(n,k) = V_h(n+k-1,k) \tag{2.17}$$

$$L(n,k,l) = V(n+k-1,k,l-1) \tag{2.18}$$

Proof. In all of these cases, n is the number of leaves and k is the number of internal nodes, so $n+k-1$ is the number of elements in the set of structures and k is the number of NSSs. The equations follow. □

Theorem 2.8.

$$L_p(n,k) = \sum_i \binom{n+k-1}{i-1} L_p^0(n-i+1,k) \tag{2.19}$$

$$L_t(n,k) = \sum_i \binom{n+i-1}{k-1} L_p^0(n-k+1,i) \tag{2.20}$$

$$L_b(n,k) = \sum_i \binom{n+k-i}{i-1} L_p^0(n-i+1,k-i+1) \tag{2.21}$$

$$L(n,k,l) = \binom{n+k-1}{l-1} L_p^0(n-l+1,k) \tag{2.22}$$

Proof. For $L(n,k,l)$, the equation can be derived from $V(n,k,l)$ in terms of sets of structures. Analogously to the proof of Theorem 2.4, the other statistics follow by holding the number of internal nodes, the number of trees, or the number of NSSs constant. □

2.4 Bicolouring Bijection Principle

The bijection between singleton-free set partitions and weighted Dyck paths with bicoloured valleys presented in Section 2.1 is part of a more general group of bicolourings which leads to an interesting class of identities. In this section we explore certain bijections between structured matchings and singleton-free sets of structures. Examples of bijections under the principle are also shown, including some new combinatorial interpretations of known identities (Equations 2.31 and 2.35). The identities include such well-known sequences as the Stirling numbers of the first and second kind, the second-order Eulerian numbers, and the Narayana numbers.

A *structured matching* is a set of structures consisting of n structures of size 2, or in other words, a matching with a structure applied to each arc. When $\phi(2) = 1$, these objects correspond directly to matchings and there are $(2n-1)!! = \prod_{i=1}^{n} 2i-1$ such objects. When $\phi(2) = 2$, there are $2^n(2n-1)!! = (n+1)!C_n$ such objects, where C_n is a Catalan number. In general, there are $\phi(2)^n(2n-1)!!$ such objects.

We are interested in bijections wherein certain *features* of the structured matchings are bicoloured. What exactly constitutes a feature depends on the specific bijection in question. Examples of such bijections are given in the following sections. The following theorem is, to the best of our knowledge, a new result.

Theorem 2.9 (Bicolouring Bijection Principle)**.** *Suppose that there exists a bijection between structured matchings with bicoloured features and singleton-free sets of structures such that a structured matching on $[2n]$ with m coloured features is in bijection with a singleton-free set of $n-m$ structures over $2n-m$ total elements, and also that $\phi(1)=1$.*

Then, if $B(n,k)$ gives the number of structured matchings on $[2n]$ with k features, the following identities hold.

$$L_p^0(n+1,k) = E_p^0(n+1,k) = V_b^0(n+k,k) = \sum_j \binom{j}{n-k} B(n,j) \tag{2.23}$$

$$\sum_k E_p^0(n+1,k) = \sum_j 2^j B(n,j) \tag{2.24}$$

$$E_p(k+1,n-k) = V_b(n,n-k) = \sum_j \binom{n+j}{2k} B(k,j) \tag{2.25}$$

$$B(n,k) = \sum_i (-1)^{n-k+i} \binom{n-i}{k} V_b^0(n+i,i) \tag{2.26}$$

$$B(n,n-k) = \sum_i (-1)^i \binom{2n+1}{i} V_b(n+k-i,k-i) \tag{2.27}$$

Proof. Equation 2.23 holds due to the constraints imposed on the bijection. Because $n+k = 2n-(n-k)$ and $k = n-(n-k)$, $V_b^0(n+k,k)$ must count structured matchings on $[2n]$ with $n-k$ coloured features. The summation on the right chooses $n-k$ features to colour for all structured matchings on $[2n]$.

Equation 2.24 follows from Equation 2.23 as $\sum_k \binom{j}{k} = 2^j$.

Equation 2.25 follows from Equation 2.7 and Equation 2.23 through a manipulation of

the sums:

$$\begin{aligned}
V_b(n, n-k) &= \sum_i \binom{n}{i} V_b^0(n-i, n-k-i) \\
&= \sum_i \binom{n}{i} \sum_j \binom{j}{2k-n+i} B(k,j) \\
&= \sum_i \sum_j \binom{n}{n-i} \binom{j}{2k-n+i} B(k,j) \\
&= \sum_j B(k,j) \sum_i \binom{n}{n-i} \binom{j}{2k-n+i} \\
&= \sum_j B(k,j) \binom{n+j}{2k}
\end{aligned}$$

Equations 2.26 and 2.27 are simply the inversions of Equations 2.23 and 2.25, respectively. □

The requirements on the bijection can also be stated as follows: Every coloured feature in the structured matching must reduce both the number of structures and the number of total elements by one. Identities between many well-known numbers can be proved by finding a bijection that satisfies the bicolouring bijection principle, as demonstrated by example in the following sections.

Note that Equations 2.26 and 2.27 define $B(n,k)$ in terms of $V_b^0(m,l)$ and $V_b(m,l)$. These equations can be used to calculate the statistics of structured matchings and their features related to a hypothetical bijection which falls under the bicolouring bijection principle. This can be a useful aid to discovering new bijections, such as the example given in Section 2.4.4.

2.4.1 Counting Peaks in Weighted Dyck Paths

Before proceeding to the examples, it will be useful to prove some statistics of weighted Dyck paths in terms of the second-order Eulerian numbers, $\left\langle\!\left\langle {n \atop k} \right\rangle\!\right\rangle$.

The second-order Eulerian numbers and their connection to Stirling numbers seems to have first appeared in the 1920s (Ginsburg [20]). They later reappeared as coefficients of polynomials in the analysis of the approximation of a class of formal power series (Buckholtz [4]). Carlitz [6] used generating functions to determine a formula for the coefficients in terms of Stirling numbers of the second kind (the number of set partitions on $[n]$ with k

parts). With the initial conditions of $\left\langle\!\left\langle {1 \atop 0} \right\rangle\!\right\rangle = 1$, $\left\langle\!\left\langle {1 \atop k} \right\rangle\!\right\rangle = 0$ $(k \neq 0)$, the second-order Eulerian numbers can be defined recursively as follows (Ginsburg [20], Carlitz [6]):

$$\left\langle\!\left\langle {n \atop k} \right\rangle\!\right\rangle = (k+1)\left\langle\!\left\langle {n-1 \atop k} \right\rangle\!\right\rangle + (2n-1-k)\left\langle\!\left\langle {n-1 \atop k-1} \right\rangle\!\right\rangle \tag{2.28}$$

Combinatorial interpretation of these numbers did not arise until much later. First Riordan [36] and then Gessel and Stanley [19] gave interpretations involving the statistics of multiset permutations. Our approach for relating statistics of weighted Dyck paths mirrors the approach of Gessel and Stanley. Namely, the recursion for the second-order Eulerian numbers implies a generation tree for combinatorial objects, as illustrated in Figure 2.17.

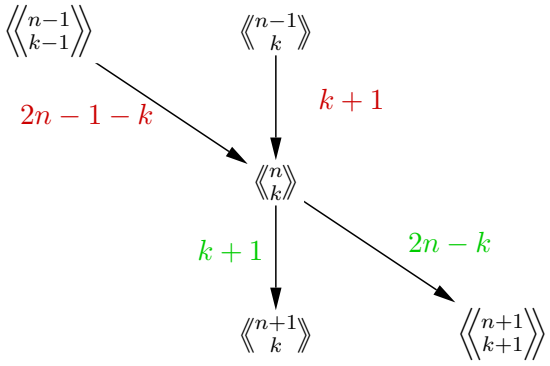

Figure 2.17: The recursion (on top) implies a generation tree profile (on bottom)

The following theorem provides another combinatorial interpretation of the second-order Eulerian numbers. The result was independently discovered by Callan [5].

Theorem 2.10. *There are $\left\langle\!\left\langle {n \atop k} \right\rangle\!\right\rangle$ weighted Dyck paths with semilength n having k strong rises (or strong falls), and thus $\left\langle\!\left\langle {n \atop n-k-1} \right\rangle\!\right\rangle$ with k valleys, and $\left\langle\!\left\langle {n \atop n-k} \right\rangle\!\right\rangle$ with k peaks.*

Proof. We show a generation tree for matchings wherein the corresponding weighted Dyck path with semilength n having k strong rises has $k+1$ children of semilength $n+1$ and k strong rises, and $2n-k$ children of semilength $n+1$ and $k+1$ rises. The generation tree corresponds to the recursion of the second-order Eulerian numbers and thus proves the result.

Recall that a weighted Dyck path with semilength n is in bijection with the arc diagram of a matching with n arcs such that the up steps correspond to left endpoints, and the down

steps to right endpoints. Consider the generation tree of matchings wherein new matchings are formed by inserting an arc with the left endpoint occupying the left-most position. (See Figure 2.18.)

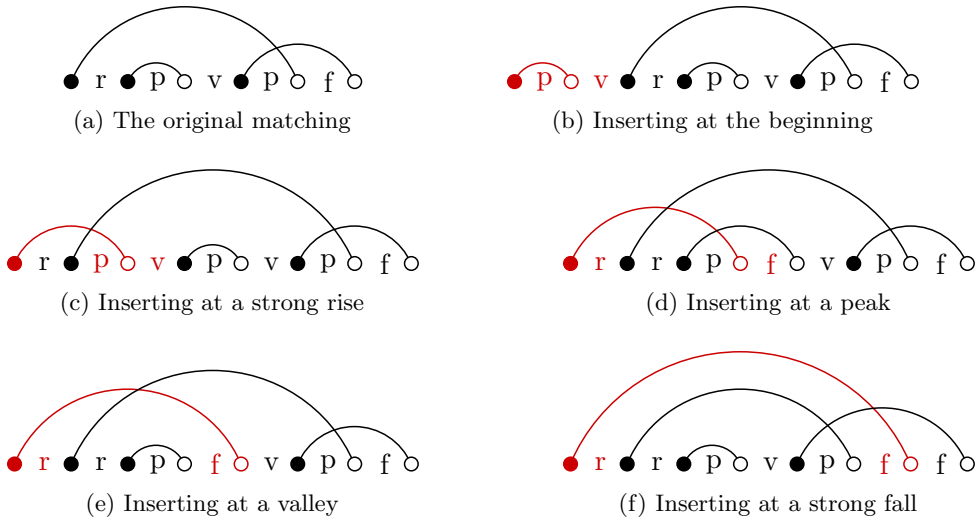

(a) The original matching
(b) Inserting at the beginning
(c) Inserting at a strong rise
(d) Inserting at a peak
(e) Inserting at a valley
(f) Inserting at a strong fall

Figure 2.18: Insertion of a new leftmost arc at various positions. Inserting the right endpoint at the far right, a peak, a strong fall, or a valley increases the number of strong rises by one, as the new right endpoint will border an existing right endpoint. However, inserting at a strong rise or at the far left will not change the number of strong rises

There are $2n+1$ possible locations to insert the right endpoint of the new arc. When the right endpoint is inserted immediately following the left endpoint of the new arc, the number of peaks and valleys in the corresponding weighted Dyck path increase by one (and the rest of the statistics do not change). The same changes occur if the right endpoint is inserted at a strong rise.

If the right endpoint is inserted at any other location, however, the number of strong rises and falls increases by 1, while the other statistics stay the same.

Therefore when there are n arcs and k strong rises, there are $k+1$ children with k strong rises, and $2n+1-(k+1) = 2n-k$ children with $k+1$ strong rises. This completes the proof. □

Note: Together with the bijections of Propositions 2.1 and 2.2 (which preserve the number of arcs), these statistics give a simple form for the number of singleton-free set partitions with n arcs (Equation 2.29) and the number of set partitions with n arcs (Equation 2.30). These also correspond to the number of phylogenetic trees and forests with $n+1$ leaves, respectively.

$$\sum_k L_p^0(n+1,k) = \sum_j 2^j \left\langle\!\!\left\langle {n \atop n-j-1} \right\rangle\!\!\right\rangle \tag{2.29}$$

$$\sum_k L_b(n+1,k) = \sum_j 2^j \left\langle\!\!\left\langle {n \atop n-j} \right\rangle\!\!\right\rangle \tag{2.30}$$

To illustrate the bicolouring bijection principle, we next present some examples. Although the identities in the examples are not new, they serve to illustrate the scope of the bicolouring bijection principle. There are some new combinatorial interpretations, namely Equations 2.31 and 2.35.

2.4.2 Example: Stirling Numbers of the Second Kind

Let $\left\{ {n \atop k} \right\}$ denote the Stirling numbers of the second kind, that is, the number of set partitions of n elements into k parts. Also let $\left\{\!\!\left\{ {n \atop k} \right\}\!\!\right\}$ denote the associated Stirling numbers of the second kind, that is, the number of set partitions of n elements into k parts, all parts having size 2 or greater.

Theorem 2.11 (Smiley [42], Ginsburg [20], Carlitz [6])**.**

$$\left\{\!\!\left\{ {n+k \atop k} \right\}\!\!\right\} = \sum_j {j \choose n-k} \left\langle\!\!\left\langle {n \atop n-j-1} \right\rangle\!\!\right\rangle \tag{2.31}$$

$$\begin{aligned} \left\{ {n \atop n-k} \right\} &= \sum_j {n+j \choose 2k} \left\langle\!\!\left\langle {k \atop k-j-1} \right\rangle\!\!\right\rangle \\ &= \sum_j {n+k-1-j \choose 2k} \left\langle\!\!\left\langle {k \atop j} \right\rangle\!\!\right\rangle \end{aligned} \tag{2.32}$$

Proof. The bijection of Section 2.1 between weighted Dyck paths with bicoloured valleys and singleton-free set partitions meets the requirements of the bicolouring bijection principle. By Theorem 2.10, $B(n,k) = \left\langle\!\!\left\langle {n \atop n-k-1} \right\rangle\!\!\right\rangle$, and the results follow from Theorem 2.9. □

Equation 2.31 is known; see, for example, Smiley [42] (Corollary 4). The bicolouring bijection gives a combinatorial interpretation of the equation; to the best of our knowledge, this is the first combinatorial interpretation.

Equation 2.32 is also known, as explored by Ginsburg [20] and Carlitz [6].

2.4.3 Example: Strongly Non-crossing Set Partitions

Let $U(n,k)$ be the number of strongly non-crossing set partitions on n elements with k parts, and let $H(n,k)$ be the number of strongly non-crossing set partitions on n elements with k parts, all of size 2 or greater. Also let $N(n,k) = \binom{n-1}{k-1}\binom{n}{k-1}/k$. ($N(n,k)$ are known as the Narayana numbers.)

Theorem 2.12 (Kreweras [30])**.**

$$H(n+k,k) = \sum_j \binom{j}{n-k} N(n, n-j) \tag{2.33}$$

$$U(n,k) = N(n,k) \tag{2.34}$$

Proof. The weighted Dyck path corresponding to a non-crossing matching must have all weights equal to 0, as shown by Kasraoui and Zeng [26]. Therefore, there is a bijection between (unweighted) Dyck paths and non-crossing matchings.

The bijection of Theorem 2.11 does not create any strong crossings. Therefore, when applied to a non-crossing matching, the result is a singleton-free strongly non-crossing set partition. Similarly, applying the bijection to any singleton-free strongly non-crossing set partition results in a non-crossing matching. Therefore we can restrict the bijection of Theorem 2.11 to be between singleton free strongly non-crossing set partitions and (unweighted) Dyck paths with bicoloured valleys.

It is well-known ([41] `A001263`) that the number of Dyck paths with k peaks is $N(n,k)$. It is also known that $N(n,k) = N(n,n-k+1)$. So the number of Dyck paths with k valleys is $N(n,k+1) = N(n,n-k) = B(n,k)$.

Not only does the bijection hold, but Equation 2.7 also holds, as adding singletons to a strongly non-crossing set partition can not cause any crossings. Equation 2.33 follows immediately from Theorem 2.9.

For Equation 2.34, some reduction is required.

$$\begin{aligned}
U(n, n-k) &= \sum_j \binom{n+j}{2k} N(k, k-j) \\
&= \sum_j \binom{n+j}{2k} N(k, j+1) \\
&= \sum_j \binom{n+j}{2k} \binom{k-1}{j} \binom{k}{j} / (j+1) \\
(k+1)U(n, n-k) &= \sum_j \binom{n+j}{2k} \binom{k-1}{j} \binom{k+1}{j+1} \\
&= \sum_j \binom{n+j}{k+k} \binom{k-(n)+(n-1)}{j} \binom{k+(n)-(n-1)}{k-j} \\
&= \binom{n}{k} \binom{n-1}{k} \\
U(n, n-k) &= \binom{n}{k} \binom{n-1}{k} / (k+1) = N(n, n-k)
\end{aligned}$$

□

Equation 2.34 was first discovered by Kreweras [30].

This example is notable in that the recursive equations of Theorem 2.3 do not apply to non-crossing partitions. However, the equations of Theorem 2.4 do apply, and we can define $V_b^0(n,k)$ in terms of the bijection with Dyck paths. By this method, all of the statistics discussed can be calculated.

It is also notable that the Narayana number are in some sense robust under the bi-colouring bijection principle. The "input" was $B(n,k) = N(n, n-k)$, and the "output" was $U(n, n-k) = N(n, n-k)$.

2.4.4 Example: Stirling Numbers of the First Kind

Let $\left[{n \atop k}\right]$ denote the Stirling numbers of the first kind, that is, permutations of n elements with k cycles. Also let $\left[\!\left[{n \atop k}\right]\!\right]$ denote the associated Stirling numbers of the first kind, that is, derangements of n elements with k cycles.

Here we demonstrate how Equations 2.26 and 2.27 can be useful in discovering new bijections. If one applies Equation 2.27 to the well-known numbers $\left[{n \atop k}\right]$ (or alternatively applies Equation 2.26 to $\left[\!\left[{n \atop k}\right]\!\right]$), the resulting numbers seem to satisfy $B(n,k) = \left\langle\!\left\langle {n \atop k} \right\rangle\!\right\rangle$. Given

the statistics of Theorem 2.10, this immediately suggests a bijection under the bicolouring bijection principle wherein the structured matchings correspond to weighted Dyck paths, and the bicoloured features are strong rises. There does in fact exist such a bijection (as demonstrated in the proof), leading to the following identities.

Theorem 2.13 (Ginsburg [20])**.**

$$\left[\!\left[{n+k \atop k} \right]\!\right] = \sum_j \binom{j}{n-k} \left\langle\!\left\langle {n \atop j} \right\rangle\!\right\rangle \tag{2.35}$$

$$\left[{n \atop n-k} \right] = \sum_j \binom{n+j}{2k} \left\langle\!\left\langle {k \atop j} \right\rangle\!\right\rangle \tag{2.36}$$

Proof. We present a bijection between weighted Dyck paths with bicoloured strong rises and derangements that meets the requirements of the bicolouring bijection principle. By Theorem 2.10, $B(n,k) = \left\langle\!\left\langle {n \atop k} \right\rangle\!\right\rangle$, and the results follow from Theorem 2.9.

In terms of matchings, a strong rise indicates two consecutive left endpoints. This can be rephrased as having two cycles with minimum elements a_1 and a_2 such that $a_1 = a_2 - 1$. We call this a *strong rise relationship*, and generalize the relationship to all derangements by allowing any cycle sizes greater than 1.

Consider the following operation to combine two cycles with a strong rise relationship:

1. In the standard notation, let the cycles be $[x_1, x_2, \ldots, x_i][y_1, y_2, \ldots, y_j]$. We require that $x_1 = y_1 - 1$.

2. Replace both cycles with a new cycle, $[x_1, x_2, \ldots, x_i, y_2, \ldots, y_j]$. Note that y_1 has been removed.

3. For any number $j > y_1$ in the derangement, renumber as $j - 1$ to account for the removal of y_1. (The new cycle is now $[x_1, x_2 - 1, \ldots, x_i - 1, y_2 - 1, \ldots, y_j - 1]$).

The operation preserves any other strong rise relationships which may exist in the derangement, and does not create any new strong rise relationships. The operation is clearly associative and also removes one vertex and one cycle, and thus meets the requirements of the bicolouring bijection principle.

The operation is also easily reversed:

1. Consider a cycle with length 3 or greater, $[x_1, x_2, \ldots, x_i]$. First, for any number in the derangement $j > x_1$, renumber as $j + 1$. The cycle is now $[x_1, x_2 + 1, \ldots x_i + 1]$.

2. Choose an inner element $x_k + 1$ $(1 < k < i)$ to be the new final element in the cycle. Replace the cycles with two cycles, $[x_1, \ldots, x_k + 1][x_1 + 1, x_{k+1} + 1, \ldots, x_i + 1]$. Note that a new element, $x_1 + 1$, has been inserted.

The requirements on k ensure that the new cycles both have size 2 or greater.
An example is given in Figure 2.19. □

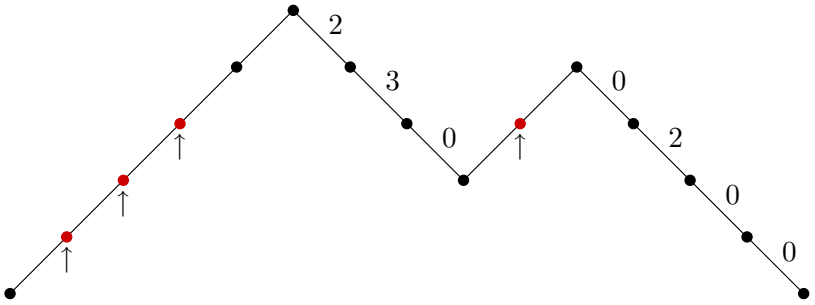

(a) A weighted Dyck path with 4 coloured strong rises.

$$[1, 8] * [2, 11] * [3, 6] * [4, 13][5, 7][9, 14] * [10, 12]$$
$$[1, 7, 10] * [2, 5] * [3, 12][4, 6][8, 13] * [9, 11]$$
$$[1, 6, 9, 4] * [2, 11][3, 5][7, 12] * [8, 10]$$
$$[1, 5, 8, 3, 10][2, 4][6, 11] * [7, 9]$$
$$[1, 5, 7, 3, 9][2, 4][6, 10, 8]$$

(b) The associated matching in cycle notation with '$*$' marking coloured strong rises. The operations of the bijection are performed to yield the final derangement

Figure 2.19: An example of the bijection in the proof of Theorem 2.13

Equation 2.36 is known; see for example [20, 21]. To the best of our knowledge, the given bijection is the first combinatorial interpretation of Equation 2.35.

Chapter 3

Permutation and Young Tableau Transformations

The connection between natural global transformations on permutations and on pairs of identically shaped increasing standard Young tableaux is one of the most interesting properties of the RSK correspondence. This chapter provides a systematic review of the properties, providing a complete classification of the symmetries in permutations and pairs of standard Young tableaux.

Of particular importance in this chapter is the fact that there is a bijection between involutions and standard Young tableaux (Corollary 3.3.2). This well-known result, as well as some properties of the global transformations, are used in Chapter 4 to develop shape-preserving transformations on the arc diagrams of involutions.

The bijection between involutions and standard Young tableaux, and most other results in this chapter, are classical results of Robinson, Schensted, Schützenberger, and Knuth. However, we also give four variations of the RSK algorithm (as indicated in the comments between Algorithm 3.4 and Theorem 3.3) which, to the best of our knowledge, have not appeared in the literature. The variations involve an operation we call the transposition of a permutation, which is related to the vacillating tableaux of Chen et al. [8] as described below Figure 3.4.

Section 3.1 introduces another method for adding and removing elements to a Young tableau called *jeu de taquin*, developed by Schützenberger [39]. Section 3.2 uses this method to define a transformation called *evacuation* on Young tableaux. Evacuation is also known

as *Schützenberger's involution*.

Section 3.3 gives the correspondence between the transformations on permutations and those on pairs of standard Young tableaux. Section 3.4 gives the analogous correspondence for variations of the RSK algorithm. The proofs of both correspondences are given in Section 3.5.

3.1 Jeu de Taquin

Section 1.2.2 introduced the operations row insertion and row deletion for adding and removing numbers from a Young tableau. Another such pair of operations is called jeu de taquin, after the sliding puzzle.

Let P be a Young tableau of size n and shape λ, and let (r, c) be a co-corner of P. We write $\text{jins}(P, r, c, i)$ for the jeu de taquin insertion of a number i at (r, c); the result is a Young tableau of size $n+1$ and shape $\lambda \cup (r, c)$. The algorithm is described as Algorithm 3.1, and an example is given in Figure 3.1.

Algorithm 3.1 $\text{jins}(P, r, c, i)$: Jeu de taquin insertion of i into Young tableau P at co-corner (r, c)

Require: (r, c) is a co-corner
  Let $(0, z) = (z, 0) = -\infty$ for all z, $x \leftarrow r$, and $y \leftarrow c$
  Create a new cell at position (r, c) and let it have the value i
  while the values at $(x-1, y)$ and $(x, y-1)$ are not both less than i **do**
    Let (x', y') be the position with the larger of the two values
    Swap the values at (x', y') and (x, y) $\{i$ is now in cell $(x', y')\}$
    Let $x \leftarrow x'$ and $y \leftarrow y'$
  end while

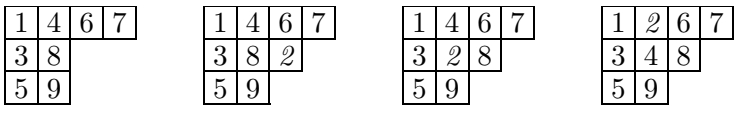

Figure 3.1: A jeu de taquin insertion of 2 into co-corner (2,3)

The algorithm slides the new number i up and left from a corner until a proper Young

tableau is formed. Jeu de taquin deletion jdel(P, i) reverses the algorithm, sliding any chosen number within the tableau down and right by swapping the lesser of two values until a corner is reached, at which point the corner and value are removed from the tableau (see Algorithm 3.2 for details). The operations are analogous for decreasing tableaux and skew tableaux.

Algorithm 3.2 jdel(P, i): Jeu de taquin deletion of value i from Young tableau P

Require: i is contained in tableau P

Let the value of all cells to the right of or below P be ∞

Let (r, c) be the location of i in P

while (r, c) is not a corner **do**

Consider the two cells $(r+1, c)$ and $(r, c+1)$. Let (x, y) be the cell containing the lesser value.

Swap the values of (x, y) and (r, c) $\{i$ is now located at $(x, y)\}$

Let $r \leftarrow x$ and $c \leftarrow y$

end while

Remove corner (r, c) and value i from the tableau

3.2 Evacuation

Repeated jeu de taquin deletion of the origin can be used to defined a transformation on Young tableaux called *evacuation*, given in Algorithm 3.3.

Algorithm 3.3 Evacuation of a Young tableau

Let the contents of P be $p_1 < p_2 < \ldots < p_n$ and let $\lambda = \mathrm{sh}(P)$

Let $P'_0 \leftarrow P$ and $Q'_0 \leftarrow \emptyset$

for $i = 1$ to n **do**

Let $P'_i \leftarrow \mathrm{jdel}(P'_{i-1}, p_i)$ and $\lambda'_i \leftarrow \mathrm{sh}(P'_i)$

Let (r, c) be the cell that was removed during the deletion of p_i from P'_{i-1}

Let $Q'_i \leftarrow Q'_{i-1}$ and then let position (r, c) in Q'_i have value p_i

$\{Q'_i$ is a decreasing skew tableau with shape $\lambda/\lambda'_i\}$

end for

Define Q'_n to be the evacuation of P

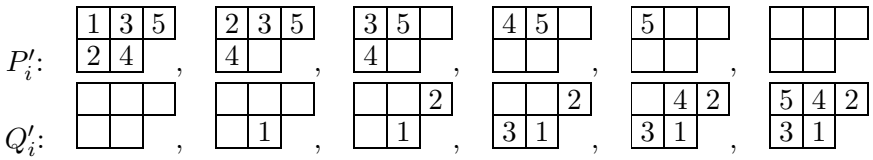

Figure 3.2: An evacuation by repeated jeu de taquin deletion of the origin

After n deletions, P'_n is empty and Q'_n is a decreasing Young tableau with shape λ, as illustrated in Figure 3.2. We define the evacuation of P to be $P^E = Q'_n$, and define evacuation for decreasing Young tableaux analogously. We also define $P^S = P^{EN} = P^{NE}$. Figure 3.3 give examples.

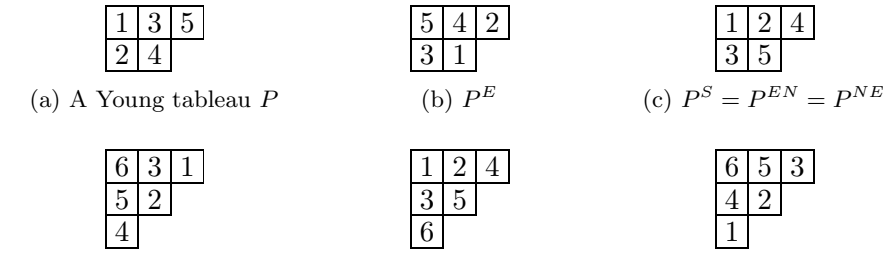

(a) A Young tableau P (b) P^E (c) $P^S = P^{EN} = P^{NE}$

(d) A decreasing Young tableau Q (e) Q^E (f) $Q^S = Q^{EN} = Q^{NE}$

Figure 3.3: Examples of the transformations P^E and P^S

In the following sections, we rely on the fact that evacuation is an involutive transformation; a sketch of a proof is provided here.

Theorem 3.1 (Schützenberger [39])**.** *Evacuation is involutive; that is, for any Young tableau P,*

$$P^{EE} = P \tag{3.1}$$

Proof sketch. It can be shown (for both increasing and decreasing Young tableaux) that

$$\text{jins}(P, r, c, \alpha)^E = \text{jins}(P^E, r, c, \alpha) \qquad (\alpha > P \text{ or } \alpha < P) \tag{3.2}$$

This allows us to prove the theorem inductively on the size of the tableau. The base case of an empty tableau is trivial. For the inductive step, let α be the largest value in a

Young tableau P, and let α be located at corner (r, c). Then,

$$\begin{aligned} P^{EE} &= \text{jins}(\text{jdel}(P, \alpha), r, c, \alpha)^{EE} \\ &= \text{jins}(\text{jdel}(P, \alpha)^{E}, r, c, \alpha)^{E} \\ &= \text{jins}(\text{jdel}(P, \alpha)^{EE}, r, c, \alpha) \\ &= \text{jins}(\text{jdel}(P, \alpha), r, c, \alpha) \\ &= P \end{aligned} \tag{3.3}$$

□

3.3 Transformations of Permutations and Young Tableaux

There are 8 natural transformations of the square when considering rotation and reflection. When applied to a permutation matrix, these can be interpreted in terms of 3 involutive transformations on a permutation.

Let $\rho \in S_n$ be the permutation such that $\rho(i) = n-i+1$. Given a permutation $\sigma \in S_n$, let σ^{-1} be the inverse permutation (such that $\sigma\sigma^{-1}$ and $\sigma^{-1}\sigma$ yield the identity permutation), and define σ^N and σ^R as follows:

$$\sigma^N = \rho\sigma \tag{3.4}$$

$$\sigma^R = \sigma\rho \tag{3.5}$$

σ^N is called the *negation* of σ, and σ^R is called the *reversal* of σ.

These 8 transformations on a permutation matrix correspond to

$$\text{Original matrix :} \quad \sigma = \sigma^{NN} = \sigma^{RR} = \sigma^{-1-1} \tag{3.6}$$

$$\text{Horizontal reflection :} \quad \sigma^R \tag{3.7}$$

$$\text{Vertical reflection :} \quad \sigma^N \tag{3.8}$$

$$\text{Diagonal reflection :} \quad \sigma^{-1} \tag{3.9}$$

$$\text{Antidiagonal reflection :} \quad \sigma^{-1RN} = \sigma^{-1NR} = \sigma^{NR-1} = \sigma^{RN-1} \tag{3.10}$$

$$90^\circ \text{ clockwise rotation :} \quad \sigma^{-1N} = \sigma^{R-1} \tag{3.11}$$

$$180^\circ \text{ clockwise rotation :} \quad \sigma^{RN} = \sigma^{NR} \tag{3.12}$$

$$270^\circ \text{ clockwise rotation :} \quad \sigma^{-1R} = \sigma^{N-1} \tag{3.13}$$

See also Figure 3.4.

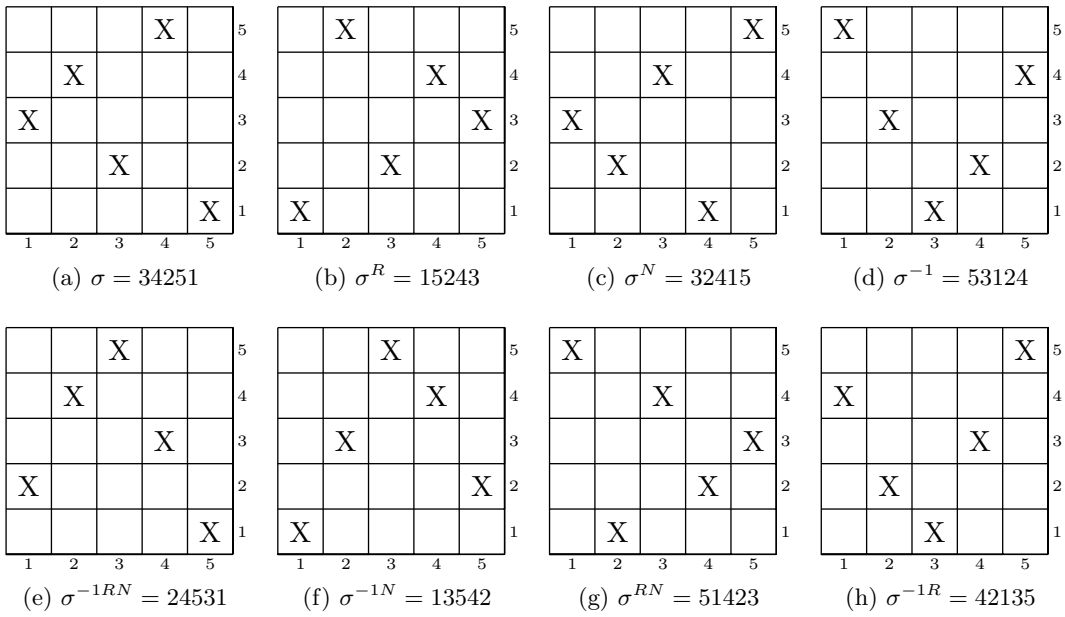

(a) $\sigma = 34251$ (b) $\sigma^R = 15243$ (c) $\sigma^N = 32415$ (d) $\sigma^{-1} = 53124$

(e) $\sigma^{-1RN} = 24531$ (f) $\sigma^{-1N} = 13542$ (g) $\sigma^{RN} = 51423$ (h) $\sigma^{-1R} = 42135$

Figure 3.4: Symmetries of the square and transformations on permutations

To complete the connection between transformations on permutations and transformations on pairs of standard Young tableaux, we define a fourth transformations on permutations, σ^T. If $\sigma \sim (P, Q)$, then σ^T is defined as the permutation corresponding to (P^T, Q^T). We define σ^T in terms of the associated Young tableaux as there is no known definition in terms of the permutation itself.

There is also a connection to Chen et al.'s paper [8]. Consider a balanced matching $\beta \in BM_{2n}$ in bijection with a permutation $f(\beta) \in S_n$. Chen et al. observe (using different notation) that applying their vacillating tableaux transformation to β results in a balanced matching in bijection with $f(\beta)^T \in S_n$. However, Chen et al.'s vacillating tableaux are constructed using row insertion and deletion, similar to RSK; again there is no direct definition in terms of permutations.

We can show close connections between the transformations on permutations and transformations on the corresponding tableaux. Firstly, note the following 4 involutive transformations on a pair of Young tableaux (P, Q) of the same shape which preserve direction of the tableaux: exchanging P and Q, transposing both P and Q, evacuating and negating P, and evacuating and negating Q. Together, these give 16 total transformations.

The connections between the 16 transformations of tableaux and permutations are stated in the following theorem.

Theorem 3.2 (Robinson [11], Schensted [38], Schützenberger [39], Knuth [27])**.** *Given that* $\sigma \sim (P, Q)$ *for a permutation* σ*, the following correspondences hold:*

$$\sigma \sim (P, Q) \tag{3.14}$$
$$\sigma^R \sim (P^T, Q^{ST}) \tag{3.15}$$
$$\sigma^N \sim (P^{ST}, Q^T) \tag{3.16}$$
$$\sigma^{RN} \sim (P^S, Q^S) \tag{3.17}$$
$$\sigma^T \sim (P^T, Q^T) \tag{3.18}$$
$$\sigma^{TR} \sim (P, Q^S) \tag{3.19}$$
$$\sigma^{TN} \sim (P^S, Q) \tag{3.20}$$
$$\sigma^{TNR} \sim (P^{ST}, Q^{ST}) \tag{3.21}$$
$$\sigma^{-1} \sim (Q, P) \tag{3.22}$$
$$\sigma^{R-1} \sim (Q^{ST}, P) \tag{3.23}$$
$$\sigma^{N-1} \sim (Q^T, P^{ST}) \tag{3.24}$$
$$\sigma^{RN-1} \sim (Q^S, P^S) \tag{3.25}$$
$$\sigma^{T-1} \sim (Q^T, P^T) \tag{3.26}$$
$$\sigma^{TR-1} \sim (Q^S, P) \tag{3.27}$$
$$\sigma^{TN-1} \sim (Q, P^S) \tag{3.28}$$
$$\sigma^{TRN-1} \sim (Q^{ST}, P^{ST}) \tag{3.29}$$

The proof will be given in terms of two-line arrays and variations of the RSK algorithm below.

Note that Equations 3.18–3.21 and 3.26–3.29 follow immediately from the other equations and the definition of σ^T, and are included above for completeness.

Before proceeding to the proof, we introduce the RSK variations.

3.4 Variations on RSK

Here, we present the RSK construction using the jeu de taquin (Algorithm 3.4 below), which is more general than the classical row insertion/row deletion presentation. Indeed, it leads to 8 variations of RSK on a two-line array A by allowing either of the Young tableaux to be decreasing instead of increasing, and also allowing the elements of the array to be inserted in reverse (from right to left) instead of forward.

4 of these variations do not require jeu de taquin and are well-known in the literature; see, for example, [28]. The other 4 variations *do* require jeu de taquin, and complete the connection between RSK and the 16 transformations on pairs of Young tableaux presented above.

Algorithm 3.4 Generalized RSK construction of tableaux from a two-line array

Let $P_0 \leftarrow \emptyset$ and $Q_0 \leftarrow \emptyset$
if reading the two-line array forward **then**
  Let $j_i = i$
else
  Let $j_i = n - i + 1$
end if
for $i = j_1$ to j_n **do**
  Let $P_i \leftarrow \text{rins}(P_{i-1}, p_i)$ and let (r_i, c_i) be the resulting new corner
  Let $Q_i \leftarrow \text{jins}(Q_{i-1}, r_i, c_i, q_i)$
  {Note that $\text{sh}(Q_i) = \text{sh}(P_i)$}
end for

Two changes have been made: The for loop can read the array either forwards or backwards, and modifications to the recording tableau Q are done using $\text{jins}(Q_{i-1}, r_i, c_i, q_i)$. Note that when Q is increasing and the array is being read forward, $\text{jins}(Q_{i-1}, r_i, c_i, q_i)$ does not shift any elements as $q_i > Q_{i-1}$. (This is similarly true when Q is decreasing and the array is being read in reverse.) In these cases, $\text{jins}(Q_{i-1}, r_i, c_i, q_i)$ is the same as creating a new cell at location (r_i, c_i) with value q_i, as was done in the original algorithm.

The four variations where $\text{jins}(Q_{i-1}, r_i, c_i, q_i)$ does not shift any elements are known in the literature; see, for example, [28]. However, to the best of our knowledge the other four variations are not in the literature.

The notation for these RSK variations is as follows. Define $F_I^I(A) \sim (P, Q)$ to be the normal RSK correspondence obtained by reading the two-line array A **F**orward from $i = 1$ to $i = n$, with both P and Q **I**ncreasing. Define $R_I^D(A)$ to be the correspondence obtained by reading A in **R**everse from $i = n$ to $i = 1$, with P **I**ncreasing but Q **D**ecreasing. The six other variations are similarly defined: $F_I^D(A), F_D^I(A), F_D^D(A), R_D^D(A), R_I^I(A), R_D^I(A)$.

The following theorem is analogous to Theorem 3.2. Equations 3.30–3.33 and 3.38–3.41 are well-known (Knuth [27, 28]). Equations 3.34–3.37 and 3.42–3.45 do not appear in the literature, and are to the best of our knowledge a new result.

Theorem 3.3. *Given that $F_I^I(A) \sim (P, Q)$ for a two-line array A, the following correspondences hold:*

$$F_I^I(A) \sim (P, Q) \quad (3.30) \qquad F_I^I(A^{-1}) \sim (Q, P) \quad (3.38)$$
$$R_I^D(A) \sim (P^T, Q^{ET}) \quad (3.31) \qquad R_I^D(A^{-1}) \sim (Q^T, P^{ET}) \quad (3.39)$$
$$F_D^I(A) \sim (P^{ET}, Q^T) \quad (3.32) \qquad F_D^I(A^{-1}) \sim (Q^{ET}, P^T) \quad (3.40)$$
$$R_D^D(A) \sim (P^E, Q^E) \quad (3.33) \qquad R_D^D(A^{-1}) \sim (Q^E, P^E) \quad (3.41)$$
$$R_I^I(A) \sim (P^T, Q^T) \quad (3.34) \qquad R_I^I(A^{-1}) \sim (Q^T, P^T) \quad (3.42)$$
$$F_I^D(A) \sim (P, Q^E) \quad (3.35) \qquad F_I^D(A^{-1}) \sim (Q, P^E) \quad (3.43)$$
$$R_D^I(A) \sim (P^E, Q) \quad (3.36) \qquad R_D^I(A^{-1}) \sim (Q^E, P) \quad (3.44)$$
$$F_D^D(A) \sim (P^{ET}, Q^{ET}) \quad (3.37) \qquad F_D^D(A^{-1}) \sim (Q^{ET}, P^{ET}) \quad (3.45)$$

3.5 Proof of Theorems 3.2 and 3.3

Here, we prove Theorems 3.2 and 3.3. The results of this section up to Lemma 3.3 are well-known (see, for example, Schensted [38] and Schützenberger [39]), and are therefore largely sketched within this thesis.

The beginning of the proof will show that inverting a two-line array exchanges the insertion and recording tableaux in the bijection.

First, we need to generalize inversion of a permutation to inversion of a two-line array. Define j_i for $1 \leq i \leq n$ such that $p_{j_1} < p_{j_2} < \ldots < p_{j_n}$. Then

$$A^{-1} = \begin{pmatrix} p_{j_1} & p_{j_2} & \cdots & p_{j_n} \\ q_{j_1} & q_{j_2} & \cdots & q_{j_n} \end{pmatrix}$$

We are now ready to state the relation.

Lemma 3.1 (Schensted [38])**.** *Inverting a two-line array A exchanges the corresponding Young tableaux P and Q; that is*

$$A \sim (P, Q) \Longleftrightarrow A^{-1} \sim (Q, P) \quad (3.46)$$

Proof sketch. Let (r, c) be the location of p_{j_n} in P. It is possible to show the following effect of removing q_{j_n} and p_{j_n} from A:

$$\begin{pmatrix} q_1 & \cdots & q_{j_n-1} & q_{j_n+1} & \cdots & q_n \\ p_1 & \cdots & p_{j_n-1} & p_{j_n+1} & \cdots & p_n \end{pmatrix} \sim (\mathrm{jdel}(P, p_{j_n}), \mathrm{rdel}(Q, r, c)) \quad (3.47)$$

The theorem holds for the trivial empty tableau. For the inductive step, let A' be the two-line array after the removal of q_{j_n} and p_{j_n}. Then we have

$$A' \sim (\text{jdel}(P, p_{j_n}), \text{rdel}(Q, r, c)) \tag{3.48}$$

$$A'^{-1} \sim (\text{rdel}(Q, r, c), \text{jdel}(P, p_{j_n})) \tag{3.49}$$

$$A^{-1} \sim (\text{rins}(\text{rdel}(Q, r, c), q_{j_n}), \text{jins}(\text{jdel}(P, p_{j_n}), p_{j_n})) \tag{3.50}$$

$$= (Q, P)$$ □

Corollary 3.3.1. *For permutation σ, $\sigma \sim (P, Q) \iff \sigma^{-1} \sim (Q, P)$*

Corollary 3.3.2. *Involutions are in bijection with SYT.*

Next, we use one of the RSK variations introduced above.

Lemma 3.2 (Schützenberger [39], Knuth [27, 28])**.** $F_I^I(A) \sim (P, Q) \iff R_I^D(A) \sim (P^T, Q^{ET})$

Proof sketch. From the RSK algorithm, it is clear that if q_n is located at r, c, then

$$\begin{pmatrix} q_1 & \cdots & q_{n-1} & q_n \\ p_1 & \cdots & p_{n-1} & p_n \end{pmatrix} \sim (P, Q) \iff \begin{pmatrix} q_1 & \cdots & q_{n-1} \\ p_1 & \cdots & p_{n-1} \end{pmatrix} \sim (\text{rdel}(P, r, c), \text{jdel}(Q, q_n)) \tag{3.51}$$

and $\text{rdel}(P, r, c)$ removes p_n.

It can also be shown that if the jeu de taquin deletion of q_1 from Q removes corner r, c, then

$$\begin{pmatrix} q_1 & q_2 & \cdots & q_n \\ p_1 & p_2 & \cdots & p_n \end{pmatrix} \sim (P, Q) \iff \begin{pmatrix} q_2 & \cdots & q_n \\ p_2 & \cdots & p_n \end{pmatrix} \sim (\text{cdel}(P, r, c), \text{jdel}(Q, q_1)) \tag{3.52}$$

and $\text{cdel}(P, r, c)$ removes p_1.

The theorem is trivial for the base case of an empty tableau. For the inductive case, let A' be A with p_1 and q_1 removed, and let the removed corner be (r, c). We then have

$$F_I^I(A') \sim (\text{cdel}(P, r, c), \text{jdel}(Q, q_1)) \tag{3.53}$$

$$R_I^D(A') \sim (\text{cdel}(P, r, c)^T, \text{jdel}(Q, q_1)^{ET})) \tag{3.54}$$

$$= (\text{rdel}(P^T, c, r), \text{jdel}(Q^{ET}, q_1))$$

$$R_I^D(A) \sim (\text{rins}(\text{rdel}(P^T, c, r), p_1), \text{jins}(\text{jdel}(Q^{ET}, q_1), q_1, c, r)) \tag{3.55}$$

$$= (P^T, Q^{ET})$$ □

From Lemmas 3.2 and 3.1, we can prove Theorem 3.2. Equation 3.22 follows from Lemma 3.1. Reversing a permutation is the same as reading the corresponding array in reverse with the top row decreasing and the bottom row increasing, except the top row has negated values. Therefore Equation 3.15 follows from Lemma 3.2. $\sigma^{-1R} = \sigma^{N-1}$, so applying Lemma 3.1 yields Equation 3.24. $\sigma^{-1N-1} = \sigma^{N}$, and therefore another application of Lemma 3.1 results in Equation 3.16. Yet another application of Lemma 3.1 gives Equation 3.23. Combining Equation 3.15 and Equation 3.16 results in Equation 3.17, and a final application of Lemma 3.1 gives Equation 3.25. As mentioned above, Equations 3.18–3.21 and 3.26–3.29 follow immediately from the other equations and the definition of σ^T. This concludes the proof of Theorem 3.2.

We can also prove half of Theorem 3.3 from Theorem 3.2. Lemma 3.2 is the same as Equation 3.31. Negation of a permutation is the same as applying RSK with the insertion tableau decreasing, and then negating the insertion tableau at the end; therefore Equation 3.16 proves Equation 3.32. Similarly, simultaneously reversing and negating a permutation is equivalent to applying RSK to a two-line array in reverse with both tableaux decreasing, and then negating the tableaux afterwards. Therefore Equation 3.17 proves Equation 3.33. Applying Lemma 3.1 to Equations 3.30–3.33 gives Equations 3.38–3.41.

However, Equations 3.34–3.37 and 3.42–3.45 do *not* immediately follow. The following lemma (to the best of our knowledge, a new result) provides the missing piece.

Lemma 3.3. *Reversing the direction of the recording tableau evacuates the recording tableau.*

Proof. For concreteness, we prove that

$$F_I^I(A) \sim (P, Q) \iff F_I^D(A) \sim (P, Q^E)$$

However, the proof applies in all cases.

The theorem is true for the trivial empty array. For a two-line array of size n, the insertion tableaux of $F_I^I(A)$ and $F_I^D(A)$ are the same by definition of the RSK algorithm. Let Q be the recording tableau of $F_I^I(A)$ and Q' that of $F_I^D(A)$; Q is increasing and Q' is

decreasing. Also let (r, c) be the location of q_n in Q. By the inductive hypothesis, we have

$$\begin{aligned} \text{jdel}(Q', q_n) &= \text{jdel}(Q, q_n)^E && (3.56) \\ Q' &= \text{jins}(\text{jdel}(Q', q_n), q_n, r, c) \\ &= \text{jins}(\text{jdel}(Q, q_n)^E, q_n, r, c) && (3.57) \\ &= \text{jins}(\text{jdel}(Q^E, q_n), q_n, r, c) \\ &= Q^E \end{aligned}$$

The equality $\text{jdel}(Q, q_n)^E = \text{jdel}(Q^E, q_n)$ holds as $q_n > \text{jdel}(Q^E, q_n)$, so we can apply Equation 3.2.

□

This completes the proof of Theorem 3.3.

Chapter 4

Involutive Transformations

In this chapter, we investigate permutations and involutions whose corresponding Young tableaux have the same shape. Section 4.1 introduces local operations on permutations discovered by Knuth which alter the contents of either the recording tableau or insertion tableau, but not their shapes. The results of Reifegerste, which describe these operations in terms of the tableaux instead of the permutation, are also presented and clarified. In particular, Theorem 4.2 and Corollary 4.2.1 show that the Knuth relations and dual Knuth relations of permutations presented in Section 4.1 can be completely identified by relations inside the corresponding Young tableaux.

Section 4.2 uses these results to describe analogous local operations on the arc diagrams of involutions, which alter the contents of the corresponding Young tableau without altering the shape. The involutive transformations are useful in proving results on involutions related to nestings and crossings, as described in Section 4.2.1. They are in fact the key tool used to prove our main result, Theorem 5.2 of Chapter 5. The transformations are also used to show connections between matchings and permutations (Proposition 5.1) and to explore properties of lattices of tableaux in Chapter 6.

4.1 Knuth Transformations in Young Tableaux

Knuth transformations were introduced in [27] in order to describe the row insertion algorithm in terms of local transformations on permutations. The results are now considered fundamental to the study of the RSK correspondence. In this section, we follow Reifegerste's lead in describing Knuth transformations in terms of Young tableaux.

4.1.1 Knuth Relations and Transformations

Let three consecutive positions of a permutation have the values a, b, and c such that $a < b < c$. The values are considered to be a *Knuth relation* if they are not in monotonic order, i.e., the order of the values is *acb*, *bac*, *bca*, or *cab*. A *Knuth transformation* exchanges the a and c values of a Knuth relation, as shown in Figure 4.1.

$$\begin{pmatrix} \dots & i-1 & i & i+1 & \dots \\ \dots & b & a & c & \dots \end{pmatrix} \leftrightarrow \begin{pmatrix} \dots & i-1 & i & i+1 & \dots \\ \dots & b & c & a & \dots \end{pmatrix}$$

$$\begin{pmatrix} \dots & i-1 & i & i+1 & \dots \\ \dots & a & c & b & \dots \end{pmatrix} \leftrightarrow \begin{pmatrix} \dots & i-1 & i & i+1 & \dots \\ \dots & c & a & b & \dots \end{pmatrix}$$

Figure 4.1: Knuth transformations ($a < b < c$)

Two permutations that can be transformed into one another by a sequence of Knuth transformations are called *Knuth-equivalent*.

Let $i-1$, i and $i+1$ be three consecutive integers. σ has a *dual Knuth relation* involving values $i-1$, i, and $i+1$ if σ^{-1} has a Knuth relation defined by its elements in positions $i-1$, i and $i+1$. A *dual Knuth transformation* exchanges the values of either $i+1$ and i if $i-1$ is between i and $i+1$ in σ, or $i-1$ and i if $i+1$ is between i and $i-1$ in σ. (See Figure 4.2.)

It follows that applying a Knuth transformation to σ, and then inverting the resulting permutation is equivalent to first inverting σ, and then applying a dual Knuth transformation on the resulting permutation σ^{-1}.

$$\begin{pmatrix} \dots & a & \dots & b & \dots & c & \dots \\ \dots & i & \dots & i-1 & \dots & i+1 & \dots \end{pmatrix} \leftrightarrow \begin{pmatrix} \dots & a & \dots & b & \dots & c & \dots \\ \dots & i+1 & \dots & i-1 & \dots & i & \dots \end{pmatrix}$$

$$\begin{pmatrix} \dots & a & \dots & b & \dots & c & \dots \\ \dots & i-1 & \dots & i+1 & \dots & i & \dots \end{pmatrix} \leftrightarrow \begin{pmatrix} \dots & a & \dots & b & \dots & c & \dots \\ \dots & i & \dots & i+1 & \dots & i-1 & \dots \end{pmatrix}$$

Figure 4.2: Dual Knuth transformations corresponding to the inverse permutation of that in Figure 4.1

Knuth transformations were introduced in [27], where the following important theorem is proved.

Proposition 4.1 (Knuth [27]). *Knuth transformations alter the contents of the recording tableau but not the contents of the insertion tableau. Dual Knuth transformations alter the contents of the insertion tableau but not the contents of the recording tableau. Neither type of transformation changes the shape of the tableaux.*

Proposition 4.2 (Knuth [27]). *Any two permutations whose tableaux have the same shape can be transformed into one another through a sequence of Knuth transformations and dual Knuth transformations.*

Theorem 4.1 (Knuth [27]). *Two permutations are Knuth-equivalent if and only if they have the same insertion tableau.*

4.1.2 Reifegerste's Results and Enclosures

In [35], Reifegerste examines the affect of Knuth transformations on the corresponding SYTs in deeper detail. To discuss these results, we first need a few definitions. Figure 4.3 below will be used for illustration.

Let us first define two positions (x_1, y_1) and (x_2, y_2) in a Ferrers diagram λ to be *antidiagonal* if $x_1 > x_2$ and $y_1 < y_2$ or vice-versa. In Figure 4.3, the positions of 5 and 7 are antidiagonal, but the positions of 1 and 9 are not. Any two positions in the same row or column are also not antidiagonal.

Next, define an *inversion* in a Young tableau to be two elements i and j such that $j < i$ and j is in a row below that of i. The two elements must necessarily be antidiagonal. Figure 4.3 contains 3 inversions, listed in the caption.

We also define the number of inversions in a Young tableau P to be $\mathrm{inv}(P)$, and the number of antidiagonal pairs of positions as $\mathrm{maxInv}(P)$. Note that $\mathrm{maxInv}(P)$ is determined by the shape of P.

Given two antidiagonal positions (x_1, y_1) and (x_2, y_2), let position (u, v) be *enclosed* by (x_1, y_1) and (x_2, y_2) if and only if $x_1 \geq u \geq x_2$ and $y_1 \leq v \leq y_2$. In such a situation, we refer to (x_1, y_1) and (x_2, y_2) as the *corners*. (If we draw a rectangle in the tableau with the lower-left corner being at (x_2, y_2) and the upper-right corner at (x_1, y_1), then (u, v) is enclosed within the rectangle.)

If the positions of $i-1$, i, and $i+1$ in a standard Young tableau are such that either i and $i+1$ enclose $i-1$, or $i-1$ and i enclose $i+1$, we say that $i-1$, i, and $i+1$ form an *enclosure*. (See Figure 4.3.)

1	2	4	5
3	6	8	
7	9		

Figure 4.3: A standard Young tableau λ with enclosures (1, 2, 3), (2, 3, 4), (4, 5, 6), (6, 7, 8), and (7, 8, 9). (5, 6, 7) is *not* an enclosure as the corners are 5 and 7. $\text{inv}(\lambda) = 3$ due to inversions (3, 4), (3, 5), and (7, 8)

We are now ready to present the connection between Knuth and dual Knuth relations in a permutation and enclosures in the corresponding SYTs. The following well-known lemma (see, for example, Fulton [18]) will be particularly useful.

Lemma 4.1. *If α is inserted into P before $\alpha - 1$ during the RSK process, then $\alpha - 1$ will remain strongly above and weakly to the right of α through any further insertion. If instead $\alpha - 1$ is inserted before α, then $\alpha - 1$ will remain weakly below and strictly to the left of α through any further insertion.*

Proof. First, recall that if a number j bumps another number j', then $j < j'$. Therefore, as the algorithm continues, the values at a given position monotonically decrease. Furthermore, RSK requires that j' is the smallest number in the row that is greater than j. Because the number immediately below j' (if present) must be greater than j' by the properties of the Young tableau, the column position of j' can never increase. That is, the position of any number j' at any point during the insertion algorithm must be weakly below and to the left of its original insertion position.

Consider two numbers α and $\alpha - 1$, inserted in that order (but not necessarily consecutively). If α is still in the first row of the Young tableau when $\alpha - 1$ is inserted, then $\alpha - 1$ will bump α. Otherwise, the value at the original insertion position of α must now be less than $\alpha - 1$, and thus $\alpha - 1$ will be inserted to the right of this position. In either case, a recursive argument shows that $\alpha - 1$ must remain weakly to the right of α so long as $\alpha - 1$ is in a row above α. But $\alpha - 1$ must always be above α, as if $\alpha - 1$ is bumped into a row containing α, it will in turn bump α to the next row.

Equation 3.15 shows that if instead $\alpha - 1$ is inserted before α, then $\alpha - 1$ will always be weakly below and strictly to the left of α. □

Theorem 4.2 (Reifegerste [35])**.** *Values $i - 1$, i, and $i + 1$ form a dual Knuth relation in a permutation if and only if the cells containing $i - 1$, i, and $i + 1$ form an enclosure in*

the corresponding insertion tableau P. Moreover, applying a dual Knuth transformation to values $i-1$, i, and $i+1$ alters the insertion tableau by swapping the corners of the enclosure formed by $i-1$, i, and $i+1$.

Reifegerste's results in [35] are stated less strongly, but a careful reading shows this theorem to be true. In particular, the structure of enclosures is not highlighted, and the fact that any three values $i-1$, i, and $i+1$ which do not form a dual Knuth relation cannot form an enclosure is not shown. For convenience, we supply a full proof here.

Proof. Firstly, any three values $i-1$, i, and $i+1$ which do not form a dual Knuth relation must be in monotonic order (either increasing or decreasing). Lemma 4.1 shows that three such values can never form an enclosure, as either $i-1$ is left of i which is left of $i+1$ (in the increasing case), or $i-1$ is above i which is above $i+1$ (in the decreasing case).

Now consider the dual Knuth transformation

$$\begin{pmatrix} q_1 & \dots & q_a & \dots & q_b & \dots & q_c & \dots \\ p_1 & \dots & i & \dots & i-1 & \dots & i+1 & \dots \end{pmatrix} \leftrightarrow \begin{pmatrix} q_1 & \dots & q_a & \dots & q_b & \dots & q_c & \dots \\ p_1 & \dots & i+1 & \dots & i-1 & \dots & i & \dots \end{pmatrix}$$

which exchanges values $i+1$ and i. Following the RSK algorithm, we let $P_0 = \emptyset$, and P_k be the insertion tableau after the insertion of p_k from the left two-line array, and define P'_k similarly for the right two-line array.

Clearly, $P_k = P'_k$ for $k < a$. Within $P_{a-1} = P'_{a-1}$, the smallest number less than i in the first row must be the same as the smallest number less than $i+1$. Therefore, P_a and P'_a are identical except for one cell in the first row, which is i in P_a and $i+1$ in P'_a. As p_k for $a < k < b$ are inserted, P_k and P'_k similarly stay identical except for the square containing i or $i+1$, as shown in Figure 4.4. (If i is the smallest number less than some other number j in P_k, then $i+1$ must be the smallest number less than j in P'_k, and vice versa.)

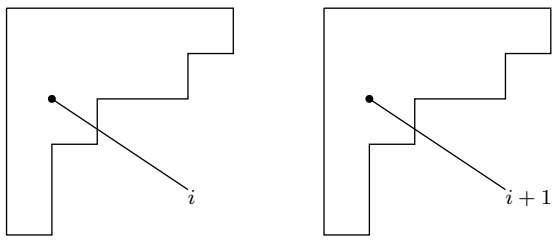

Figure 4.4: Tableaux P_{b-1} and P'_{b-1} differ only in the value of one square

We next insert $i-1$ into P_{b-1} and P'_{b-1}. If i and $i+1$ are still in the first rows of P_{b-1} and P'_{b-1} (respectively), then $i-1$ will bump i and $i+1$, after which point the algorithm will run identically in both tableaux. Otherwise, $i-1$ is inserted at the same position in both P_{b-1} and P'_{b-1}, and the algorithm still runs identically. Therefore, P_b and P'_b remain identical except for the values of i and $i+1$.

Recall from Lemma 4.1 that $i-1$ must stay strictly above and weakly to the right of i. As p_k for $b < k < c$ is inserted, $i-1$ can never occupy the same row as i or $i+1$, as it would bump these values into the next row. The algorithm continues to run identically in both tableaux.

Next, $i+1$ is inserted into P_{c-1} and i is inserted into P'_{c-1}: i (resp. $i+1$) cannot be in the first row of P_{c-1} (resp. P'_{c-1}), and thus the insertion once again runs identically. In P'_c, i must be weakly above and strictly to the right of $i-1$, and so $i+1$, i, and $i-1$ form an enclosure in P'_c, and swapping the corners of this enclosure yields P_c. (See Figure 4.5.)

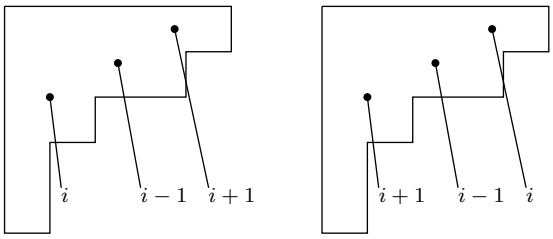

Figure 4.5: Tableaux P_c and P'_c differ by swapping i and $i+1$, which enclose $i-1$

As p_k for $k > c$ is inserted, the enclosure holds, as $i-1$ must remain strongly above i in P_k and i must remain weakly above $i-1$ in P'_k. If i and $i-1$ are in the same row in P'_k, then i cannot be bumped by construction; any $j < i$ must also be less than $i-1$. In this situation, $i+1$ must remain below both i and $i-1$. (i and $i+1$ can occupy the same row in neither P_k nor P'_k.)

This proves the theorem for the first type of dual Knuth transformation. Next we consider the second type of dual Knuth transformation:

$$\begin{pmatrix} q_1 & \dots & q_a & \dots & q_b & \dots & q_c & \dots \\ p_1 & \dots & i-1 & \dots & i+1 & \dots & i & \dots \end{pmatrix} \leftrightarrow \begin{pmatrix} q_1 & \dots & q_a & \dots & q_b & \dots & q_c & \dots \\ p_1 & \dots & i & \dots & i+1 & \dots & i-1 & \dots \end{pmatrix}$$

Using similar reasoning to above, we can show that $i-1$ and i enclose $i+1$ in P_c and P'_c, as illustrated in Figure 4.6.

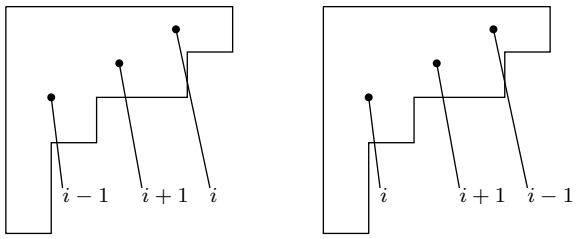

Figure 4.6: Tableaux P_c and P'_c differ by swapping $i-1$ and i, which enclose $i+1$

For the remaining insertions, i must remain strictly above and weakly to the right of $i+1$ in P_k, and i must remain weakly below and strictly to the left of $i+1$ in P'_k. It is possible for the values to remain in this enclosure configuration through the remaining insertions, in which case the theorem is complete.

However, in this case, it is possible for the configuration to change. If i and $i+1$ are in the same row in P'_k, then $i+1$ cannot be bumped, and $i-1$ must be above both i and $i+1$. At the same time in P_k, $i-1$ would be next to $i+1$, and $i+1$ can only be bumped by i. If some value $j \neq i-1, i$ bumps i in P'_k and $i-1$ in P_k, then the configuration is preserved. However, if $i-1$ bumps i in P'_k and i bumps $i+1$ in P_k, the configuration changes, as shown in Figure 4.7.

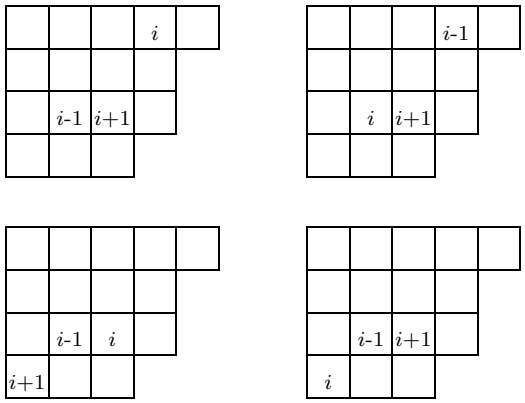

Figure 4.7: If the lower two enclosure elements end up in the same row, they must be side-by-side. If the third element also enters the same row, a new enclosure configuration results

The new configuration is still an enclosure, and P_k and P'_k can still be transformed into

one another by exchanging the corners of the enclosure. The configuration is now the same that was encountered with the first type of dual Knuth relation, so the values must stay in this configuration through any further insertions. Therefore, the theorem holds in all cases. □

Corollary 4.2.1 (Reifegerste [35]). *Positions $i-1$, i, and $i+1$ form a Knuth relation in a permutation if and only if the cells containing $i-1$, i, and $i+1$ form an enclosure in the corresponding recording tableau Q. Moreover, applying a Knuth transformation to positions $i-1$, i, and $i+1$ alters the recording tableau by swapping the corners of the enclosure formed by $i-1$, i, and $i+1$.*

Proof. If positions $i-1$, i, and $i+1$ form a Knuth relation in σ, then values $i-1$, i, and $i+1$ form a dual Knuth relation in σ^{-1}. Performing a Knuth transformation on positions $i-1$, i, and $i+1$ in σ is equivalent to inverting σ, applying a dual Knuth transformation on values $i-1$, i, and $i+1$ in σ^{-1}, and then inverting the result.

By Corollary 3.3.1, inversion of a permutation exchanges the insertion and recording tableaux. This corollary follows. □

Corollary 4.2.2 (Reifegerste [35]). *Applying a Knuth transformation changes* $\mathrm{inv}(Q)$ *by* ± 1*, and applying a dual Knuth transformation changes* $\mathrm{inv}(P)$ *by* ± 1.

An example of Theorem 4.2 and Corollary 4.2.1 is given in Figure 4.8.

$$\begin{pmatrix} 1 & 2 & 3 & 4 & 5 & 6 & 7 & 8 \\ 7 & 3 & 4 & 6 & 8 & 2 & 5 & 1 \end{pmatrix}$$

1	4	5	8
2	6		
3			
7			

1	3	4	5
2	7		
6			
8			

Figure 4.8: A permutation and the associated tableaux. The enclosures in the insertion tableau correspond to the values in dual Knuth relations in the permutation: $(2,3,4)$, $(4,5,6)$, and $(6,7,8)$. The enclosures in the recording tableau correspond to the positions in Knuth relations in the permutation: $(1,2,3)$, $(4,5,6)$, $(5,6,7)$, and $(6,7,8)$

It is also easy to show that enclosures are robust with regard to transformations on tableaux. The following proposition can be seen as a translation of properties of Knuth transformations and dual Knuth transformations (Knuth [27]) to the context of enclosures.

Proposition 4.3. *$i-1$, i and $i+1$ form an enclosure in P if and only if they also form an enclosure in P^E, P^T, and P^{ET}.*

Proof. The proof is trivial for transposition.

For evacuation, consider a permutation $\sigma \sim (P, Q)$. We also know that $\sigma^R \sim (P^T, Q^{ST}) = (P^T, Q^{ENT})$. If $\sigma(i) = j$ and $\sigma \in S_n$, then $\sigma^R(n-i+1) = j$. Any positions $p-1$, p and $p+1$ that originally formed a Knuth relation in σ will result in positions $n-p+2$, $n-p+1$, and $n-p$ forming a Knuth relation in σ^R. Positions which are *not* in a Knuth relation are similarly preserved. It follows that taking Q to (the decreasing, non-negated tableau) Q^{ET} preserves enclosures. As transposition preserves enclosures, evacuation must also preserve enclosures. □

4.2 Involutive Transformations

4.2.1 The Case for Involutions

We will next next introduce transformations on arc diagrams of involutions based on the Knuth transformations of permutations. Central to this section is Corollary 3.3.2, which states that involutions are in bijection with standard Young tableaux (i.e. the insertion and recording tableaux of an involution are identical).

Our motivation is to define local shape-preserving transformations on involutions in terms of arc diagrams. Involutions are the natural choice as they are in bijection with standard Young tableaux. A property of Knuth transformations which will be inherited by involutive transformations is that any two involutions with the same shape can be transformed into one another through a sequence of involutive transformations.

This property allows for a type of induction on the arc diagrams of involutions. For example, it can be shown that for every tableau shape, there as at least one non-crossing involution having that shape. A theorem can be proved for all involutions by first proving the result for non-crossing involutions (as a base case for each shape), and then showing that all involutive transformations preserve the result. Proving that involutive transformations preserve the result acts as the inductive step, and extends the theorem to all involutions.

Using this form of induction is, in fact, the method used to prove the main result of this thesis, Theorem 5.2. The rest of this chapter defines involutive transformations and gives a complete enumeration of involutive transformations in terms of the arc diagrams of

involutions.

4.2.2 Definitions and Enumeration

Let a permutation σ have a Knuth relation at (consecutive) positions $i-1$, i, and $i+1$ involving the respective values $\sigma(i-1)$, $\sigma(i)$, and $\sigma(i+1)$. Then by definition, its inverse σ^{-1} has a dual Knuth relation involving values $i-1$, i, $i+1$ at the (not necessarily consecutive) positions $\sigma(i-1)$, $\sigma(i)$, and $\sigma(i+1)$.

Let π be an involution. If the value at position j is $\pi(j)$, then the value at position $\pi(j)$ must be j. Consider a set $S = \{s_1, \ldots, s_k, \pi(s_1), \ldots, \pi(s_k)\}$. S contains between k and $2k$ numbers. In terms of the two-line array of π, for any i, $q_i \in S \Leftrightarrow p_i \in S$. In terms of the arc diagram defined by π, there is no arc with one endpoint in the set and the other outside. In other words, any such set is a sub-involution of π. (See Figure 4.9.)

$$\begin{pmatrix} 1 & 2 & 3 & 4 & 5 & 6 & 7 \\ 4 & 6 & 3 & 1 & 7 & 2 & 5 \end{pmatrix} \qquad \begin{pmatrix} 1 & 3 & 4 \\ 4 & 3 & 1 \end{pmatrix}$$

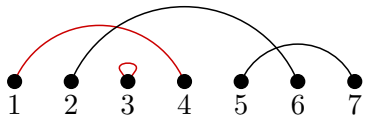

Figure 4.9: An involution and a sub-involution involving $(1, 3, 4)$

Because the insertion and recording tableaux of an involution are identical, they must contain exactly the same enclosures. Due to Theorem 4.2, this means that if positions $i-1$, i, and $i+1$ are in a Knuth relation, then the *values* $i-1$, i, and $i+1$ must be in a dual Knuth relation. Applying the Knuth transformation defined by $i-1$, i, and $i+1$ will swap the corners of the corresponding enclosure in the recording tableau, and applying the dual Knuth transformation defined by $i-1$, i, and $i+1$ will swap the corners in the insertion tableau (see Figure 4.10).

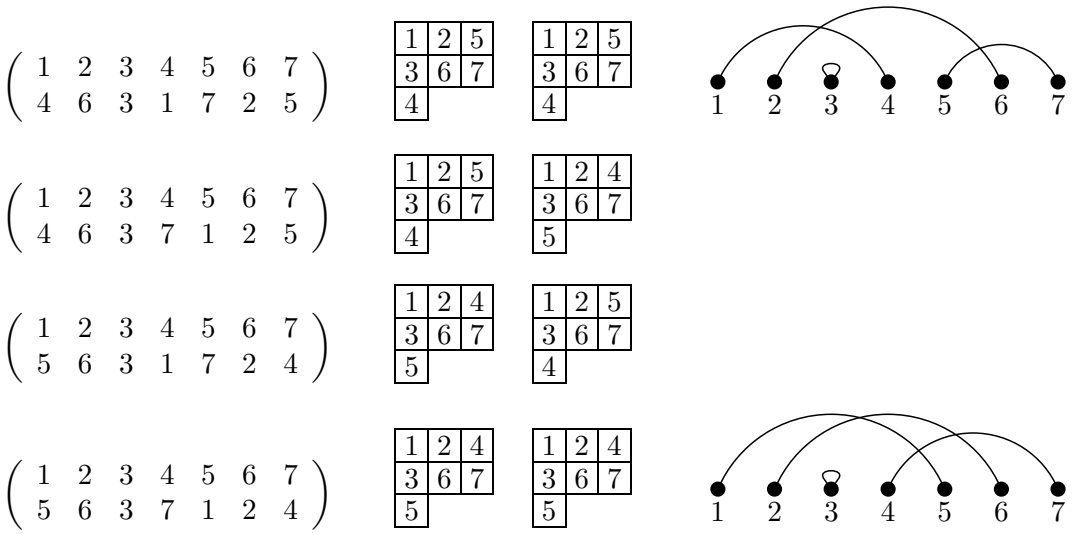

Figure 4.10: In the first row, an involution, its insertion tableau, recording tableau, and its arc diagram. In the second row, a Knuth transformation has been applied to the original involution at positions 3, 4, 5. In the third row, a dual Knuth transformation has been applied to the original involution at *values* 3, 4, 5. In the final row, both the Knuth and dual Knuth transformations have been applied. The tableaux are again identical, and the arc diagram of the resulting involution is shown

Because Knuth transformations change only the recording tableau, and dual Knuth transformations only the insertion tableau, applying a Knuth transformation to positions $i-1$, i, and $i+1$ does not remove the dual Knuth transformation at values $i-1$, i, and $i+1$ (and vice versa). If both transformations are applied (in either order), the same changes will be made to the insertion and recording tableaux, and a new involution will result.

We define such compound transformations as *involutive transformations*. More formally, if positions $i-1$, i, and $i+1$ form a Knuth transformation in an involution π, an involutive transformation on $i-1$, i, and $i+1$ consists of applying a Knuth transformation to positions $i-1$, i, and $i+1$ followed by a dual Knuth transformation to values $i-1$, i, and $i+1$. The result is another involution.

In terms of arc diagrams, an exhaustive examination reveals 10 involutive transformations up to left-to-right reflection, shown in Figure 4.11 below.

Involutive transformations inherit some useful properties from Knuth and dual Knuth transformations. The following theorem is key to the use of involutive transformations as a

form of induction.

Theorem 4.3. *Any two involutions whose tableaux have the same shape can be transformed into one another through a sequence of involutive transformations.*

Proof. The theorem is directly implied by Proposition 4.2. □

Finally, Figure 4.11 below provides a complete enumeration of involutive transformations in terms of arc diagrams, up to left-to-right reflection. They will be used in the following chapter in the proof of our main result, Theorem 5.2, as well as Proposition 5.1. They are also used throughout Chapter 6.

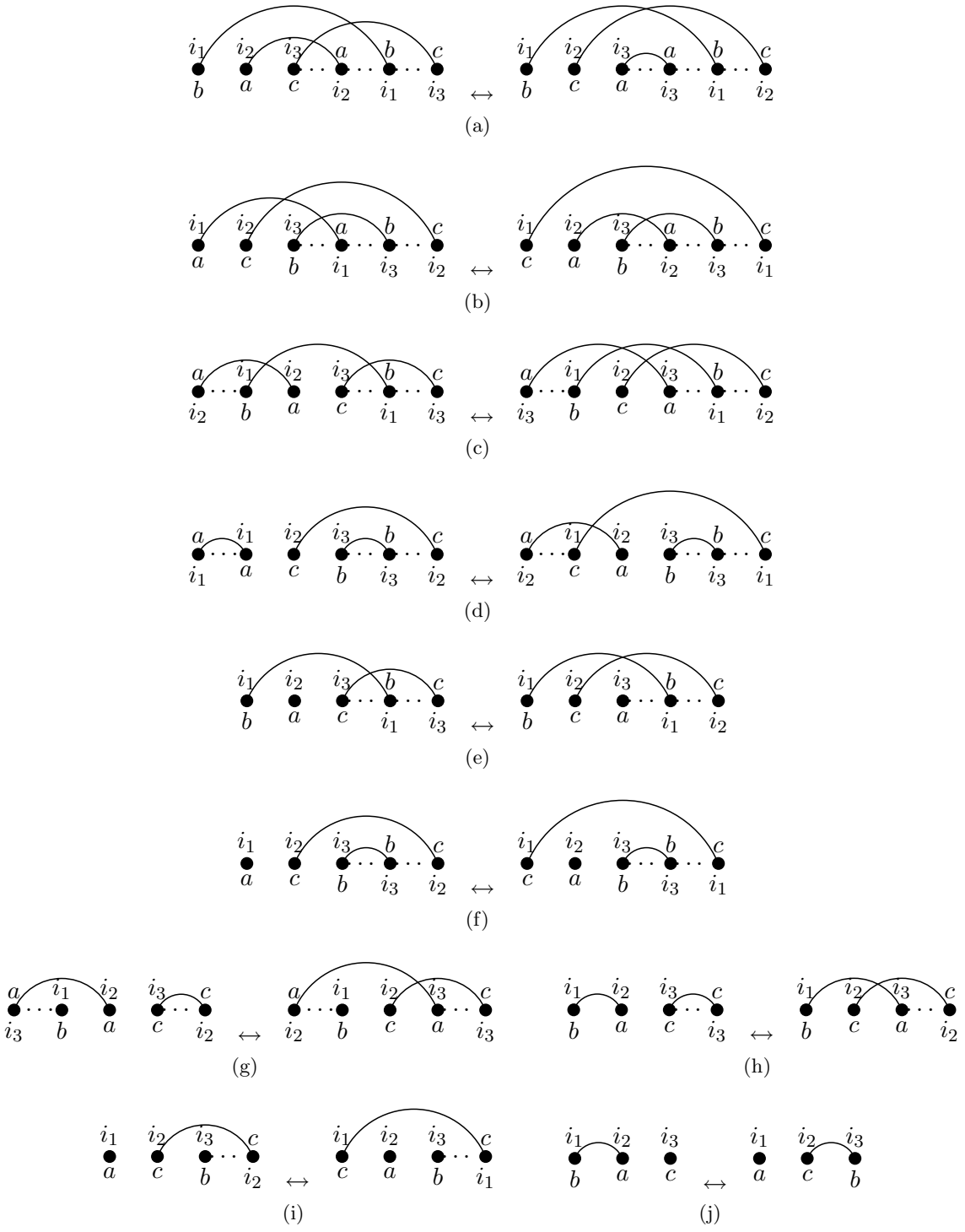

Figure 4.11: The 10 involutive transformations, up to left-to-right reflection

Chapter 5

A Greene-like Correspondence for Nestings

Greene proved in [22] a surprising result that links sets of increasing subsequences of a permutation to the shape of the corresponding Young tableaux given by the RSK construction, extending the work of Schensted [38]. Since then, similar results have been found for several variants of the RSK construction, such as the one described in [8] for set partitions.

In the present chapter, we first use involutive transformations to prove an analogous result that relates decreasing sequences in involutions and the k-nestings in the corresponding arc diagrams (Theorem 5.2). By way of Greene's result, this shows that the nestings of involutions directly correspond to the shape of its associated tableau.

We then extend these results to arc diagrams that represent set partitions for both the weak and strong nesting interpretations (Theorem 5.4). We also show a connection with permutations by surjection (Corollary 5.5.2), which both extends and gives an alternate proof to some of the results of Chen et al. [8]. The surjection from matchings to permutations is also examined in terms of involutive transformations in Proposition 5.1; the results of the proposition are later used in Section 6.4.

5.1 Greene's Result for Permutations

To state Greene's result, we first we need some notation. Given a permutation σ, let d_i be the maximal combined length of i disjoint decreasing subsequences of σ. Also let $d_0 = 0$,

and define the *maximal decreasing structure* of σ to be the vector $\mathrm{mds}(\sigma) = d_1 - d_0, d_2 - d_1, \ldots, d_i - d_{i-1}, \ldots$.

For example, the permutation $\sigma = 5416327$ has a decreasing sequence 5432, but there are no decreasing subsequences of longer length, so $d_1 = 4$. Similarly, the two disjoint decreasing subsequences 541 and 632 have a combined length of 6, and no other two disjoint decreasing subsequences can exceed this length, so $d_2 = 6$. All 7 elements of σ can be contained in three disjoint decreasing subsequences: 541, 632, and 7. Thus $d_3 = 7$, and $d_i = 7$ for $i > 3$ as well. Combining the results, $\mathrm{mds}(\sigma) = 4 - 0, 6 - 4, 7 - 6, 7 - 7, \ldots = 4, 2, 1, 0, 0, \ldots$.

Analogously define the *maximal increasing structure*, $\mathrm{mis}(\sigma)$, in terms of disjoint increasing subsequences of σ.

Theorem 5.1 (Greene [22])**.** *For any permutation* σ*,* $\mathrm{mis}(\sigma) = \mathrm{sh}(\sigma)$ *and* $\mathrm{mds}(\sigma) = \mathrm{sh}(\sigma)^T$

In other words, the maximal increasing structure of a permutation corresponds to its shape, and the maximal decreasing structure to the conjugate shape. This result generalizes in a very natural way Schensted's result [38] that the length of the longest increasing subsequence of a permutation is the length of the largest row of the corresponding Young tableaux shape.

5.2 Maximal Nesting Structures

Recall that a k-nesting is a set of k pairwise nested arcs. In this section, we interpret singletons within an involution to be $\frac{1}{2}$-*nestings*. Note that under this interpretation, a k-nesting involves $2k$ vertices, and thus corresponds to a decreasing subsequence of length $2k$. A k-nesting under this interpretation corresponds to a strong $\lfloor k \rfloor$-nesting and to a weak $\lceil k \rceil$-nesting. An example is given in Figure 5.1.

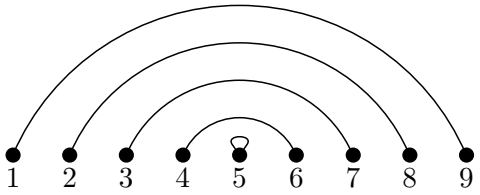

Figure 5.1: A 4.5-nesting

Our goal is a Greene-like result for matchings that relates the shape of a Young tableau to the k-nestings in the arc diagram of some class of objects. By Corollary 3.3.2, involutions are in bijection with standard Young tableaux, and thus are the natural class of objects to consider.

Given an involution π, let m_i be the maximal combined size of i disjoint k-nestings within π. Also let $m_0 = 0$, and define the *maximal nesting structure* of π to be the vector $\mathrm{mns}(\pi) = m_1 - m_0, m_2 - m_1, \ldots, m_i - m_{i-1}, \ldots$. Also define a *certificate of* m_i to be any maximal set of i disjoint k-nestings with combined size m_i.

With these definitions, we can state our main results, which are proved together.

Theorem 5.2. *For any involution* π, $\mathrm{mds}(\pi) = 2\mathrm{mns}(\pi) = 2(m_1 - m_0), \ldots, 2(m_i - m_{i-1}), \ldots$.

Theorem 5.3 (Odd column property)**.** *Let* π *be an involution corresponding to the SYT* P*, and let* o_i *be the number of columns of odd height from the first* i *columns of* P*. Any certificate of* m_i *must contain* o_i *singletons.*

Proof. Note that by Greene's result, if an involution π corresponds to the SYT P, then $\mathrm{mds}(\pi) = \mathrm{sh}(\pi)^T$. Therefore Theorem 5.2 states that all involutions with the same shape also have the same maximal nesting structure.

We prove both theorems using the same method. First, we show that the theorems hold for at least one involution of each shape. Next, we show that involutive transformations preserve the results. This form of induction is possible due to Theorem 4.3, which states that any two involutions with the same shape can be transformed into one another through a sequence of involutive transformations.

For the base case, consider an involution π which consists of a sequence of j k-nestings, such that the ith nesting is a k_i-nesting. Moreover, order the sequence of k-nestings such that $k_i \geq k_{i+1}$. In terms of a permutation, the ith k-nesting is a decreasing sequence of length $2k_i$ such that all elements are greater than those in the $(i-1)$th nesting and less than those in the $(i+1)$th nesting. The result is that each k-nesting in the sequence corresponds directly to a column in the standard Young tableau. More specifically, the ith k-nesting, which is a k_i-nesting, corresponds to the ith column from the left, which contains $2k_i$ cells. Therefore, both theorems hold. An example is given in Figure 5.2.

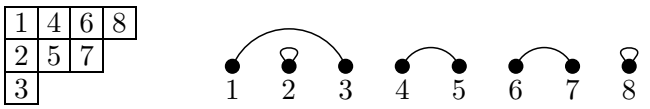

Figure 5.2: The unique SYT with maxInv(λ) inversions for $\lambda = 4, 3, 1$ and the corresponding involution

For the inductive case, we can show that the involutive transformations preserve both the maximal nesting structure and the odd column property. As an example, the proof for Involutive Transformation 4.11a follows.

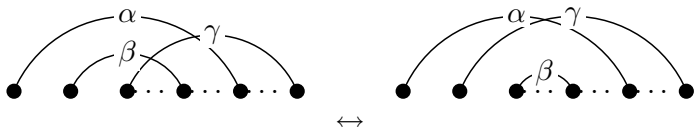

Figure 5.3: Involutive Transformation 4.11a with labeled arcs

Consider Figure 5.3. The only difference between the two involutions is that arc β is nested inside of arc γ on the right, but not on the left. We need to show that we can preserve the certificates of m_l, for any l, when transforming the right hand side to the left hand side. (Recall that a certificate of m_l is a set of l k-nestings.)

If γ and β are not contained within the same k-nesting on the right, the certificate is trivially preserved.

Next we consider certificates in which both γ and β appear in the same k-nesting. No other arcs in the k-nesting may appear between γ and β, as their left endpoints are adjacent. Therefore, any such k-nesting consists of some number of arcs nested above γ, then γ, β, and some number of arcs nested below β. We represent this k-nesting by $G^+\gamma\beta B^-$.

That fact that the left endpoints of α and γ are adjacent also means that any arcs which are nested above γ are also nested above α, and any arcs which are nested below α are also nested below γ.

In the first case, consider certificates which do not contain α. α is nested above β in the arc diagram as well, so for these certificates, we can simply replace γ with α to obtain another certificate of the same size that does not have γ and β in the same k-nesting.

For the second case we must consider certificates that contain both α and $G^+\gamma\beta B^-$. α must be part of a different k-nesting than $G^+\gamma\beta B^-$, as α crosses γ. We represent the

k-nesting containing α by $A^+\alpha A^-$, where A^+ are arcs in the k-nesting which are above α, and A^- are those which are below α. For any such certificate, we replace the k-nestings $G^+\gamma\beta B^-$ and $A^+\alpha A^-$ by two new k-nestings $G^+\gamma A^-$ and $A^+\alpha\beta B^-$. The k-nestings are valid as β is nested below α, and any arc nested below α must also be nested below γ.

In either case, in the new certificate α and γ are not in the same k-nesting, and thus it is preserved on the left side as well as the right side. This proves that Involutive Transformation 4.11a preserves $\mathrm{mns}(\pi)$.

The proofs for the other 9 involutive transformations are analogous. Because the number of singletons in each certificate is preserved, the odd column property is also preserved. The odd column property must hold in the base case and it is always possible to reach a base case through a sequence of involutive transformations, and therefore the odd column property must always hold. □

Remark: An alternative proof of Theorem 5.2 is possible using permutation matrices. The key facts are that involutions are reflective around the main diagonal, and that k-nestings correspond to decreasing subsequences that are also reflective around the main diagonal.

Corollary 5.3.1 (Schützenberger [40])**.** *The number of singletons in an involution corresponds to the number of odd columns in its shape.*

Note: The odd column property is a refinement of Corollary 5.3.1. Corollary 5.3.1 is itself a well-known result of Schützenberger [40]. A more direct proof of this result was also given by Beissinger [1].

5.3 Set Partitions, Matchings, and Permutations

The results of the previous section are important in that they provide a Greene-like result between nestings in involutions and the shape of the same involutions under RSK. However, maximal nesting structure is defined in terms of $\frac{1}{2}$-nestings. Our goal in this section is to both extend the results to the larger class of set partitions, and to restate the results in terms of weak nestings and strong nestings, as is conventional.

This section relies heavily on the surjections of Section 2.1.4. Recall that $\check{\eta}(\nu)$ is a surjection to involutions which preserves strong crossings and all nestings; $\hat{\eta}(\nu)$ is a surjection to involutions which preserves weak crossings and all nestings; $\check{h}(\nu)$ is a surjection to matchings

which preserves strong nestings and crossings; and $\hat{h}(\nu)$ is a surjection to matchings which preserves weak nestings and crossings.

The following theorem gives results for set partitions in the $\frac{1}{2}$-nesting, strong nesting, and weak nesting interpretations.

Theorem 5.4. *For any set partition ν,*

$$\begin{aligned}
\mathrm{mns}(\nu) &= \mathrm{mns}(\check{\eta}(\nu)) = \mathrm{mns}(\hat{\eta}(\nu)) \\
\mathrm{mns}(\check{h}(\nu)) &= \lfloor \mathrm{mns}(\nu) \rfloor = \lfloor m_1 - m_0 \rfloor, \ldots, \lfloor m_i - m_{i-1} \rfloor, \ldots \\
\mathrm{mns}(\hat{h}(\nu)) &= \lceil \mathrm{mns}(\nu) \rceil = \lceil m_1 - m_0 \rceil, \ldots, \lceil m_i - m_{i-1} \rceil, \ldots \\
2\mathrm{mns}(\nu) &= \lfloor \mathrm{mns}(\nu) \rfloor + \lceil \mathrm{mns}(\nu) \rceil
\end{aligned}$$

Proof. The first equation is trivially true, as $\check{\eta}(\nu)$ and $\hat{\eta}(\nu)$ do not alter k-nestings in any way. This extends Theorem 5.2 to set partitions under the $\frac{1}{2}$-nesting interpretation.

$\check{h}(\nu)$ changes k-nestings into $\lfloor k \rfloor$-nestings, and $\hat{h}(\nu)$ changes them into $\lceil k \rceil$-nestings. The odd column property allows us to extend this to the maximal nesting structure as a whole, as $m_i - m_{i-1}$ is not an integer if and only if certificate m_i involves one more singleton than certificate m_{i-1}.

Therefore the second equation states that the maximal nesting structure of a set partition ν under the strong nesting interpretation is $\lfloor \mathrm{mns}(\nu) \rfloor$. Similarly, under the weak nesting interpretation, it is $\lceil \mathrm{mns}(\nu) \rceil$.

The final equation is true as $2(m_i - m_{i-1})$ is always an integer, so $2(m_i - m_{i-1}) = \lfloor m_i - m_{i-1} \rfloor + \lceil m_i - m_{i-1} \rceil$. □

The above theorem describes the maximal nesting structures of a set partition ν purely in terms of matchings ($\hat{h}(\nu)$ or $\check{h}(\nu)$ for the weak and strong interpretations, respectively).

We next follow the lead of Chen et al. [8] and show a connection between the maximal nesting structure of a matching μ and the maximal decreasing structure of a permutation $f(\mu)$. The following theorem can be considered a special case of Corollary 5.5.2 below; as later noted, Corollary 5.5.2 includes one of the results of Chen et al. [8]. We provide an alternate proof that uses the relatively simple connection between the Ferrers filling and the permutation matrix of a matching.

Theorem 5.5 (Chen et al. [8])**.**

$$\mathrm{mns}(\mu) = \mathrm{mds}(f(\mu)) \qquad (\mu \in M_{2n})$$

Proof. Recall the relationship between a matching μ and its Ferrers filling. The Ferrers filling corresponds to the upper triangular half of the permutation matrix of μ. A k-nesting in the matching is in bijection with a decreasing subsequence in the upper half of the permutation matrix, as can be evidenced in the Ferrers filling. (See Figure 5.4.)

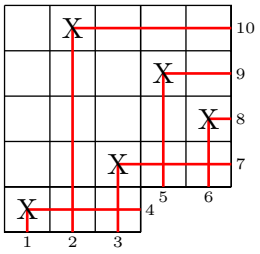

Figure 5.4: A Ferrers filling of a matching, with arcs

$f(\mu)$ is defined by extending the Ferrers filling of μ to be an $n \times n$ permutation matrix. The contents of the filling are not changed, and thus the decreasing subsequences of $f(\mu)$ correspond to the decreasing subsequences in the upper half of the permutation matrix of μ, which in turn are in bijection with the k-nestings of μ. □

The theorem implies that applying involutive transformations to a matching μ does not change the shape of $f(\mu)$. The following proposition (a new result) makes the relationship more explicit, and is later used in Section 6.4.

Proposition 5.1. *Given a matching μ,*

1. *applying Involutive Transformations 4.11a or 4.11b to μ applies a Knuth transformation on $f(\mu)$,*

2. *applying the reflections of Involutive Transformations 4.11a or 4.11b to μ applies a dual Knuth transformation on $f(\mu)$,*

3. *all other involutive transformations on μ have no effect on $f(\mu)$.*

Proof. We originally formulated $f(\mu)$ in terms of the Ferrers filling of μ. To prove the proposition, we note some properties of the surjection. Figure 5.5 is included for reference.

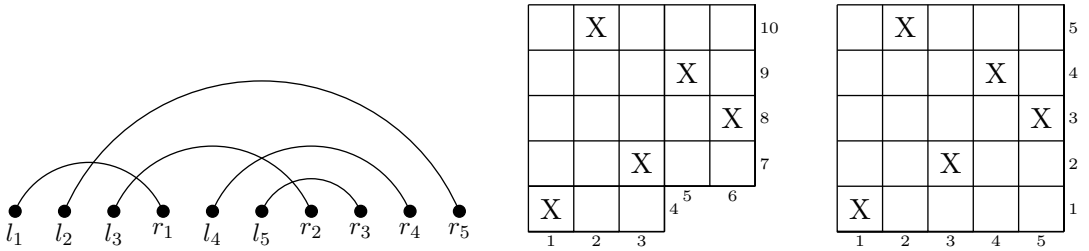

(a) A matching μ with labeled left and right endpoints

(b) The Ferrers filling of μ

(c) The permutation matrix of $f(\mu)$

Figure 5.5: The relationship between μ and $f(\mu)$ for a matching μ

Let $\mu \in M_{2n}$ be a matching and let $f(\mu) = \sigma \in S_n$. Label the left endpoints of μ from left to right as $l_1, \ldots, l_n$, and label the right endpoints from left to right as $r_1, \ldots, r_n$. The key property is that $\sigma(i) = j$ if and only if there is an arc between l_i and r_j in μ.

Involutive Transformations 4.11a and 4.11b involve three consecutive left endpoints l_{i-1}, l_i, and l_{i+1}, two of which are exchanged. Due to the above property and the definition of involutive transformations, positions $i-1$, i, and $i+1$ form a Knuth transformation in σ. Applying the involutive transformation to μ results in the Knuth transformation being applied in σ.

Similarly, the reflections of Involutive Transformations 4.11a and 4.11b involve three consecutive *right* endpoints, which correspond to a dual Knuth relation in σ.

Involutive Transformations 4.11c, 4.11d, 4.11h, and their reflections exchange the positions of a left and a right endpoint, and this has no affect on σ as shown by the property above. (The relative positions of all left points is not affected, nor is the relative positions of all right points.)

The remaining transformations do not apply to matchings, and thus the proof is complete. □

Next, we state two corollaries of the preceding theorems. Corollary 5.5.1 is new, and Corollary 5.5.2 is partially new (as discussed following the proof).

Corollary 5.5.1.

$$\mathrm{mds}(\pi) = 2\mathrm{mns}(\pi) = \mathrm{mds}(\check{f}(\pi)) + \mathrm{mds}(\hat{f}(\pi)) \qquad (\pi \in I_n) \qquad (5.1)$$

$$\mathrm{mds}(\mu) = 2\mathrm{mns}(\mu) = 2\mathrm{mds}(f(\mu)) \qquad (\mu \in M_{2n}) \qquad (5.2)$$

Corollary 5.5.2.

$$\lfloor \mathrm{mns}(\nu) \rfloor = \mathrm{mns}(\check{h}(\nu)) = \mathrm{mds}(\check{f}(\nu)) \qquad (\nu \in P_n) \tag{5.3}$$

$$\lceil \mathrm{mns}(\nu) \rceil = \mathrm{mns}(\hat{h}(\nu)) = \mathrm{mds}(\hat{f}(\nu)) \qquad (\nu \in P_n) \tag{5.4}$$

Proof. Equation 5.1 follows from Theorems 5.2 and 5.4.

Equation 5.2 follows from Equation 5.1, as for matchings μ, $\check{f}(\mu) = \hat{f}(\mu) = f(\mu)$.

Corollary 5.5.2 follows from Theorems 5.4 and 5.5. □

The practical result is that the maximal nesting structures of matchings can be described in terms of their Ferrers fillings. In combination with the previous results, the maximal nesting structures of set partitions under the weak or strong interpretations can also be described in terms of Ferrers fillings after applying the surjections of Section 2.1.4.

Note: Recall that $\check{h}(\nu)$ corresponds to the strong nesting interpretation of a set partition. In [8] (Proposition 8 and Corollary 9), Chen et al. use the machinery of vacillating tableaux to prove (using a different notation) that

$$\mathrm{mns}(\check{h}(\nu)) = \mathrm{mds}(\check{f}(\nu)^{-1}) \quad (\nu \in P_n) \tag{5.5}$$

Inversion of a permutation preserves the maximal decreasing structure, so this is equivalent to the second equality of Equation 5.3.

Corollary 5.5.2 provides an alternate proof Chen et al.'s result, and also gives an analogous result for the weak nesting interpretation. Additionally, it extends the result to show an explicit connection with the $\frac{1}{2}$-nesting interpretation ($\lfloor \mathrm{mns}(\nu) \rfloor$ and $\lceil \mathrm{mns}(\nu) \rceil$).

The authors also state that "[i]t would be interesting to get a result for $cr_r(P)$ [(maximal crossing structure)] analogous to Corollary 9." However, as the shape of an involution is determined completely by its maximal nesting structure while the maximal crossing structure varies, this seems unlikely in the general case.

The exception is for $\beta \in BM_{2n}$. Similar to decreasing subsequences and nestings, $g(\sigma)$ translates increasing subsequences in permutation σ to crossings in $g(\sigma)$. That is, $\mathrm{mcs}(g(\sigma)) = \mathrm{mis}(\sigma) = \mathrm{sh}(\sigma)$ where mcs represents maximal crossing structure.

Chapter 6

Knuth Graphs

In Chapter 4 we used the results of Knuth [27] and Reifegerste [35] to show that all standard Young tableaux of a constant shape can be transformed into one another through a sequence of transformations on enclosures within the tableaux.

In this section, we use the enclosure transformations to define graphs on Young tableaux of a constant shape. The graphs can be interpreted as the Hasse diagram of a poset; two examples of such posets are given. Some graph theoretical properties are also explored, with the aid of involutive transformations.

To the best of our knowledge, these graphs are unexplored in the literature. In Section 6.3 we prove some results for special shapes of Young tableaux.

6.1 Introducing Knuth Graphs

Consider a graph on all involutions of a given shape λ, where there is an edge between two involutions if and only if they differ by a single involutive transformation. We define such a graph to be K_λ. K_λ is equivalent to a graph on all SYTs with shape λ. Under this interpretation, the edges correspond to two SYT that can be transformed into one another by swapping the corners of an enclosure. By Corollary 4.2.1, K_λ can also be considered to be a graph on Knuth-equivalent permutations, wherein the edges correspond to Knuth transformations.

As transposition of a Young tableau preserves enclosures, K_λ is isomorphic to K_{λ^T}. If $\lambda = \lambda^T$, then K_λ is automorphic around transposition. Evacuation and negation of a Young tableau preserves the shape of the tableau, and corresponds to the left-to-right reflection

of the arc diagram of an involution, as shown in Figure 6.1. The values of the enclosures are negated, but still exist, so K_λ (for any shape λ) is automorphic around evacuation and negation. Examples of Knuth graphs appear in Figures 6.3 and 6.4.

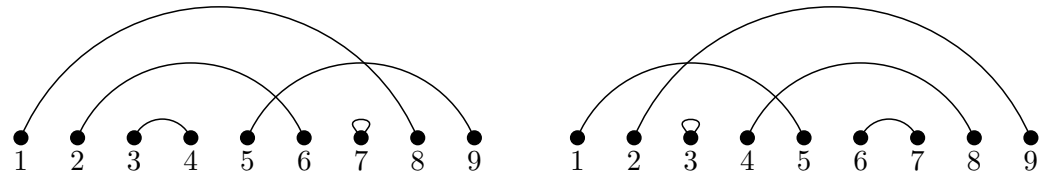

(a) An involution $\pi \sim (P, P)$ (b) $\pi^{RN} \sim (P^S, P^S)$

Figure 6.1: Reflecting the arc diagram of an involution is equivalent to evacuating and negating the tableau

6.2 Posets

The study of *partially ordered sets* or *posets* is an active research area. We refer the interested reader to the works of Stanley [43, 44].

First, let us introduce some terminology of posets. A poset is a tuple $(S, \leq)$ where S is a set and $\leq$ is a reflexive, antisymmetric, and transitive relation. The relation does not need to apply to all pairs of elements in S. s_2 *covers* s_1 if $s_1 < s_2$ and there does not exist any element x such that $s_1 < x < s_2$. The *Hasse diagram* of a poset is a graph wherein the vertices are elements of S, and there is an edge between x and y if and only if y covers x.

x is a *maximal element* of the poset if there does not exist a $y \in S$ such that $x < y$; *minimal elements* are analogously defined. A poset has a *least element* x if $x \leq y$ for all $y \in S$. *Greatest element* is analogously defined. A *bounded poset* is a poset with both a least and greatest element.

A *graded poset* is a poset with a rank function $\rho : S \to \mathbb{Z}$ such that if $x \leq y$, then $\rho(x) \leq \rho(y)$. A *ranked poset* has the additional property that all maximal elements have the same rank, and all minimal elements have the same rank. A bounded, graded poset is necessarily ranked, and has the property that any three elements in the Hasse diagram can be contained in a single path.

It is possible to define statistics on Young tableaux which change by ± 1 whenever the corners of an enclosure are swapped. As a result, Knuth graphs can be interpreted as the

Hasse diagram of a graded poset defined by both the statistic (which acts as a rank function), and the restriction that tableau P covers tableau Q if and only if they differ only by a swap of the corners of an enclosure.

One such statistic which applies to any shape λ is the number of inversions within the tableau, as discussed in Section 4.1.2. We refer to this poset as the inversion poset. Although for any shape λ there is only one SYT with $\text{inv}(P) = \text{maxInv}(\lambda)$ and one with $\text{inv}(P) = 0$, the poset is not necessarily ranked, as demonstrated in Figure 6.2. In fact, there exist Knuth graphs which cannot be the Hasse diagram of *any* bounded and graded poset, as noted in Figure 6.3. However, the poset may be ranked in special cases, as discussed in Section 6.3.1.

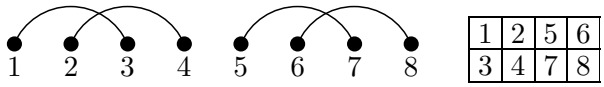

Figure 6.2: An involution and the corresponding SYT P; $\text{inv}(P) = 4$. There are four enclosures in the tableau, two of which have the corners 2 and 3, and two of which have the corners 6 and 7. Swapping 2 and 3 or swapping 6 and 7 would both increase the number of inversions. Therefore, P is minimal in the inversion poset, even though $\text{inv}(P) > 0$, and thus the poset is not ranked

If we restrict λ to have columns of even height, we can define statistics in terms of matchings. There are only 5 involutive transformations (up to reflection) for matchings, namely 4.11a, 4.11b, 4.11c, 4.11d, and 4.11h. Clearly, each of these transformations changes the number of crossings by 1. Therefore, the number of crossings defines another poset corresponding to K_λ when all columns of λ have even height. We refer to this poset as the crossing poset. In general the number of crossings does not equal the number of inversions (or its complement), as shown in Figure 6.3. However, they are related in special cases, as discussed in Section 6.3.3.

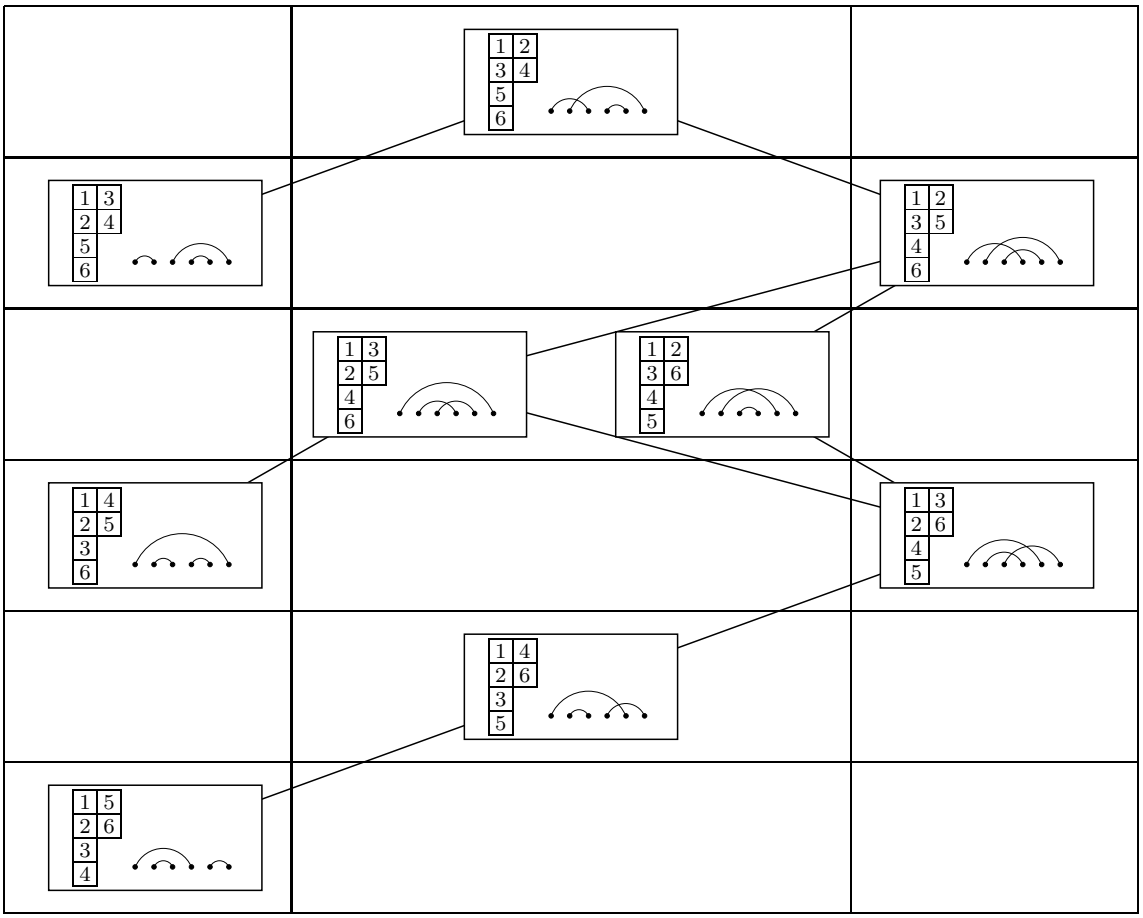

Figure 6.3: The inversion poset and the crossing poset as defined on K_λ, $\lambda = 2, 2, 1, 1$. The number of crossings increases from 0 to 2, left to right. The number of inversions increases from 0 to 5, top to bottom. The two posets are not isomorphic; for example the crossing poset has 4 minimal elements, while the inversion poset has 1. Also note that the three non-crossing involutions have degree 1. Therefore, no single path can contain them, and thus K_λ cannot be the Hasse diagram of any bounded, graded poset

6.3 Special Shapes

By restricting the class of Young tableaux to specific shapes, we can find specialized results on Knuth graphs which are not applicable in the general case.

6.3.1 Hook Shapes and Young's Lattice

There is a bijection between Young's lattice and Knuth graphs in certain cases. Let $\rho_{r,c}$ be a rectangular integer partition with r rows and c columns, and let $Y_{\rho_{r,c}}$ be the sublattice of Young's lattice induced by the Ferrers diagrams contained within $\rho_{r,c}$. Let $R_{r,c}$ be the L-shaped integer partition

$$(c+1)\overbrace{11\ldots1}^{r \text{ copies}}$$

(which has $r+1$ rows and $c+1$ columns), and $K_{R_{r,c}}$ be the Knuth graph of $R_{r,c}$. (Shapes conforming to $R_{r,c}$ are also referred to as *hook shapes*.) We then have the following theorem.

Theorem 6.1. *There is a bijection between SYTs with shape $R_{r,c}$ and partitions contained within $\rho_{r,c}$ which preserves the edges of $Y_{\rho_{r,c}}$ and $K_{R_{r,c}}$.*

Proof. The bijections are as follows. Define a grid G from $(1,1)$ to $(r+1, c+1)$, with an SYT of shape R in the northwest corner such that it fills column and row 1. For all $1 < i \leq r+1$, $1 < j \leq c+1$, the positions (i,j) are marked as full or empty. If positions $(i,1)$ and $(1,j)$ form an inversion in the SYT, then mark position (i,j) as full; else as empty. The full positions define an integer partition contained within $\rho_{r,c}$, with the origin to the northeast. (See Figure 6.4 for an example.)

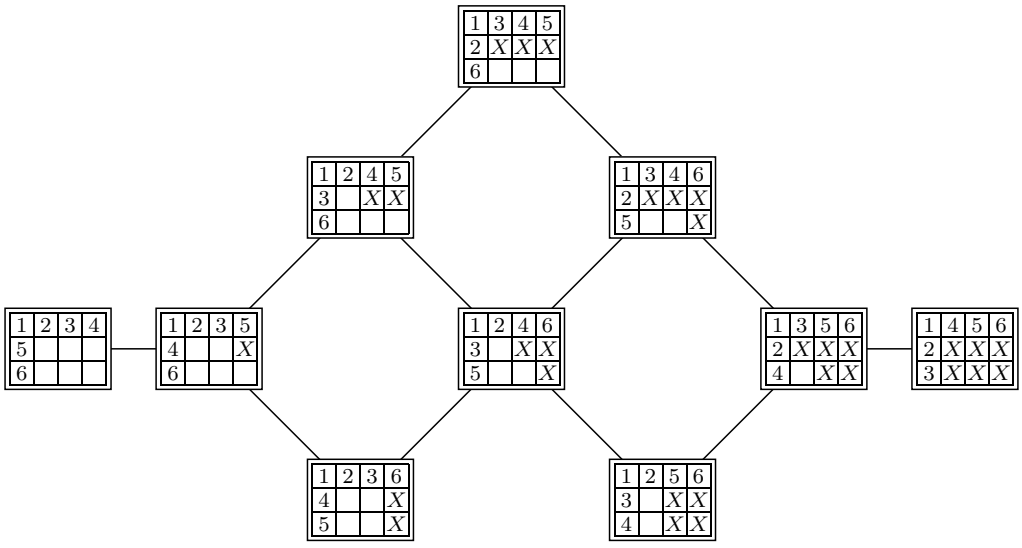

Figure 6.4: An example with $r = 2$, $c = 3$

First we show that the vertices are in bijection. Let $i' < i$ and let $j' > j$. Then $(i', 1) < (i, 1)$ and $(1, j') > (1, j)$. Therefore if $(i, 1)$ and $(1, j)$ are inverted, so are $(i', 1)$ and $(1, j')$. This shows that the shape defined by the marked positions is a Ferrers diagram.

Following an edge in a Knuth graph changes the number of inversions in the corresponding SYT by 1, so edges in $K_{R_{r,c}}$ correspond to edges in $Y_{\rho_{r,c}}$.

It remains to show that edges in $Y_{\rho_{r,c}}$ also correspond to edges in $K_{R_{r,c}}$. Let position (i, j) be a corner in the Ferrers diagram. Then $(1, j-1) < (i, 1) < (1, j) < (i+1, 1)$. If $(i, 1)$ and $(1, j)$ are exchanged, the result will still be a SYT. We need to show that $(i, 1)$ and $(1, j)$ are the corners of an enclosure; that is, we must prove that $(1, j) - (i, 1) = 1$.

The proof is by contradiction. Assume that there exists a value x such that $(i, 1) < x < (1, j)$. If x is at location $(i', 1)$, then $i' > i$ and position (i', j) must be filled. But this contradicts with (i, j) being a corner in the Ferrers filling. Similarly, x cannot be at any position $(1, j')$.

Therefore we must have $(i, 1) = k$ and $(1, j) = k + 1$ for some $k > 1$. $k - 1$ must be above $(i, 1)$ or to the left of $(1, j)$, so $(i, 1)$ and $(1, j)$ form an enclosure and thus correspond to an edge in $K_{R_{r,c}}$.

□

6.3.2 Crossings and Inversions in Non-nesting Matchings

Here we show that the crossing poset and inversion poset are isomorphic in the special case of non-nesting matchings, modulo a complement of rank.

Note that by Theorem 5.2, the standard Young tableau corresponding to a non-nesting matching is a two row tableau having shape $\lambda = n, n$.

Lemma 6.1. *Given a non-nesting matching μ that corresponds to the standard Young tableau P, i is at position $(1, k)$ in P and j is at position $(2, k)$ if and only if there is an arc between i and j in the arc diagram of μ.*

Proof. We prove the lemma by considering the recording tableau during the RSK algorithm. Recall that the value of the left endpoint of an arc is the position of the right endpoint, and vice versa.

When the value of a left endpoint is inserted, it must be larger than any other value seen beforehand. A left endpoint must have a value greater than any previous right endpoint (in any arc diagram), and it must also have a value greater than that of any previous

left endpoint (or it would be nested underneath the arc associated with the previous left endpoint). Therefore, the values of left endpoints enter the Young tableau at the far end of the top row, and do not bump any elements.

The shape of the final tableau is (n, n), which implies that the values of the right endpoints always bump elements. A right endpoint must similarly have a value greater than any previous right endpoint, and thus the position of bumped elements in the top row must proceed from left to right. Together, these observations imply that the final tableau will consist of the values of the right endpoints (the positions of the left endpoints) from left to right in the top row, and of the values of the left endpoints (the positions of the right endpoints) from left to right in the bottom row.

In order to avoid nesting, the kth left endpoint from the left must be connected by an arc to the kth right endpoint from the left. This completes the proof. □

Figure 6.5 gives an example of the lemma.

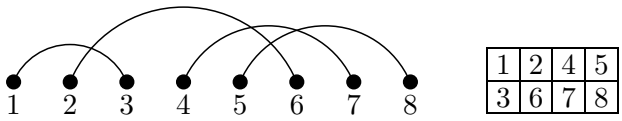

Figure 6.5: A non-nesting matching with arcs $(1, 3)$, $(2, 6)$, $(4, 7)$, and $(5, 8)$ corresponds to the standard Young tableau with columns $(1, 3)$, $(2, 6)$, $(4, 7)$, and $(5, 8)$

Theorem 6.2. *Given a non-nesting matching $\mu \in M_{2n}$ that corresponds to the standard Young tableau P, the number of crossings in μ is $\binom{n}{2} - \mathrm{inv}(P)$.*

Proof. A non-nesting matching with n arcs has shape $\lambda = n, n$. By definition, every one of the $\binom{n}{2}$ pairs of arcs are either crossing or in alignment. There are also $\sum_{1 \le i < n} i = \binom{n}{2}$ possible inversions in λ.

Consider two arcs (i, i') and (j, j') with $i < j$. These arcs correspond to two columns with i above i' and j above j'. By the properties of Young tableaux, $i' < j'$.

If there is an inversion between the two columns, then $i < i' < j < j'$. In terms of the arc diagram, the two arcs must form alignment. (See Figure 6.6.)

If there is not an inversion, then $i < j < i' < j'$. In terms of the arc diagram, the two arcs must cross.

Therefore, a non-nesting matching on $[2n]$ whose corresponding SYT has c inversions must have c alignments and thus $\binom{n}{2} - c$ crossings.

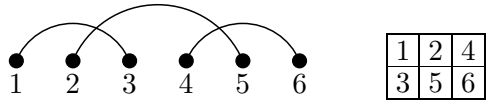

Figure 6.6: 3 and 4 are inverted, and the corresponding arcs (13) and (46) are in alignment. 3 and 2 are not inverted, and the corresponding arcs (13) and (25) are crossed

□

6.3.3 Knuth Graph Diameter of Non-nesting Involutions

We next consider the two row shape $(k + c), k$ with $c > 0$. By Theorem 5.2, these tableaux correspond to weakly non-nesting involutions with c singletons and k non-singleton arcs. Figure 6.7 gives an example.

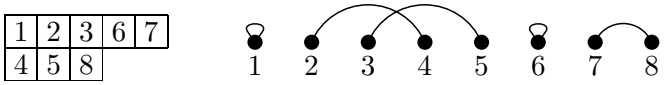

Figure 6.7: A standard Young tableau with shape $5, 3 = (3 + 2), 3$, and corresponding involution with 2 singletons and 3 non-singleton arcs

Theorem 6.3. *Let λ be a two row shape $(k + c), k$ with $c > 0$. Then the diameter of K_λ is $k(k + c - 1)$.*

Proof. Consider the length of the path between the involution with c singletons to the right of a k-crossing and the one with c singletons to the left of a k-crossing, as demonstrated in Figure 6.8.

Figure 6.8: An example for k = 3 and c = 2. The path between these two involutions has length $k(k + c - 1) = 12$

Because there are no weak nestings, the only involutive transformation that can change

the position of the singletons is Involutive Transformation 4.11j. Involutive Transformation 4.11j allows a singleton to "jump" a non-singleton arc, but only if both endpoints of the non-singleton arc are immediately adjacent to the singleton; in other words, the arc must not be crossed by any other arc.

An arc can be removed from a m-crossing by one application of Involutive Transformation 4.11c followed by $m-2$ applications of Involutive Transformation 4.11d (or their reflections); thus an entire m-crossing can be deconstructed (or reconstructed) in $\binom{m}{2}$ transformations.

The total number of transformations required for the path described is $\binom{k}{2}$ to deconstruct the k-crossing, ck to move each of the c singletons over all k non-singleton arcs, and then another $\binom{k}{2}$ to reconstruct the k-crossing. The total is $k(k-1)+ck = k(k+c-1)$, giving a lower bound for the diameter of the path.

An m-crossing consists of m pairwise crossing arcs, and thus consists of $\binom{m}{2}$ total crossings. This is maximum number of crossings possible in an arc diagram with m non-singleton arcs. Because there are no weak nestings, it is always possible to use Involutive Transformation 4.11c or 4.11d to reduce the number of crossings present, if any. Therefore $\binom{k}{2}$ is the maximum number of transformations needed to deconstruct (or construct) any arc crossings in the arc diagram. Likewise, ck is the maximum number of transformations needed to move the singletons, as this involves moving every singleton to the opposite side of every non-singleton arc. Therefore, $k(k+c-1)$ is also the maximum path in, and thus the diameter of, K_λ.

□

It is also interesting to note that the difference between the diameter and the number of possible inversions is independent of the number of singletons.

The number of possible inversions is

$$\sum_{i=c}^{k+c-1} i = \frac{k(k+2c-1)}{2} \tag{6.1}$$

And the difference is

$$\frac{2k(k+c-1)}{2} - \frac{k(k+2c-1)}{2} = \frac{k^2-k}{2} = \binom{k}{2} \tag{6.2}$$

When $c=0$, i.e. for matchings, $\binom{k}{2}$ is still a valid lower bound for the diameter, and

$2\binom{k}{2} = k(k-1)$ is still a valid upper bound. However these bounds are not tight. Empirically, the diameter appears to be closer to $\binom{k}{2}$ than $2\binom{k}{2}$, yet is not always equal to $\binom{k}{2}$.

6.4 Permutations and Knuth Graphs

Given two permutations with the same shape λ, Proposition 4.2 states that it is possible to transform them into each other through a sequence of Knuth transformations and dual Knuth transformations. Knuth relations correspond to enclosures in the recording tableau and dual Knuth transformations to those in the insertion tableau. Therefore the graph of all Knuth and dual Knuth transformations for permutations of shape λ is the box product of K_λ with itself, $K_\lambda \square K_\lambda = K_\lambda^2$.

K_λ^2 also appears within the Knuth graphs of shapes related to λ.

Theorem 6.4. *Given a shape λ with column heights $(c_1, c_2, \ldots, c_k)$, let μ be the shape with column heights $(2c_1, 2c_2, \ldots, 2c_k)$. Then K_μ contains an induced copy of K_λ^2.*

Proof. Recall the bijection g between permutations on $[n]$ and balanced matchings on $[2n]$. Let the permutation $\sigma \sim (P, Q)$ be in bijection with the balanced matching $\beta \sim (R, R)$. By Theorem 5.2, the column heights of R are exactly twice those of P.

Also recall that $f(\beta) = g^{-1}(\beta)$ for $\beta \in BM_{2n}$. By Proposition 5.1, applying Involutive Transformations 4.11a or 4.11b to β applies a Knuth transformation to $g^{-1}(\beta)$, and applying the reflections of 4.11a or 4.11b to β applies a dual Knuth transformation to $g^{-1}(\beta)$.

Any other involutive transformation exchanges a left and right endpoint of β, and thus transforms β into a matching which is not balanced. Therefore, the vertices of K_μ which correspond to balanced matchings induce a subgraph which is isomorphic to K_λ^2. □

A similar result applies to the Knuth graph of tableau shapes which consist entirely of odd columns.

Theorem 6.5. *Given a shape μ with odd column heights $(2c_1{+}1, 2c_2{+}1, \ldots, 2c_n{+}1, 1, 1, \ldots, 1)$, let j be the number of columns of height 1 ($j \geq 0$), and let λ be the shape with column heights $(c_1, c_2, \ldots, c_n)$. Then K_μ contains $\binom{j+2}{2}$ induced copies of K_λ^2.*

Proof. Let π be a balanced matching whose corresponding Young tableau has column heights $(2c_1, 2c_2, \ldots, 2c_n)$. Let π' be the involution that results from inserting n singletons in the middle of the arc diagram, between the left and right endpoints, as illustrated in Figure 6.9.

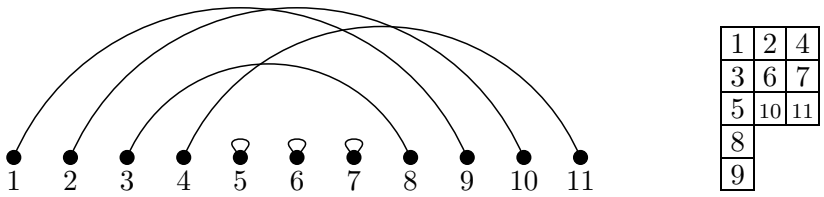

Figure 6.9: A balanced matching with singletons inserted in the middle, and the corresponding Young tableau

By inserting singletons in the center of π, they are nested below every non-singleton arc in the diagram. Therefore, it is possible to extend every maximal nesting structure certificate m_i by adding i singletons, one for each k-nesting, for $1 \leq i \leq n$. Therefore, by Theorem 5.2, the Young tableau corresponding to π' must have column heights $(2c_1+1, 2c_2+1, \ldots, 2c_n+1)$.

By Corollary 5.3.1, the number of odd columns in the shape of the Young tableau must equal the number of singletons in the arc diagram. If more singletons are inserted into π', they cannot extend the maximal nesting structure certificates any further, as there is at most one singleton in every k-nesting. Therefore, if j additional singletons are inserted, the resulting shape of the Young tableau will be $(2c_1 + 1, 2c_2 + 1, \ldots, 2c_n + 1, 1, 1, \ldots, 1)$ with j columns of height 1.

If the j additional singletons are inserted either at the far left of the arc diagram, the far right of the arc diagram, or with the other singletons in the middle of the arc diagram, all left endpoints will remain adjacent and all right endpoints will remain adjacent.

By keeping the left endpoints adjacent, the possible Involutive Transformations 4.11a and 4.11b are maintained, and by keeping the right endpoints adjacent, their reflections of 4.11a and 4.11b are also maintained. Therefore, every arrangement of singletons which preserves these properties induces a subgraph that is isomorphic to K^2_λ.

There are $\binom{j+2}{j} = \binom{j+2}{2}$ ways to insert j additional singletons into the three viable locations, and thus the theorem is proved. □

Note: Similar results are possible for shapes whose columns, from left to right, consist of columns of odd height, then columns of even height, and finally 0 or more columns of height 1.

Chapter 7

Conclusions and Perspectives

In this chapter, we highlight topics encountered in this thesis that are promising areas for further research.

7.1 Transposition of a Pair of SYT in Terms of Permutations

Section 3 defined the transformation σ^T on $\sigma \in S_n$ such that if $\sigma \sim (P, Q)$ then $\sigma^T \sim (P^T, Q^T)$.

Given $\mu \in M_{2n}$, let μ^V be the result of applying Chen et al.'s [8] transposition transformation on vacillating tableaux to μ. If $\beta \in BM_{2n}$ and $f(\beta) = \sigma$, then $f(\beta^V) = \sigma^T$. (This observation appears in the Chen et al. paper, using different terminology.) Therefore, σ^T could be defined in terms of vacillating tableaux, or Krattenthaler's generalization to growth diagrams [29].

However, both of these definitions rely on some form of tableaux and their shapes, and thus at least indirectly on RSK. To our knowledge, there is no formulation of the transformation in terms of permutations themselves.

Such a formulation could lead to a better understanding of oscillating tableaux, vacillating tableaux, and growth diagrams. For example, consider the definition of oscillating tableaux presented in Figure 7.1.

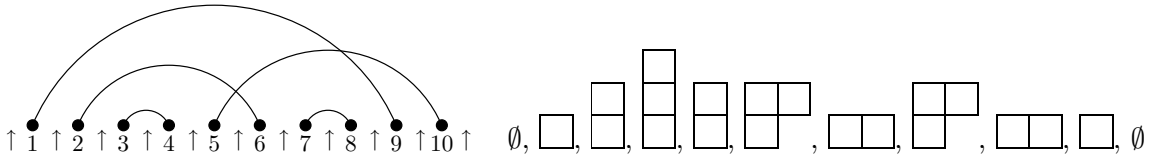

Figure 7.1: For $\mu \in M_{2n}$, consider the $2n+1$ places between the vertices of the arc diagram. The arcs above each place i form a balanced matching, β_i. Let the oscillating tableau of μ be a sequence of $2n+1$ Ferrers diagrams such that the ith diagram has the shape $\mathrm{sh}(f(\beta_i))$

Under this formulation, transposing the oscillating tableau is the same as transposing the permutations $f(\beta_i)$ at each place i in the oscillating tableau.

7.2 Transformations on Ferrers Fillings

Complementing the previous section, it is possible generalize the transformations on permutations presented in Section 3 to transformations on Ferrers fillings. As discussed above, Chen et al.'s [8] transposition transformation generalizes σ^T. Any Ferrers diagram may also be reflected around the antidiagonal, generalizing the transformation σ^{RN-1}. (See Figure 7.2.) Denote this transformation on $\mu \in M_{2n}$ as μ^F.

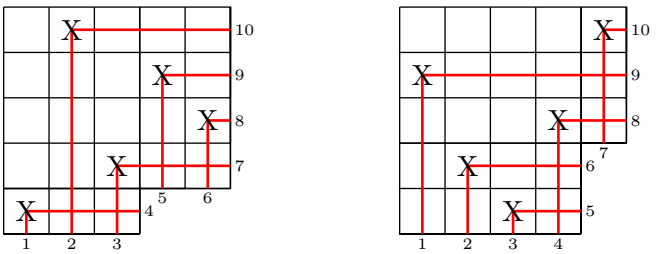

(a) A matching μ (b) μ^F

Figure 7.2: An example of transformation μ^F on a matching μ. Note that $f(\mu^F) = f(\mu)^{RN-1}$

Let D be a weighted Dyck path, and let D' be the Dyck path with complemented weights, as discussed in Kasraoui and Zeng's paper [26]. If $\mu \in M_{2n}$ is in bijection with D, define μ^K to be the matching in bijection with D'. It can be shown that if $\beta \in BM_{2n}$ such that $f(\beta) = \sigma$, then $f(\beta^K) = \sigma^R$.

Instead of weighting the down steps of Dyck paths, it is possible to weight the up steps, as shown in Figure 7.3. Let μ^Z be the transformation of complementing these alternate weights. Note that $\mu^Z = \mu^{FKF}$. For $\beta \in BM_{2n}$ such that $f(\beta) = \sigma$, $f(\beta^Z) = \sigma^N$.

(a) A matching and its weighted Dyck path after filling rows from bottom to top, weighting the down steps

(b) Alternatively, columns can be filled from right to left, weighting the up steps

Figure 7.3: Weighting up steps in a Dyck path

Together, these four transformations – μ^V, μ^F, μ^K, and μ^Z – generalize the four transformations on permutations (σ^T, σ^{-1}, σ^R, and σ^N).

μ^K and μ^Z are of particular interest. Although $\sigma^{RN} = \sigma^{NR}$, it is not always true that $\mu^{KZ} = \mu^{ZK}$. Figure 7.4 provides an example.

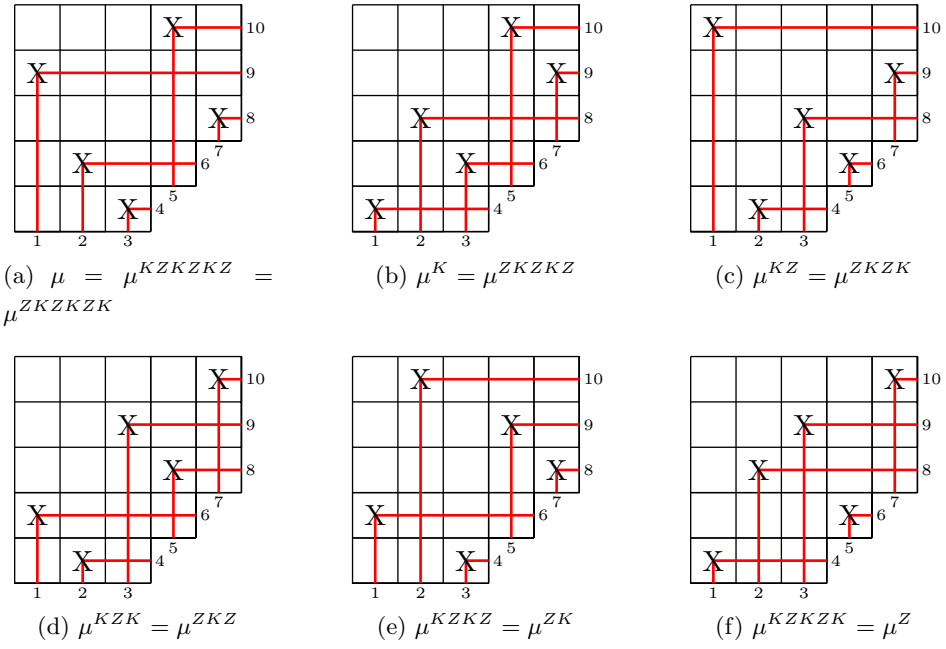

(a) $\mu = \mu^{KZKZKZ} = \mu^{ZKZKZK}$ (b) $\mu^{K} = \mu^{ZKZKZ}$ (c) $\mu^{KZ} = \mu^{ZKZK}$

(d) $\mu^{KZK} = \mu^{ZKZ}$ (e) $\mu^{KZKZ} = \mu^{ZK}$ (f) $\mu^{KZKZK} = \mu^{Z}$

Figure 7.4: Repeated application of μ^{Z} and μ^{K}

Repeated application of the compound transformation μ^{KZ} results in an equivalence class of matchings with the same Ferrers shape, same number of nestings, and same number of crossings. In the example above, Figures 7.4a, 7.4c, and 7.4e have 2 crossings and 5 nestings, while Figures 7.4b, 7.4d, and 7.4f have 5 crossings and 2 nestings.

7.3 Extending Results on Matchings

Many of the recent results on nestings and crossings, including those of Kasraoui and Zeng [26] and Chen et al. [8], can first be formulated in terms of matchings and then automatically extended to set partitions with the weak nesting and crossing interpretations using the bijection of Proposition 2.1, or to singleton-free set partitions with the strong nesting and crossing interpretations using the bijection of Proposition 2.2. This approach can be generalized to apply to unrestricted Ferrers fillings and unrestricted arc diagrams, as explored (for the strong interpretations) by de Mier [12].

If statistics could be found for the number of Dyck paths with semilength n and p peaks

in bijection with matchings having c crossings and m nestings, for example, the bicolouring bijections would immediately extend the results to set partitions and singleton-free set partitions with the weak and strong interpretations, respectively.

Recall the arc diagrams for permutations briefly introduced in Section 1.3; Figure 7.5a gives another example. In Corteel's paper [10], the arcs above the axis (which are analogous to a set partition) are considered under the weak nesting and crossing interpretation, and the arcs below the axis (which are analogous to a singleton-free set partition) are considered under the strong nesting and crossing interpretation. This is equivalent to creating two Ferrers fillings from the permutation matrix by dividing the matrix using a zig-zag pattern immediately below the main diagonal, as illustrated in Figure 7.5b. The cells strictly below the main diagonal correspond to the arcs below the axis, and the cells weakly above the diagonal, to the arcs above the axis. Similarly, Chen et al.'s triangular matrices can be considered to be the part of a permutation matrix contained strictly above the main diagonal.

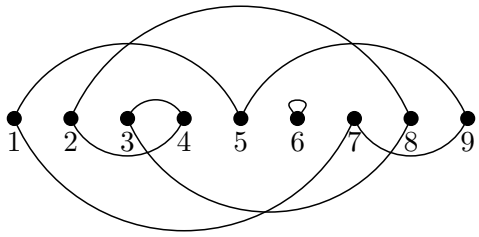

(a) The arc diagram of a permutation $\sigma = 584296137$

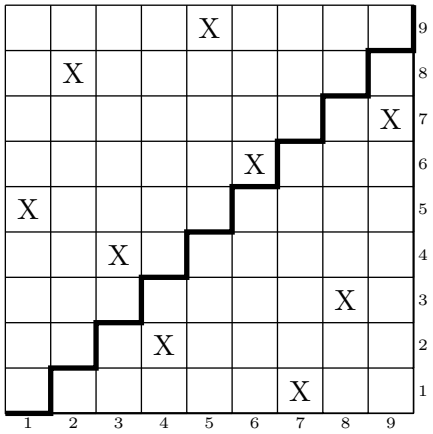

(b) The permutation matrix of σ, divided near the diagonal

Figure 7.5: Dividing a permutation matrix

This suggests dividing permutation matrices by walks on the grid of a permutation matrix which are allowed to stray further from the main diagonal.

7.4 Trees, Structured Matchings, and the Bicolouring Bijection Principle

Section 2.2 gives bijections between sets of structures and semilabeled structured trees, and between sets of structures and series-reduced semilabeled structured forests. Section 2.3 examines the statistics of all three of these families of objects. The bicolouring bijection principle of Section 2.4 is presented in terms of singleton-free sets of structures and structured matchings, but by the bijections of Section 2.2, can be restated in terms of semilabeled structured binary trees and series-reduced semilabeled structured trees.

The connection between semilabeled structured trees and sets of structures could benefit from further development. As mentioned before, the bijections can be related to the Lagrange formal power series inversion formula (such as in [31]), one of the main tools to enumerate fully-labeled tree-like objects. Our bijections may be of use in the inversion of formal power series and in the extraction of the coefficients of the generating functions of semilabeled structured trees. One interesting property of these bijections, however, is that they do not in general preserve the number of labeled objects.

There are also connections with fully-labeled trees which deserve deeper study. Mahmoud [32] has shown that the number of fully-labeled increasing plane trees with $n+1$ nodes and $k-1$ leaves is enumerated by the second-order Eulerian numbers $\left\langle\!\left\langle {n \atop k} \right\rangle\!\right\rangle$ (see also Bergeron et al. [2]). This implies a bijection between fully-labeled increasing plane trees with $n+1$ nodes and k internal nodes and matchings on $[2n]$ whose corresponding weighted Dyck paths have k peaks. (Chen and Ni [7] give a bijection between fully-labeled increasing plane trees with $n+1$ nodes and matchings on $[2n]$; their bijection does not transport the statistic between internal nodes and peaks as presented, but can be modified such that it does.)

The bijections of Chen and Ni [7] and of Diaconis and Holmes [14] (or alternatively Erdös and Székely [15]) can be combined to create a bijection between fully-labeled increasing plane trees with $n+1$ nodes and unordered semilabeled binary trees with $n+1$ leaves.

These numerous connections suggest, for example, that there may be a form of the bicolouring bijection principle that applies to bijections between families of trees, or that a more general framework of bijections between families of semilabeled and fully-labeled trees could be developed.

Bibliography

[1] J.S. Beissinger. Similar constructions for Young tableaux and involutions, and their application to shiftable tableaux. *Discrete Mathematics*, 67:149–163, 1987.

[2] F. Bergeron, P. Flajolet, and B. Salvy. Varieties of increasing trees. In *CAAP '92: 17th Colloquium on Trees in Algebra and Programming*, Lecture Notes in Computer Science, pages 24–48, 1992.

[3] F. Bergeron, G. Labelle, and P. Leroux. *Combinatorial Species and Tree-like Structures*. Cambridge University Press, Cambridge, UK, 1997.

[4] J.D. Buckholtz. Concerning an approximation of Copson. In *August 1963*, volume 14.4 of *Proceedings of the American Mathematical Society*, pages 564–568, 1963.

[5] D. Callan. A combinatorial survey of identities for the double factorial. arXiv:0906.1317v1 [math.CO], 2009.

[6] L. Carlitz. The coefficients in an asymptotic expansion. In *April 1965*, volume 16 of *Proceedings of the American Mathematical Society*, pages 248–252, 1965.

[7] W.C. Chen and W.C. Ni. Heap-ordered trees, 2-partitions and continued fractions. *European Journal of Combinatorics*, 15.6:513–517, 1994.

[8] W.Y.C. Chen, E.Y.P. Deng, R.R.X. Du, R.P. Stanley, and C.H. Yan. Crossings and nestings of matchings and partitions. *Transactions of the American Mathematical Society*, 359:1555–1575, 2006.

[9] W.Y.C. Chen, H.S.W. Han, and C.M. Reidys. Random k-noncrossing RNA structures. arXiv:0906.5553v1 [math.CO], 2009.

[10] S. Corteel. Crossings and alignments of permutations. *Advances in Applied Mathematics*, 38.2:149–163, 2007.

[11] G. de B. Robinson. On representations of the symmetric group. *American Journal of Mathematics*, 60:745–760, 1934.

[12] A. de Mier. k-noncrossing and k-nonnesting graphs and fillings of Ferrers diagrams. *Combinatorica*, 27:699–720, 2007.

[13] E. Deutsch. Dyck path enumeration. *Discrete Mathematics*, 204:167–202, 1999.

[14] P.W. Diaconis and S.P. Holmes. Matchings and phylogenetic trees. In *December 1998*, volume 95.25 of *Proceedings of the National Academy of Sciences of the United States of America*, pages 14600–14602, 1998.

[15] P.L. Erdös and L.A. Székely. Applications of antilexicographic order. I. An enumerative theory of trees. *Advances in Applied Mathematics*, 10.4:488–496, 1989.

[16] P. Flajolet. Combinatorial aspects of continued fractions. *Discrete Mathematics*, 32:125–161, 1980.

[17] P. Flajolet and R. Sedgewick. *Analytic Combinatorics*. Cambridge University Press, Cambridge, UK, 2009.

[18] W. Fulton. *Young Tableaux (London Mathematical Society Student Texts 35)*. Cambridge University Press, Cambridge, UK, 1997.

[19] I.M. Gessel and R.P. Stanley. Stirling polynomials. *Journal of Combinatorial Theory, Series A*, 24:24–33, 1978.

[20] J. Ginsburg. Note on Stirling's numbers. *American Mathematical Monthly*, 35:77–80, 1928.

[21] R.L. Graham, D.E. Knuth, and O. Patashnik. *Concrete Mathematics: A Foundation for Computer Science*. Addison-Wesley Longman Publishing Co., Inc., Boston, MA, USA, 1994.

[22] C. Greene. An extension of Schensted's theorem. *Advances in Mathematics*, 14:254–265, 1974.

[23] F.W.D. Huang, W.W.J. Peng, and C.M. Reidys. Folding 3-noncrossing RNA pseudoknot structures. arXiv:0809.4840v1 [math.CO], 2008.

[24] E.Y. Jin, J. Qin, and C.M. Reidys. Combinatorics of RNA structures with pseudoknots. *Bulletin of Mathematical Biology*, 70.1:45–67, 2008.

[25] E.Y. Jin, C.M. Reidys, and R.R. Wang. Asymptotic analysis of k-noncrossing matchings. arXiv:0803.0848v1 [math.CO], 2008.

[26] A. Kasraoui and J. Zeng. Distribution of crossings, nestings, and alignments of two edges in matchings and partitions. *Electronic Journal of Combinatorics*, 13:#R33, 2006.

[27] D.E. Knuth. Permutations, matrices, and generalized Young tableaux. *Pacific Journal of Mathematics*, 34:709–727, 1970.

[28] D.E. Knuth. *The Art of Computer Programming 3. Sorting and Searching*. Addison-Wesley, 2 edition, 1998.

[29] C. Krattenthaler. Growth diagrams, and increasing and decreasing chains in fillings of Ferrers shapes. *Advances in Applied Mathematics*, 37:404–431, 2006.

[30] G. Kreweras. Sur les partitions noncroisées d'un cycle. *Discrete Mathematics*, 1:333–350, 1972.

[31] G. Labelle. Une nouvelle démonstration combinatoire des formules d'inversion de Lagrange. *Advances in Mathematics*, 42.3:217–247, 1981.

[32] H.M. Mahmoud, R.T. Smythe, and J. Szymański. On the structure of random plane-oriented recursive trees and their branches. *Random Structures and Algorithms*, 4.2:151–176, 1993.

[33] S. Poznanović. A bijection between partially directed paths in the symmetric wedge and matchings. arXiv:0803.4233v1 [math.CO], 2008.

[34] G.N. Raney. Functional composition patterns and power series reversion. *Transactions of the American Mathematical Society*, 94:441–451, 1960.

[35] A. Reifegerste. Permutation sign under the Robinson-Schensted-Knuth correspondence. 8:103–112, 2004.

[36] J. Riordan. The blossoming of Schröder's fourth problem. *Acta Mathematica*, 137:1–16, 1976.

[37] M. Rubey. Nestings of matchings and permutations and north steps in PDSAWs. arXiv:0712.2804v4 [math.CO], 2008.

[38] C. Schensted. Longest increasing and decreasing subsequences. *Canadian Journal of Mathematics*, 13:179–191, 1961.

[39] M.P. Schützenberger. Quelques remarques sur une construction de Schensted. *Mathematica Scandinavica*, 12:117–128, 1963.

[40] M.P. Schützenberger. La correspondance de Robinson. In *Combinatoire et représentation du groupe symétrique*, volume 579 of *Lecture Notes in Mathematics*, pages 59–113. Springer, 1977.

[41] N.J.A. Sloane. On-line encyclopedia of integer sequences (OEIS). `http://www.research.att.com/~njas/sequences/`.

[42] L.M. Smiley. Completion of a rational function sequence of Carlitz. arXiv:math/0006106v1 [math.CO], 2001.

[43] R.P. Stanley. *Enumerative Combinatorics, Volume 1.* Cambridge University Press, Cambridge, UK, 1996.

[44] R.P. Stanley. *Enumerative Combinatorics, Volume 2.* Cambridge University Press, Cambridge, UK, 1999.

[45] D. Stanton and D. White. *Constructive Combinatorics.* Springer-Verlag New York, Inc., New York, NY, USA, 1986.